THE WORLD BANK
IBRD • IDA | WORLD BANK GROUP

ESMAP
Energy Sector Management Assistance Program

SOLAR RESOURCE AND PV POTENTIAL OF ZAMBIA

SOLAR RESOURCE ATLAS

April 2019

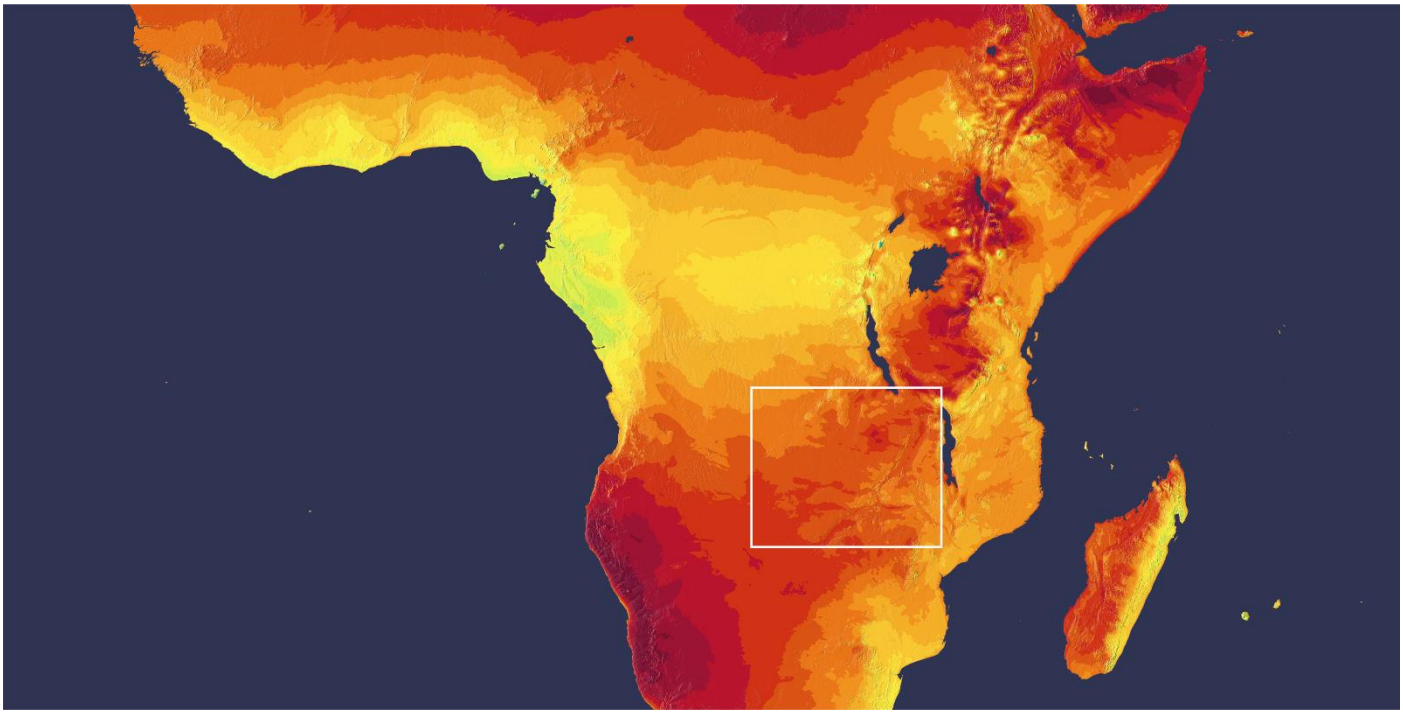

This report was prepared by Solargis, under contract to the World Bank.

It is one of several outputs from the solar resource mapping component of the activity "Capacity Building for Renewable Energy Resource Mapping and Grid Integration in Zambia" [Project ID: P145271]. This activity is funded and supported by the Energy Sector Management Assistance Program (ESMAP), a multi-donor trust fund administered by the World Bank, under a global initiative on Renewable Energy Resource Mapping. Further details on the initiative can be obtained from the ESMAP website.

The content of this document is the sole responsibility of the consultant authors. Any improved or validated solar resource data will be incorporated into the Global Solar Atlas.

Washington DC 20433
Telephone: +1-202-473-1000
Internet: www.worldbank.org

Attribution

Please cite the work as follows: World Bank. 2019. Solar resource and PV potential of Zambia: Solar Resource Atlas. Washington, DC: World Bank.

Solar Resource Atlas

Based on regional adaptation of Solargis model

Republic of Zambia

Reference No. **128-09/2019**

Customer

World Bank
Energy Sector Management Assistance Program
Contact: Mr. Tigran Parvanyan
1818 H St NW, Washington DC, 20433, USA
Phone: +1-202-473-3159
E-mail: mailto: tparvanyan@worldbank.org
http://www.esmap.org/RE_Mapping

Consultant

Solargis s.r.o.
Contact: Mr. Marcel Suri
Mytna 48, 811 07 Bratislava, Slovakia
Phone +421 2 4319 1708
E-mail: marcel.suri@solargis.com
https://solargis.com

Table of contents

Acronyms

AC	Alternating current
AERONET	The AERONET (AErosol RObotic NETwork) is a ground-based remote sensing network dedicated to measuring atmospheric aerosol properties. It provides a long-term database of aerosol optical, microphysical and radiative parameters.
AOD	Aerosol Optical Depth at 670 nm. This is one of atmospheric parameters derived from MACC database and used in Solargis. It has a notable impact on the accuracy of solar calculations in arid zones.
CFSR	Climate Forecast System Reanalysis. The meteorological model operated by the US service NOAA.
CFSv2	The Climate Forecast System Version 2. CFSv2 meteorological models operated by the US service NOAA (Operational extension of Climate Forecast System Reanalysis, CFSR).
CPV	Concentrated Photovoltaic systems, which uses optics such as lenses or curved mirrors to concentrate a large amount of sunlight onto a small area of photovoltaic cells to generate electricity.
CSP	Concentrated solar power systems, which use mirrors or lenses to concentrate a large amount of sunlight onto a small area, where it is converted to heat for a heat engine connected to an electrical power generator.
DC	Direct current
DIF	Diffuse Horizontal Irradiation, if integrated solar energy is assumed. Diffuse Horizontal Irradiance, if solar power values are discussed.
DNI	Direct Normal Irradiation, if integrated solar energy is assumed. Direct Normal Irradiance, if solar power values are discussed.
ECMWF	European Centre for Medium-Range Weather Forecasts is independent intergovernmental organisation supported by 34 states, which provide operational medium- and extended-range forecasts and a computing facility for scientific research.
ESMAP	Energy Sector Management Assistance Program, a multi-donor trust fund administered by the World Bank
EUMETSAT	European Organisation for the Exploitation of Meteorological Satellites, an intergovernmental organisation for establishing, maintaining and exploiting European systems of operational meteorological satellites
GFS	Global Forecast System. The meteorological model operated by the US service NOAA.
GHI	Global Horizontal Irradiation, if integrated solar energy is assumed. Global Horizontal Irradiance, if solar power values are discussed.
GIS	Geographical Information System
GTI	Global Tilted (in-plane) Irradiation, if integrated solar energy is assumed. Global Tilted Irradiance, if solar power values are discussed.
KSI	Kolmogorov–Smirnov Index, a statistical index for comparing functions or samples

MACC	Monitoring Atmospheric Composition and Climate – meteorological model operated by the European service ECMWF (European Centre for Medium-Range Weather Forecasts)
Meteosat MFG and MSG	Meteosat satellite operated by EUMETSAT organization. MSG: Meteosat Second Generation; MFG: Meteosat First Generation
MERRA	Modern-Era Retrospective Analysis for Research and Applications, a NASA reanalysis for the satellite era using an Earth observing systems
MERRA-2	Modern-Era Retrospective analysis for Research and Applications, Version 2
NASA	National Aeronautics and Space Administration organization
NOAA NCEP	National Oceanic and Atmospheric Administration, National Centre for Environmental Prediction
NOAA ISD	NOAA Integrated Surface Database with meteorological data measured by ground-based measurement stations
NOCT	The Nominal Operating Cell Temperature, is defined as the temperature reached by open circuited cells in a module under the defined conditions: Irradiance on cell surface = 800 W/m^2, Air Temperature = 20°C, Wind Velocity = 1 m/s and mounted with open back side.
PV	Photovoltaic
PVOUT	Photovoltaic electricity output calculated from solar resource and air temperature time series.
RSR	Rotating Shadowband Radiometer
SOLIS	Solar Irradiance Scheme, Solar clear-sky model for converting meteorological satellite images into radiation data
SRTM	Shuttle Radar Topography Mission, a service collecting topographic data of Earth's land surfaces
STC	Standard Test Conditions, used for module performance rating to ensure the same measurement conditions: irradiance of 1,000 W/m², solar spectrum of AM 1.5 and module temperature at 25°C.
TEMP	Air Temperature at 2 metres
UV	Ultraviolet radiation

Glossary

AC power output of a PV power plant	Power output measured at the distribution grid at a connection point.
Aerosols	Small solid or liquid particles suspended in air, for example desert sand or soil particles, sea salts, burning biomass, pollen, industrial and traffic pollution.
All-sky irradiance	The amount of solar radiation reaching the Earth's surface is mainly determined by Earth-Sun geometry (the position of a point on the Earth's surface relative to the Sun which is determined by latitude, the time of year and the time of day) and the atmospheric conditions (the level of cloud cover and the optical transparency of atmosphere). All-sky irradiance is computed with all factors taken into account
Bias	Represents systematic deviation (over- or underestimation) and it is determined by systematic or seasonal issues in cloud identification algorithms, coarse resolution and regional imperfections of atmospheric data (aerosols, water vapour), terrain, sun position, satellite viewing angle, microclimate effects, high mountains, etc.
Clear-sky irradiance	The clear sky irradiance is calculated similarly to all-sky irradiance but without considering the impact of cloud cover.
Fixed-mounted modules	Photovoltaic modules assembled on fixed bearing structure in a defined tilt to the horizontal plane and oriented in fixed azimuth.
Frequency of data (30-minute, hourly, daily, monthly, yearly)	Period of aggregation of solar data that can be obtained from the Solargis database.
Installed DC capacity	Total sum of nominal power (label values) of all modules installed on photovoltaic power plant.
Long-term average	Average value of selected parameter (GHI, DNI, etc.) based on multiyear historical time series. Long-term averages provide a basic overview of solar resource availability and its seasonal variability.
P50 value	Best estimate or median value represents 50% probability of exceedance. For annual and monthly solar irradiation summaries it is close to average, since multiyear distribution of solar radiation resembles normal distribution.
P90 value	Conservative estimate, assuming 90% probability of exceedance (with a 90% probability the value should be exceeded). When assuming normal distribution, the P90 value is also a lower boundary of the 80% probability of occurrence. P90 value can be calculated by subtracting uncertainty from the P50 value. In this report we apply a simplified assumption of normal distribution of yearly values.
PV electricity production	AC power output of a PV power plant expressed as percentage part of installed DC capacity.
Root Mean Square Deviation (RMSD)	Represents spread of deviations given by random discrepancies between measured and modelled data and is calculated according to this formula: $$RMSD = \sqrt{\frac{\sum_{k=1}^{n}\left(X^{k}{}_{measured} - X^{k}_{modeled}\right)^{2}}{n}}$$ On the modelling side, this could be low accuracy of cloud estimate (e.g. intermediate clouds), under/over estimation of atmospheric input data, terrain,

	microclimate and other effects, which are not captured by the model. Part of this discrepancy is natural - a satellite monitors a large area (of approx. 3 x 4 km), while a sensor sees only a micro area of approx. 1 sq. centimetre. On the measurement side, the discrepancy may be determined by accuracy/quality and errors of the instrument, pollution of the detector, misalignment, data loggers, insufficient quality control, etc.
Solar irradiance	Solar power (instantaneous energy) falling on a unit area per unit time [W/m^2]. Solar resource or solar radiation is used when considering both irradiance and irradiation.
Solar irradiation	Amount of solar energy falling on a unit area over a stated time interval [Wh/m^2 or kWh/m^2].
Spatial grid resolution	In digital cartography the term applies to the minimum size of the grid cell or in other words, minimum size of the pixels in the digital map.

Executive summary

This report presents results of the solar resource assessment and mapping activity undertaken by The World Bank in Zambia, as a part of a broader technical assistance project covering biomass, solar and wind mapping funded by the Energy Sector Management Assistance Program (ESMAP).

The data used in this report is based on the Solargis model. The uncertainty of the solar resource data has been reduced by the regional model adaptation based on the ground measurements collected at six solar meteorological stations across Zambia, commissioned by The World Bank during the years 2015 to 2017 under the same activity. The ground-based solar resource measurements have been supplied by GeoSUN Africa, based in South Africa. The measurement campaign has been technically supported by SGS Inspection Services, Zambia.

The report has two objectives:

- To explain the methodologies and outcomes of the solar resource and photovoltaic power potential assessment, based on the combined use of models and measured data. The report documents the uncertainty of solar and meteorological data, as key inputs in the technical and financial evaluation of solar energy systems.
- To improve the awareness and knowledge of resources for solar energy technologies by producing a comprehensive countrywide dataset and maps based on the accuracy-enhanced models. The report evaluates key solar climate features, and the geographic and time variability of solar power potential in the country.

The results of this report compare to interim solar resource validation at the beginning of the project, which were based on the Solargis model, validated by the ground measurements available in a wider region (*ESMAP Solar Resource Mapping for Zambia, Interim Solar Modelling Report, 128-01/2014, November 2014*). The uncertainty estimates in this report have been found as too optimistic. The validation of the model based on 24 months of measurements conducted at six solar meteorological stations revealed higher uncertainty of originally used Solargis model.

The uncertainty of the Solargis model yearly estimates for yearly values of DNI, has been reduced from the original assumptions, made in 2014, for the original model ±9.0% to the range of ±5% and ±7% for the regionally adapted model. For yearly GHI, the uncertainty was reduced from ±6.5% for original model to the range of ±4% and ±5% for the regionally adapted model. These figures represent a majority of the country's territory with flat and monotonous terrain. In specific conditions with complex terrain we expect a higher model uncertainty. The key achievement of this project is supplying country-wide data and maps, based on the extensive validation of the solar model by high accuracy solar measurements acquired in Zambia.

The data underlying this report are delivered in two formats:

- Raster GIS data for the whole territory of the Republic of Zambia, representing long-term monthly and yearly average values. This data layers are accompanied by geographical data layers in raster and vector data formats.
- High-resolution digital maps prepared for poster printing, as well as Google Earth maps.

The maps show that, throughout most of Zambia, yearly sum of global horizontal irradiation is in the range of 1900 to 2100 kWh/m^2. This translates to a specific yearly PV electricity output in the range of 1550 kWh/kWp to more than 1700 kWh/kWp. The seasonal variability is smaller, compared to other countries further away from the equator. This qualifies Zambia as a country with high potential for PV power generation.

The aggregated data for Zambia can be accessed online via an interactive map-based application, or as downloadable files and maps at http://globalsolaratlas.info/. The ground-measured data is accessible through https://energydata.info/.

1 Introduction

Solar electricity offers a unique opportunity to achieve long-term sustainability goals, such as the development of a modern economy, healthy and educated society, clean environment, and improved geopolitical stability. Solar power plants exploit local solar resources; they do not require heavy support infrastructure, they are scalable, and improve electricity services. A key feature of solar electricity is that it is accessible in remote locations, thus providing development opportunities anywhere.

While solar resources are fuel to solar power plants, the local geographical and climate conditions determine the efficiency of their operation. Free fuel makes solar technology attractive; however, effective investment and technical decisions require **detailed, accurate and validated solar and meteorological data**. Accurate data are also needed for the cost-effective operation of solar power plant. High quality solar resource and meteorological data can be obtained by satellite-based meteorological models and by measuring instruments installed at meteorological stations.

1.1 Past and on-going solar resource assessment initiatives

Several solar resource assessment initiatives are documented below as publications and online data resources. The works show steadily growing interest and different stages of development of solar resource assessment and energy modelling in the region. Below we compare a selection of solar databases.

NASA Power, NASA

Monthly and yearly averages are available from the NASA Power project [1]. The data and documentation are updated in 2018. Specific parameters are available at higher time resolution (e.g. daily). The data includes numerous atmospheric and solar radiation parameters, the solar data represents a period from 1983 to 2005, resolution of approx. 55 km. Data is not validated for the region and it can be accessed from https://power.larc.nasa.gov/.

Photovoltaic Geographical Information System (PVGIS), European Commission JRC

Geographical Assessment of Solar Resource and Performance of Photovoltaic Technology. The online tools are accessible from http://re.jrc.ec.europa.eu/pvgis.html. The database is based on Meteosat satellite data calculation and offers solar resource long-term averages as well as hourly data.

PVGIS HelioClim-1 is an older version of PVGIS based on HelioClim-1 product by Ecole des Mines, Paris, that makes use of interpolation of clear-sky index derived from low resolution Meteosat MFG satellite images and terrain shading. The PVGIS Helioclim-1 database has been validated at only very limited number of ground stations in Africa and the outputs are of lower accuracy [2].

PVGIS CM-SAF is more modern and more accurate version of satellite database which makes use of Meteosat MSG satellite images. CM-SAF data is primarily offered at hourly resolution, the accuracy is better, compared to HelioClim 1. Yet the data has also limited validation in Africa and no validation in this region. The most recent update of the project has been made in 2017 [3].

HelioClim Project, Ecole des Mines Paris (Mines ParisTech), ARMINES, Transvalor

Online solar radiation satellite-derived database is available for free on http://www.soda-pro.com/web-services/radiation/helioclim-1. This database is one of first attempts in Europe to provide satellite-based solar radiation database covering Europe and Africa. HelioClim 1 uses reduced dataset of Meteosat Prime MFG satellite images, with temporal resolution from 3 hours and the cloud index is calculated via Heliosat-2 method. With the coverage period from 1985 to 2005, it represents daily values of solar radiations with a coarse resolution: 20 to 30km [4]. The group developed and operates a commercial version of HelioClim-3 database, which also covers the territory of Meteosat Prime satellite. More information at http://www.soda-is.com.

CAMS - JADE, European Union's Earth observation programme

CAMS (Copernicus Atmosphere Monitoring Service) solar radiation services provide detailed assessment of optical variables in the atmosphere. Developed and operated by ARMINES,/MINES ParisTech/TRANSVALOR and implemented by ECMWF (European centre for Medium-range Weather Forecasts) as part of the Copernicus programme, https://atmosphere.copernicus.eu/, it covers Europe, Africa and adjacent territories between ±66° latitude and longitude and it processes Meteosat satellites (MFG and MSG) images with Heliosat-4 method to create the dataset of solar radiation components with JADE being the specific CAMS radiation service dataset over Africa [5]. CAMS solar radiations services are validated at BSRN network of ground stations, but without a reference station in the wide region of South-eastern Africa. The service is still in the phase of accuracy improvements.

Meteonorm, Meteotest

Meteonorm, https://meteonorm.com/en/ is a global meteorological database of ground stations around the world, with a support from satellite-based solar radiation for Europe and Africa available from CM-SAF data service. The measurements are used to interpolate the specific conditions from nearby stations for the site of interest and to calculate synthetic hourly data for one artificial year. This approach provides data with limited accuracy and use, and there are little prospects for meeting the needs of development and operation of commercial PV power plants. The accuracy of calculation database depends the density of good-quality solar meteo stations. In Africa however, the availability of high-quality solar meteorological stations (based on the use of high-accuracy sensors and good maintenance) is very limited, with only a handful sites available in the region of Central/Southeast Africa. Moreover, the micro-climate conditions of a specific site would be completely overlooked by spatial interpolation, which may result in large errors in the calculation output. Synthetic hourly data cannot be validated by high resolution ground measurements [6].

Other projects

The list above is not exhaustive as there are some other projects, historical and on-going, in various stages of development, also offering solar radiation data, for example:

- SOLEMI by DLR (Germany); https://wdc.dlr.de/data_products/SERVICES/SOLARENERGY/description.php
- Solar database by 3E (Belgium); https://solardata.3e.eu/
- Solar database by Reuniwatt (France); https://reuniwatt.com/

Global Solar Atlas, World Bank Group

The World Bank Group have provided the Global Solar Atlas to support the scale-up of solar power in their client countries. This work is funded by the Energy Sector Management Assistance Program (ESMAP), a multi-donor trust fund administered by The World Bank. The Atlas has been prepared by Solargis under a contract to The World Bank. The primary aim is to provide quick and easy access to solar resource data and maps globally [7, 8]. The project is ongoing, and a substantial update is planned for year 2019; https://globalsolaratlas.info.

Renewable Energy Resource Mapping for Zambia, World Bank (ESMAP)

This report refers to the outcomes achieved within this project, closed in 2019. A set of data and reports for Zambia has been prepared by Solargis and its subcontractor GeoSUN Africa, working on this project until the present. Three areas were addressed, in consecutive phases:

- Preliminary modelling that has been conducted by Solargis
- Installation, operation and data acquisition for six ground-based solar meteorological stations by GeoSUN Africa, South Africa supported by SGS Inspection Services, Zambia. All the measured data is accessible via the portal https://energydata.info/
- This report refers to final Phase 3 of the project, and it accompanies the delivery of the final outputs based on the combination of the modelled and the measured data. Solargis provides the final mapping outputs for Zambia. All outputs are accessible from https://globalsolaratlas.info.

1.2 Evaluation of the existing data and studies

Zambia has considerable though diverse potential for solar power generation. Many of the solar and meteorological data sets, listed in Chapter 1.1, do not fulfil the requirements for accuracy, reliability and features needed for commercial development of solar PV power plants in present times. Table 1.1 compares Solargis results to some of other solar data initiatives. The features that differ Solargis from most of other data sets:

- Solargis models are based on the best available algorithms and approaches, in-house adapted over years, validated worldwide for all climate zones and geographies
- Best available input data are used for the models (satellite, atmospheric and meteorological), harmonized over time and geographically, to assure the same level of performance globally
- Data is available globally at 250-metres spatial resolution and subhourly time resolution. Historically the data goes back to 1994, 1999 and 2007 (depending on the satellite region).
- Time series data is updated in real time, thus it can be used for project development as well as for monitoring and forecasting; data is systematically validated and quality controlled.
- There is customer support and supporting consultancy services available.

The new Solargis database focuses on supply of data and services for the development and financing of large-scale solar power plants worldwide, including Zambia. The main objective is to systematically supply reliable, validated and high-resolution data to the solar industry with low uncertainty and systematic quality control.

Table 1.1: Comparison of long-term GHI estimate: Solargis vs. other databases
Lusaka site (Lat: -15.39463, Lon: 28.33722)

Source	Reference	Daily GHI estimate (kWh/m2)	Yearly GHI estimate (kWh/m2)	GHI difference to validated Solargis	Indicated uncertainty of yearly value	Year of publication (data access)	Data coverage
NASA POWER	[1]	5.63	2056	2.5%	?	2018	1983 – 2005
PVGIS HelioClim-1	[2]	5.71	2086	3.9%	?	2017	1998 – 2011
PVGIS CMSAF	[3]	5.91	2159	7.1%	?	2016	1985 – 2004
Helioclim-1	[4]	5.65	2064	2.8%	?	(2018)	1985 – 2005
CAMS-JADE	[5]	5.84	2131	5.9%	?	2018	1991 – 2010
Meteonorm 7.3	[6]	5.45	1990	-0.8%	±4.0%	2018	1991 – 2010
Solargis and Global Solar Atlas	[7]	5.79	2114	5.2%	±6.0%	2017	1994 – 2016
Solargis	This report	5.49	2005	-	±4.0%	2019	1994 – 2017

(regionally adapted)

The solar industry requires models that offer map-based data covering extensive territories at a high level of a detail using historical and real time data. Modern solar measuring stations are used for accuracy enhancement of such models and to gain a better understanding of the local climate. Thus, a combination of the model data with modern solar and meteorological measurements is used to support solar energy development in all stages of its lifecycle.

High accuracy solar resource and meteorological data is needed for the development and operation of commercial solar power plants. Typically, detailed data describing the local climate is needed for a location of interest; however, high accuracy meteorological measurements for sites of interest are rarely available. Therefore, data from solar and meteorological models are initially used to evaluate the energy yield and assess the performance of the power plants. When the location for commercial project development is selected, a solar meteorological station is installed in the second step. The high accuracy meteorological equipment is used to collect local data for an initial period of at least one year. Such measurements are then used for the site adaptation of solar models and for delivering high accuracy solar resource and meteorological time series that covers a long historical period. At larger power plants, solar measurements are collected continuously over the lifetime of the project.

The solar and meteorological data is used for the following tasks related to solar power generation:

1. Country-level evaluation and strategical assessment
2. Prospection; selection of candidate sites for future power plants, and prefeasibility analysis
3. Project evaluation; solar and energy yield assessment, technical design and financing
4. Monitoring and performance assessment of solar power plants and forecasting of solar power
5. Quality control of solar measurements.

This report addresses the first topic from the list above.

1.3 Structure of this study

Following an introduction to the activity (Chapter 1), Chapter 2 of this Solar Resource Atlas provides an outline of solar radiation basics and principles of photovoltaic power potential calculation. Chapters 2.1 and 2.2 describe measuring and modelling approaches for developing reliable solar and meteorological data, including information about solar and meteorological data uncertainty. These chapters document the role of solar measurements in reducing the uncertainty of solar, meteorological and PV power potential data for the country. Chapter 2.3 and 2.4 explain the relevance of solar resource and meteorological information for the deployment of solar power technologies. An emphasis is given to photovoltaic (PV) technology, which has high potential for developing utility-scale projects close to larger load centres, as well as deployment of rooftop PV systems, off-grid, hybrid systems and mini-grids for community electrification.

Chapter 3 presents an analysis and evaluation of meteorological and solar resource data in Zambia. Six representative sites are selected to show potential regional differences in Zambia through tables and graphs. Chapter 3.1 introduces ancillary geographical data that influence the performance of solar power plants. Chapter 3.2 to 3.5 summarizes geographical differences and seasonal variability of the solar resource in Zambia, while Chapter 3.6 presents the PV power generation potential of the country. The theoretical specific PV electricity output is calculated from the most commonly used PV technology: a fixed system with crystalline-silicon (c-Si) PV modules, optimally tilted and oriented towards the Equator. Chapter 3.7 summarizes the analytical information and presents conclusions. Chapter 4 summarizes the technical features of the delivered data products. Chapters 5 to 8 provide support information.

2 Methods and data

2.1 Solar resource data

2.1.1 Introduction

Solar resource (physical term solar radiation) is fuel to solar energy systems. The solar radiation available for solar energy systems at the ground level depends on processes in the atmosphere. This leads to a high spatial and temporal variability at the Earth's surface. The interactions of extra-terrestrial solar radiation with the Earth's atmosphere, surface and objects are divided into three groups:

1. Solar geometry, trajectory around the sun and Earth's rotation (declination, latitude, solar angle)
2. Atmospheric attenuation (scattering and absorption) by:
    2.1 Atmospheric gases (air molecules, ozone, NO_2, CO_2 and O_2)
    2.2 Solid and liquid particles (aerosols) and water vapour
    2.3 Clouds (condensed water or ice crystals)
3. Topography (elevation, surface inclination and orientation, horizon)
4. Shadows, reflections from surface or local obstacles (trees, buildings, etc.) and re-diffusion by atmosphere.

The atmosphere attenuates solar radiation selectively: some wavelengths are associated with high attenuation (e.g. UV) and others with a good transmission. Solar radiation called "short wavelength" (in practice, 300 to 4000 nm) is of primary interest to solar power technology and is used as a reference. The component that is neither reflected nor scattered, and which directly reaches the surface, is called *direct radiation*; this is the component that produces shadows. The component scattered by the atmosphere that also reaches the ground is called *diffuse radiation*. A small portion of the radiation reflected by the surface that reaches an inclined plane is called the *reflected radiation*. These three components together create *global radiation*. A proportion of individual component at any time is given by Sun position and by the actual state of atmosphere – mainly the occurrence of clouds, air pollution and humidity.

According to the generally adopted terminology, in solar radiation two terms are distinguished:

- **Solar irradiance** indicates power (instant energy) per second incident on a surface of 1 m^2 (unit: W/ m^2).
- **Solar irradiation**, expressed in MJ/ m^2 or Wh/m^2; it indicates the amount of incident solar energy per unit area during a lapse of time (hour, day, month, etc.).

Often, the term *irradiance* is used by the authors of numerous publications in both cases, which can sometimes cause confusion.

In **solar energy applications**, the following three solar resources are relevant:

- **Direct Normal** Irradiation/Irradiance (DNI): it is the direct solar radiation from the solar disk and the region closest to the sun (circumsolar disk of 5° centred on the sun). DNI is the component that is important to concentrating solar collectors used in Concentrating Solar Power (CSP) and high-performance cells in Concentrating Photovoltaic (CPV) technologies.
- **Global Horizontal** Irradiation/Irradiance (GHI): sum of direct and diffuse radiation received on a horizontal plane. GHI is a reference radiation for the comparison of climatic zones; it is also the essential parameter for calculation of radiation on a flat plate collector.
- **Global Tilted** Irradiation/Irradiance (GTI) or total radiation received on a surface with defined tilt and azimuth, fixed or sun-tracking. This is the sum of the scattered radiation, direct and reflected. A term Plane of Array (POA) irradiation//irradiance is also used. In the case of photovoltaic (PV) applications, GTI can

occasionally be affected by shading from the surrounding terrain or objects, and GTI is then composed only from diffuse and reflected components. This typically occurs for sun at low angles over the horizon.

Solar radiation data can be acquired by two complementary approaches:

1. **Ground-mounted sensors** are good in providing high frequency and accurate data (for well-maintained, high accuracy measuring equipment) for a specific location.
2. **Satellite-based models** provide data with a lower frequency of measurement, but cover a long history over lager areas. Satellite-models are not capable of producing instantaneous values at the same accuracy as ground sensors, but can provide robust aggregated values.

Chapter 2 summarizes approaches applied for measuring and computing solar resource parameters, for Zambia, and the main sources of uncertainty. It also discusses methods for combining data acquired by these two complementary approaches with the aim of maximizing strengths of both approaches.

2.1.2 ESMAP Solar resource measurements in Zambia

Data from six ESMAP measuring stations in Zambia was collected and harmonized with the objective of acquiring reference solar radiation data for reducing the uncertainty of the model. Quality data from these meteorological stations is available for this assessment (Tables 2.1 and 2.2, Figure 2.1, Map 2.1). Detailed information about the measurement sites is also available at the web sites http://energydata.info/ and http://globalsolaratlas.info/.

More detailed information related to the measurement campaign in Zambia can be found in the report *"Annual solar resource report for solar meteorological stations after completion of 24 months of measurements"*, Ref. Nr. 128-07/2018 (August 2018) [12]. The report presents quality control of ground measured data and results of site adaptation of the Solargis model for six solar meteorological sites, with estimate of relevant data uncertainties.

Table 2.1: Overview information on measurement stations operated in the region

No.	Site name	Nearest town	Latitude [°]	Longitude [°]	Altitude [m a.s.l.]	Measurement station host*
1	Lusaka UNZA	Lusaka	-15.39463°	28.33722°	1263	UNZA
2	Mount Makulu	Chilanga	-15.54830°	28.24817°	1227	ZARI/ZMD
3	Mochipapa	Choma	-16.83828°	27.07046°	1282	ZARI/ZMD
4	Longe	Kaoma	-14.83900°	24.93100°	1169	ZARI
5	Misamfu	Kasama	-10.17165°	31.22558°	1380	ZARI/ZMD
6	Mutanda	Mutanda	-12.42300°	26.21500°	1316	ZARI/ZMD

**Zambia Meteorological Department (ZMD), Zambia Agriculture Research Institute (ZARI) and School of Agricultural Sciences at University of Zambia (UNZA)*

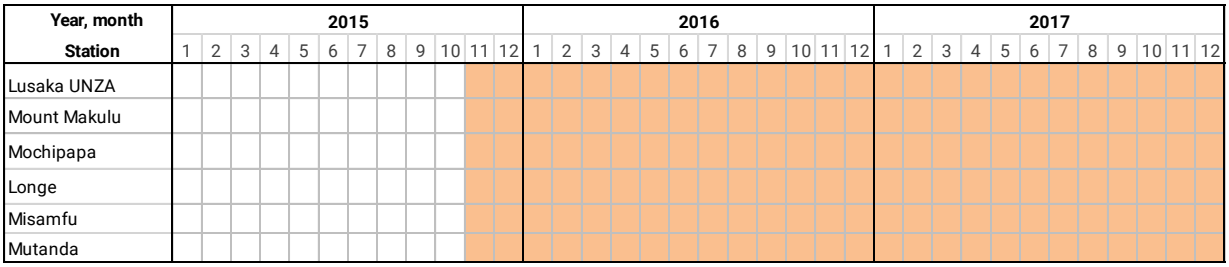

Figure 2.1: Solar resource data availability.

Table 2.2: Overview information on solar meteorological stations in Zambia

No.	Site name	Type	Solar parameters	Time step	Period of data used in study
1	Lusaka UNZA	TIER1	GHI, DNI, DIF	1 min	7 November 2015 – 31 December 2017
2	Mount Makulu	TIER2	GHI, GHI2, DNI2, DIF2	1 min	13 November 2015 – 31 December 2017
3	Mochipapa	TIER2	GHI, GHI2, DNI2, DIF2	1 min	5 November 2015 – 31 December 2017
4	Longe	TIER2	GHI, GHI2, DNI2, DIF2	1 min	10 November 2015 – 31 December 2017
5	Misamfu	TIER2	GHI, GHI2, DNI2, DIF2	1 min	18 November 2015 – 31 December 2017
6	Mutanda	TIER2	GHI, GHI2, DNI2, DIF2	1 min	21 November 2015 – 31 December 2017

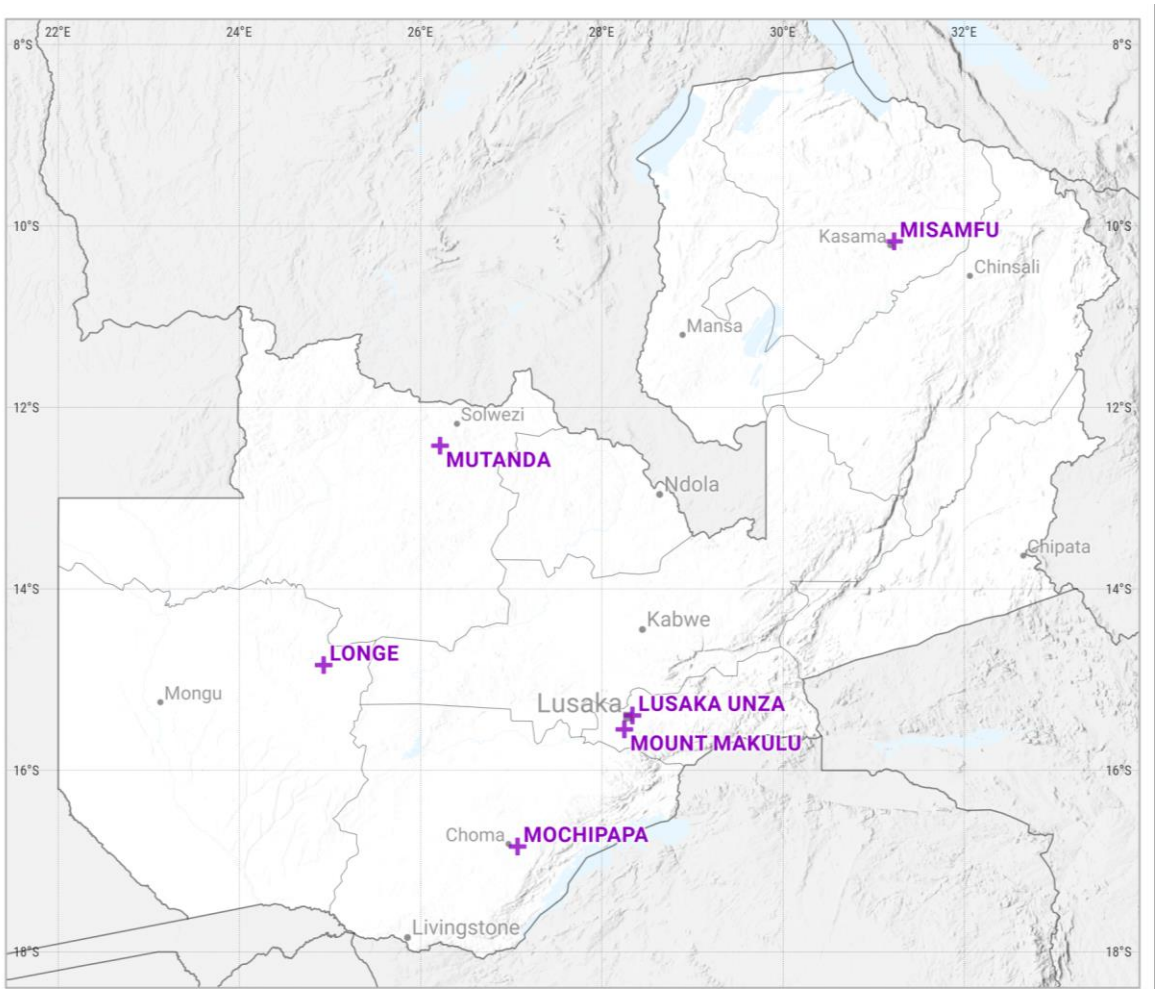

Map 2.1: Position of the solar meteorological stations used for the model validation

2.1.3 Solargis satellite-based model

Models using satellite and atmospheric data have become a standard for calculating solar resource time series and maps. The same models are also used for real-time data delivery for system monitoring and solar resource forecasting. Data from reliable operational solar models are routinely used by the solar industry.

In this study, we applied a model developed and operated by the company Solargis. This model operationally calculates high-resolution solar resource data and other meteorological parameters. Its geographical extent covers most of the land surface between 60° North and 45° South latitudes. A comprehensive overview of the Solargis model was made available in several publications [9, 10, 11]. The related uncertainty and requirements for bankability are discussed in [12, 13, 14].

In the Solargis approach, solar irradiance is calculated in 5 steps:

1. Calculation of clear-sky irradiance, assuming all atmospheric effects except clouds,
2. Calculation of cloud properties from satellite data,
3. Integration of clear-sky irradiance and cloud effects and calculation of global horizontal irradiance (GHI)
4. Calculation of direct normal irradiance (DNI) from GHI and clear-sky irradiance.
5. Calculation of global tilted irradiance (GTI) from GHI and DNI.

Models used in individual calculation steps are parameterized by a set of inputs characterizing the cloud properties, state of the atmosphere and terrain conditions.

The **clear-sky irradiance** is calculated by the simplified SOLIS model [15]. This model allows the fast calculation of clear-sky irradiance from the set of input parameters. Sun position is a deterministic parameter, and it is described by the algorithms with satisfactory accuracy. Stochastic variability of clear-sky atmospheric conditions is determined by changing concentrations of atmospheric constituents, namely aerosols, water vapour and ozone. Global atmospheric data, representing these constituents, are routinely calculated by world atmospheric data centres:

- In Solargis, the new generation **aerosol data set** representing Atmospheric Optical Depth (AOD) is used. The core data set, representing a period from 2003 to the present, is from the MACC-II/CAMS project (ECMWF) [16, 17]. An important feature of this data set is that it captures daily variability of aerosols and allows simulating more precisely the events with extreme atmospheric load of aerosol particles. Thus, it reduces uncertainty of instantaneous estimates of GHI and especially DNI, and it allows for improved statistical distribution of irradiance values [18, 19]. For years 1994 to 2002, data from the MERRA-2 model (NASA) [20] is used and it is homogenized with MACC-II/CAMS model are used. The Solargis calculation accuracy of the clear-sky irradiance is especially sensitive to information on aerosols.
- **Water vapour** is also highly variable in space and time, but it has lower impact on the values of solar radiation, compared to aerosols. The daily GFS and CFSR values (NOAA NCEP) are used in Solargis, thus representing the daily variability from 1994 to the present [21, 22, 23].
- **Ozone** absorbs solar radiation at wavelengths shorter than 0.3 μm, thus having negligible influence on the broadband solar radiation.

The **clouds** are the most influencing factor modulating clear-sky irradiance. The effect of clouds is calculated from satellite data in the form of the cloud index (cloud transmittance). The cloud index is derived by relating irradiance recorded by the satellite in several spectral channels and surface albedo to the cloud optical properties. In this study, a data from the Meteosat MFG and MSG satellites is used. Data is available for a period from 1994 to the present (24-hour delay) in a time step of 30 and 15 minutes. In Solargis, the modified calculation scheme by Cano has been adopted to retrieve cloud optical properties from the satellite data [25]. A number of improvements have been introduced to better cope with specific situations such as snow, ice, or high albedo areas (arid zones and deserts), and complex terrain.

To calculate **Global Horizontal Irradiance** (GHI) for all atmospheric and cloud conditions, the clear-sky global horizontal irradiance is coupled with the cloud index.

From GHI, other solar irradiance components (direct, diffuse and reflected) are calculated. **Direct Normal Irradiance** (DNI) is calculated by the modified Dirindex model [26]. Diffuse horizontal irradiance is derived from GHI and DNI according to the following equation:

$$DIF = GHI - DNI * Cos\ Z \quad (1)$$

Where Z is the zenith angle between the solar position and the Earth's surface.

Calculation of **Global Tilted Irradiance (GTI)** from GHI deals with direct and diffuse components separately. While calculation of the direct component is straightforward, estimation of diffuse irradiance for a tilted surface is more complex, and it is affected by limited information regarding shading effects and albedo of nearby objects. For converting diffuse horizontal irradiance for a tilted surface, the Perez diffuse transposition model is used [27]. The reflected component is also approximated considering that knowledge of local conditions is limited.

A model for the simulation of **terrain** effects (elevation and shading) based on high-resolution elevation and horizon data is used in the standard Solargis methodology [28]. The model by Ruiz Arias is used to achieve enhanced spatial representation – from the resolution of satellite (several km) to the resolution of the digital terrain model.

Solargis model version 2.1 has been used for computing the data. Table 2.3 summarize technical parameters of the model inputs and of the primary outputs.

Table 2.3: Input data for Solargis solar radiation model and related GHI and DNI outputs for Zambia

Inputs into the Solargis model	Source of input data	Time representation	Original time step	Approx. grid resolution
Cloud index	Meteosat MFG Meteosat MSG satellites (EUMETSAT)	1994 to 2004 2005 to date	30 minutes 15 minutes	2.8 x 3.3 km 3.3 x 4.0 km
Atmospheric optical depth (aerosols)*	MACC/CAMS (ECMWF) MERRA-2 (NASA)	2003 to date 1994 to 2002	3 hours 1 hour	75 km and 125 km 50 km
Water vapour	CFSR/GFS (NOAA)	1994 to date	1 hour	35 and 55 km
Elevation and horizon	SRTM-3 (SRTM)	-	-	250 m
Solargis primary data outputs (GHI and DNI)	**-**	**1994 to date**	**15 minutes**	**250 m**

2.1.4 Measured vs. satellite data – adaptation of solar model

For a qualified solar resource assessment, it is important to understand the characteristics of ground measurements and satellite-modelled data (Table 2.4). The ground measurements and satellite data complement each other, and it is beneficial to correlate them and adapt the satellite model for the specific site or region.

Within this project, regional model adaptation has been performed using the data from six measuring stations (Table 2.1, Map 2.1). In addition, the data from the three stations in Malawi were used to improve model performance in the broader context. The model adapted for regional conditions provides long history solar resource time series as well as recent data with lower uncertainty.

The model adaptation procedure has two steps:

1. Identification of systematic differences between hourly satellite data and local measurements for the period when both data sets overlap;

2. Development of a correction method that is applied for the whole period represented by the satellite time series over the whole region.

In the case of regional adaptation, the method aims to identify and reduce regional systematic deviations of a model compared to the measured data, typically driven by the insufficient characterization of aerosols or specific cloud patterns. The result of regional adaptation is an improved solar resource database in the regional context with overall reduction of systematic errors.

The regional-adaptation of satellite-based model data was performed for the whole territory of Zambia and the methodology and results are described in the report *"Solar Model Validation Report; Regional adaptation of Solargis model based on data acquired in 24-months solar measurement campaign; Republic of Zambia"*, Ref. Nr. 128-08/2019 [29].

The regional-adaptation improves knowledge about uncertainty of the model in specific conditions of Zambia, and more generally in tropical regions, where the Solargis model shows higher uncertainty. The new knowledge developed from the analysis of ground measurements collected during the project creates an important base for further model developments and improvements.

Table 2.4: Comparing solar data from solar measuring stations and from satellite models

	Data from solar measuring stations	Data from satellite-based models (Solargis)
Availability/ accessibility	Available only for limited number of sites. Mostly, data covers only recent years.	Data are available for any location within latitudes 60° N and 45° S. Data covers long period, in Zambia, historical data for more than 25 years.
Original spatial resolution	Data represent the microclimate of a site.	Satellite models represent area with complex spatial resolution: clouds are mapped at approx. 3 km, aerosols at 50-125 km and water vapour at 34 km. Terrain can be modelled at spatial resolution of up to 250 m. Methods for enhancement of spatial resolution are often used.
Original time resolution	Seconds to minutes	15 and 30 minutes in Africa
Quality	Data need to go through rigorous quality control, gap filling and cross-comparison.	Quality control of the input data is necessary. Outputs are regularly validated. Under normal operation, the data have only minimum occurrence of gaps, which are filled by intelligent algorithms.
Stability	Instruments need regular cleaning and control. Instruments, measuring practices, maintenance and calibration may change over time. Thus, regular calibration is needed. Long-term stability is typically a challenge.	If data are geometrically and radiometrically pre-processed, a complete history of data can be calculated with one single set of algorithms. Data computed by an operational satellite model may change slightly over time, as the model and its input data evolve. Thus, regular reanalysis and temporal harmonization of inputs is used in state-of-the-art models.
Uncertainty	Uncertainty is related to the accuracy of the instruments, maintenance and operation of the equipment, measurement practices, and quality control.	Uncertainty is given by the characteristics of the model, resolution and accuracy of the input data. Uncertainty of models is higher than high quality local measurements. The data may not exactly represent the local microclimate, but are usually stable and may show systematic deviation, which can be reduced by good quality local measurements (regional adaptation or site adaptation of the model).

2.1.5 Validation and regional adaptation of Solargis model

Regional model adaptation has been performed in order to reduce overall model uncertainty in the region. Tables 2.5 and 2.6 show the Solargis model quality indicators for solar primary parameters, DNI and GHI, after the regional model adaptation. The uncertainty is evaluated for the version that has been regionally adapted.

All information shown in this report is derived from the regionally adapted Solargis model.

Comparison of the validation statistics, computed for the solar meteorological sites in Zambia, shows overall stability of the Solargis model and of the underlying input data. Locally, an increased bias exceeding expectations was identified (Mutanda station), which reflects the limited accuracy of the model and its input data, as well as the properties of ground measurements. The statistics show that the model uncertainty has been reduced after the regional adaptation. The results of the regional model adaptation are comparable to those achieved in other regions [30, 31].

Table 2.5: Direct Normal Irradiance: bias before and after regional model adaptation

Meteo station	Original DNI data		DNI after regional adaptation	
	Bias	Bias	Bias	Bias
	[kWh/m^2]	[%]	[kWh/m^2]	[%]
Lusaka UNZA	44	10.5	8	2.0
Mount Makulu	42	9.9	3	0.7
Mochipapa	41	9.0	2	0.4
Longe	32	6.9	3	0.6
Misamfu	44	10.1	-1	-0.2
Mutanda	43	10.5	5	1.2
Mean	41	9.5	3	0.8
Standard deviation	5	1.4	3	0.7

Table 2.6: Global Horizontal Irradiance: bias before and after regional model adaptation

Meteo station	Original GHI data		GHI after regional adaptation	
	Bias	Bias	Bias	Bias
	[kWh/m^2]	[%]	[kWh/m^2]	[%]
Lusaka UNZA	32	6.8	6	1.2
Mount Makulu	30	6.4	1	0.2
Mochipapa	26	5.4	-1	-0.2
Longe	33	6.6	4	0.8
Misamfu	32	6.4	-3	-0.5
Mutanda	46	9.5	10	2.0
Mean	33	6.9	3	0.6
Standard deviation	7	1.4	5	0.9

2.1.6 Uncertainty of solar resource estimates

The **uncertainty of regionally adapted satellite-based DNI and GHI** is determined by uncertainty of the model, ground measurements, and the model adaptation method. More specifically it depends on [15]:

1. Parameterization and adaptation of **numerical models integrated in Solargis** for the given data inputs and their ability to generate accurate results for various geographical and time-variable conditions:
   - Data inputs into Solargis model: accuracy of Meteosat satellite data, MACC-II/CAMS and MERRA-2 aerosols and CFSR/GFS water vapour
   - Solis clear-sky model and its capability to properly characterize various states of the atmosphere
   - Simulation accuracy of the Solargis cloud transmittance algorithms, being able to properly distinguish different states of various surface types, albedo, clouds and fog
   - Diffuse and direct decomposition by Perez model
   - Transposition from global horizontal to in-plane irradiance (for GTI) by Perez model
   - Terrain shading and disaggregation by Ruiz-Arias model
2. Uncertainty of the **ground-measurements**, which is determined by:
   - Accuracy of the instruments
   - Maintenance practices, including sensor cleaning, service and calibration
   - Data post-processing and quality control procedures.
3. Uncertainty of the **model adaptation** at regional scale and residual uncertainty after adaptation

The uncertainty from the interannual variability of solar resource is not considered in this study.

Accuracy statistics, such as bias (Chapter 2.1.5) characterize the accuracy of the Solargis model in the given validation points, relative to the ground measurements. The validation statistics are affected by local geography and by the quality and reliability of ground-measured data. Therefore, the validation statistics only indicate performance of the model in this region.

The majority of Zambia territory has uncertainty of the regionally-adapted model yearly values in the range of ±4% to ±5% for GHI and ±5% to ±7% for DNI. We expect higher uncertainty in regions with more complex geography, which is partly a result of uncertainty of ground measurements, limited number of solar meteorological stations and higher model uncertainty in regions with specific micro-climatic conditions (e.g. occurrence of convective clouds close to steep mountain slopes).

Table 2.7: Uncertainty of the model estimate for original and regionally-adapted annual GHI, DNI and GTI and how does it compare to the best-achievable uncertainty case.

	Direct Normal Irradiation		Global Horizontal Irradiation		Global Tilted Irradiation	
	Low	Medium	Low	Medium	Low	Medium
Original data	< ±9.0%	< ±13%	< ±6.5%	< ±8.0%	< ±7.0%	< ±9.0%
After adaptation	±5% to ±7%	< ±10%	±4% to ±5%	< ±6%	±4.5% to ±5.5%	< ±7%
Best-achievable	±3.5%	-	±2.5%	-	±3.0%	

The lowest (best achievable) uncertainty in Table 2.7 can only be achieved by the model site-adaptation so that it would represent only the very local microclimate of the site recorded in the ground measurements. In the case of the regional adaptation, used in this study, the uncertainty is usually higher because it describes data uncertainty in the regional context.

Moreover, a residual discrepancy between ground measurements, and the model data can be found after regional adaptation (Tables 2.5 and 2.6). This model adaptation approach is designed to correct only regional discrepancy patterns, not to resolve site-specific issues.

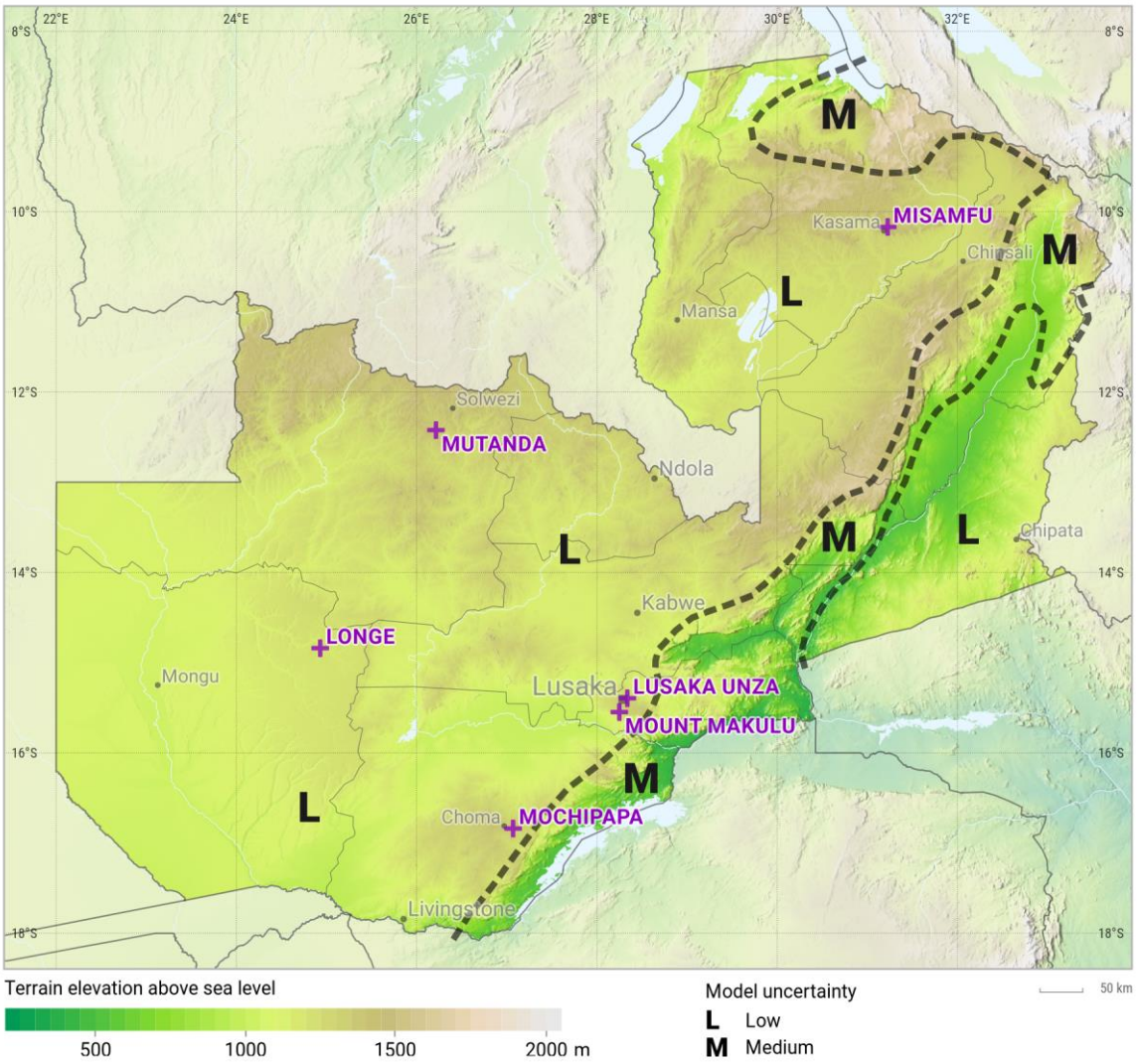

Map 2.2: Geographic distribution of the regionally adapted model uncertainty in Zambia
L: low; M: medium

2.2 Meteorological data

2.2.1 Measured vs. modelled data

Meteorological parameters are an important part of a solar energy project assessment as they determine the operating conditions and the effectiveness of solar power plant operations. The most important meteorological parameter for the operation of photovoltaic power plants is air temperature, which directly impacts power production (energy yield is decreasing when temperature is increasing). Meteorological data can be collected by two approaches: (1) by measuring at meteorological sites and (2) computing by meteorological models.

The requirements for the meteorological data for solar energy projects are:

- Long and continuous record of data, preferably covering the same time period as satellite-based solar resource data,
- Data should reliably represent the local climate,
- Data should be accurate, quality-controlled and without gaps.

Table 2.8: Comparing data from meteorological stations and weather models

	Meteorological station data	Data from meteorological models
Availability/ accessibility	Available only for selected sites. Data may cover different periods of time	Data are available for any location. Data cover long continuous and equal period of time (decades)
Original spatial resolution	Local measurement representing microclimate with all local weather occurrences	Regional simulation, representing regional weather patterns with relatively coarse grid resolution. Therefore, local values can be smoothed, especially extreme values.
Original time resolution	From 1 minute to 1 hour	1 hour
Quality	Data has to go through rigorous quality control, gap filling and cross-comparison.	No need of special quality control. No gaps, relatively stable outputs if data processing systematically controlled.
Stability	Sensors, measuring practices, maintenance and calibration may change over time. Thus, achieving long-term stability needs systematic attention.	In case of reanalysis, long history of data is calculated with one single stable model. Data for operational models may slightly change over time, as model development evolves
Uncertainty	Uncertainty is related to the quality and maintenance of sensors and measurement practices, usually sufficient for solar energy applications.	Uncertainty is given by the resolution and accuracy of the model. Uncertainty of meteorological models is higher than uncertainty of high quality measurements. The model data may not exactly represent the local microclimate; accuracy can be enhanced by correlating them with the ground measurements.

Several models are available: a good option is to use Modern-Era Retrospective analysis for Research and Applications (MERRA-2) model (source NASA, USA) [23] and the Climate Forecast System Version 2 (CFSv2) model (source NOAA, NCEP, USA), which cover a long period of time with continuous data [24]. The results of these models are implemented in Solargis.

The role of meteorological ground measurements in solar energy development has two aspects:

- Measurements are used for the validation and accuracy enhancement of historical data derived from the solar and meteorological models
- The high frequency measurements (typically one-minute data) are used for improved understanding of the microclimate of the site, especially for capturing the extremes.

Data from the two sources described above have their advantages and disadvantages (Table 2.8). Air temperature derived from the meteorological models has lower spatial and temporal resolution compared to ground measurements, and lower accuracy. Thus, the modelled parameters characterize regional climate patterns rather than the local microclimate. Extreme values, in particular, may not be well represented.

2.2.2 Method and validation

In this project, the air temperature data is delivered. It is derived from the meteorological models: MERRA-2 and CFSv2 (Table 2.9). As explained in Chapter 2.2.1, the numerical weather models have lower spatial and temporal resolution compared to the solar resource data. The original spatial resolution of the models is enhanced to 1 km for air temperature by spatial disaggregation and the use of the Digital Elevation Model SRTM-3.

Table 2.9: Original source of Solargis air temperature at 2 m for Zambia: MERRA-2 and CFSv2.

	Modern-Era Retrospective analysis for Research and Applications (MERRA-2)	Climate Forecast System (CFSv2)
Time period	1994 to 2010	2011 to the present time
Original spatial resolution	45 x 50 km	19 x 22 km
Original time resolution	1 hour	1 hour

For the purpose of validating the meteorological models in Zambia, we have used the data collected at six meteorological stations (Table 2.1, Map. 2.1). The summary of basic statistical parameters is presented in Table 2.10.

The main issue identified is the underestimation or overestimation of night-time temperature by the model depending on the station and the month, yet the day-time temperature is represented with higher accuracy. More details about the validation of meteorological parameters can be seen in the report *"Annual Solar Resource Report for solar meteorological stations after completion of 24 months of measurements, Republic of Zambia, Report number: 128-07/2018"* [8].

Table 2.10: Air temperature at 2 m: accuracy indicators of the model outputs [°C].

Meteorological station	Validation period	Bias mean	RMSD hourly	RMSD daily	RMSD monthly
Lusaka UNZA	11/2015 – 12/2017	-1.6	2.5	1.8	1.6
Mount Makulu	11/2015 – 12/2017	-1.7	2.7	2.0	1.8
Mochipapa	11/2015 – 12/2017	-1.1	2.2	1.5	1.2
Longe	11/2015 – 12/2017	0.2	2.5	1.4	0.9
Misamfu	11/2015 – 12/2017	-1.7	2.7	2.0	1.8
Mutanda	11/2015 – 12/2017	0.8	3.4	2.2	1.9

2.2.3 Uncertainty of air temperature

In general, the data from the meteorological models represent larger area, and it is not capable to represent accurately the microclimate. The main issue identified is underestimation or overestimation of night-time temperature by the model, yet the day-time temperature is represented with higher accuracy than nigh-time.

The uncertainty of the model estimate for air temperature is summarised in Table 2.11.

Table 2.11: Expected uncertainty of air temperature in Zambia.

	Unit	Annual	Monthly	Hourly
Air temperature at 2 m	°C	±2.0	±2.0	±3.5

2.3 Simulation of solar photovoltaic potential

Solar radiation is the most important parameter for PV power simulation, as it is fuel for solar power plants. The intensity of global irradiance received by the tilted surface of PV modules (GTI) is calculated from two primary parameters stored in the Solargis database and delivered in this project:

- Global Horizontal Irradiance (GHI)
- Direct Normal Irradiance (DNI)

There are two main types of solar energy technologies: photovoltaic (PV) and concentrating solar power (CSP). Photovoltaics have high potential in Zambia, and this technology is discussed in this Chapter. CSP technology is not expected to be implemented in Zambia.

Photovoltaic technology exploits global horizontal or tilted irradiation, which is the sum of direct and diffuse components (see Equation (1) in Chapter 2.1.3). To simulate power production from a PV system, global irradiance received by a flat surface of PV modules must be calculated. Due to clouds, PV power generation reacts to changes in solar radiation in a matter of seconds or minutes (depending on the size of a module field), thus intermittency (short-term variability) of the PV power production is to be considered. Similarly, the effect of seasonal variability is to be considered as well.

For possible PV installations, several technical options are available. They are briefly described below.

Two types of mounting of PV modules can be considered:

- PV modules mounted on the ground in a fixed position or on sun-trackers
- PV modules mounted on rooftops or façades of buildings
- Three types of PV systems can be considered for Zambia:
- Grid-connected PV power plants
- Mini-grid PV systems
- Off-grid PV systems

The majority of larger PV power plants are built in an **open space** and often these have **PV modules mounted at a fixed position**. Fixed mounting structures offer a simple and efficient choice for implementing PV power plants. A well-designed structure is robust and ensures long-life performance, even during harsh weather conditions, at low maintenance costs. **Sun-tracking systems** are another alternative for the design of a PV module field. Solar trackers adjust the orientation of the PV modules during the day towards the sun, so the PV modules collect more solar radiation.

Roof or façade mounted PV systems are typically small to medium size, i.e. ranging from hundreds of watts to hundreds of kilowatts. Modules can be mounted on rooftops, façades or can be directly integrated as part of a building structure. PV modules in this type of system are often installed in a suboptimal position (deviating from the optimum angle), and this results in a lower performance efficiency. Some reduction of PV power output can be expected due to nearby shading structures. Trees, masts, neighbouring buildings, roof structures or self-shading of PV modules determine the reduced PV system performance.

Mini-grid PV systems include power generation facility and distribution grids connecting the local consumers. The typical size of installed PV systems is in the range of 10s to 100s of kWp. Mini-grids may be adapted to meet the requirements of local needs, they can be combined with diesel generators and battery storage. This option appears to be most economic for supply of electricity for small rural communities.

Off-grid PV systems are small systems that are not connected into a distribution grid. They are usually equipped with energy storage (classic lead acid or modern-type batteries, such as Li-on) and/or connected to diesel generators. Batteries are maintained through charge controllers for protection against overcharging or deep discharge. Depending on size and functionality of the off-grid PV system, it can work with AC (together with inverter) or DC voltage source.

In this study, the PV power potential is studied for **a system with fixed-mounted monofacial PV modules**, considered here as the mainstream technology. Installed capacity of a PV power plant is usually determined by the available space and options to maintain the stability of the local grid.

2.3.1 Principles of PV electricity simulation

Results of PV electricity simulation, presented in Chapter 3.6, are based on software developed by Solargis. This Chapter summarizes key elements of the simulation chain.

Table 2.12: Specification of Solargis database used in the PV calculation in this study

Data inputs for PV simulation	**Global tilted irradiation (GTI) derived from GHI and DNI** **Air temperature at 2 m (TEMP)**
Spatial grid resolution (approximate)	250 m (9 arc-sec)
Time resolution	15-minute
Geographical extent (this study)	Republic of Zambia
Period covered by data (this study)	01/1994 to 12/2017

The PV software implemented by Solargis has scientifically proven methods [32 to 37] and uses full historical time series of solar radiation and air temperature data on the input (Table 2.12). Data and model quality are checked using field tests and ground measurements.

In PV energy simulation procedure, there are several energy losses that occur in the individual steps of energy conversion (Figure 2.2):

1. **Losses due to terrain shading** caused by far horizon**.** On the other hand, shading of local features such as nearby building, structures or vegetation is not considered in the calculation,
2. Energy conversion in PV modules is reduced by **losses due to angular reflectivity**, which depends on the relative position of the sun and plane of the module and **temperature losses,** caused by the performance of PV modules working outside of STC conditions defined in datasheets,

3. DC output of PV array is further reduced by **losses due to dirt or soiling** depending mainly on the environmental factors and module cleaning**, losses by inter-row shading** caused by preceding rows of modules, **mismatch** and **DC cabling losses**, which are caused by slight differences between the nominal power of each module and small losses on cable connections,
4. DC to AC energy conversion is performed by an inverter. The efficiency of this conversion step is reduced by **inverter losses**, given by the inverter efficiency function. Further factors reducing AC energy output are **losses in AC cabling** and **transformer losses** (applies only to large-scale open space systems),
5. **Availability.** This empirical parameter quantifies electricity losses incurred by the shutdown of a PV power plant due to maintenance or failures, including issues in the power grid. Availability of well operated PV systems is approximately 99%.

According to experience in many countries, the crystalline silicon PV modules show a relatively low performance reduction over time. The rate of the performance degradation is higher at the beginning of exposure, and then stabilizes at a lower level. Initial degradation may be close to the value of 0.8% for the first year and 0.5% or less for subsequent years [37]. The performance ageing of PV modules is not considered in this study. The calculation results of PV power potential for Zambia are shown in Chapter 3.6.

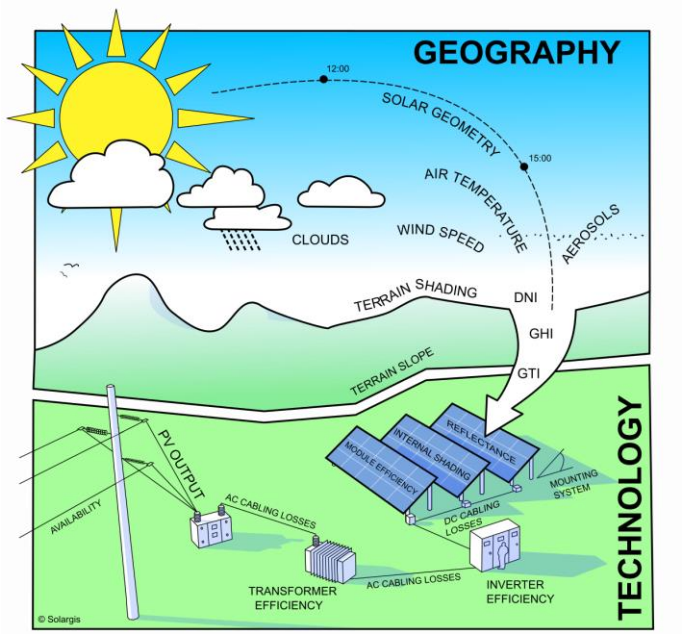

Figure 2.2: Simplified Solargis PV simulation chain

2.3.2 Technical configuration of a reference PV system

Theoretical photovoltaic power production in Zambia has been calculated using numerical models developed and implemented in-house by Solargis. As introduced in Chapter 2.1, 15-minute **time series of solar radiation and air temperature**, representing last 24 years, are used as an input to the simulation. The models are developed based on the advanced algorithms, expert knowledge and recommendations given in [38] and tested using monitoring results from existing PV power plants. Table 2.14 summarizes losses and related uncertainty throughout the PV computing chain.

PV electricity potential is calculated based on a set of assumptions shown in Tables 2.13 and 2.14. These assumptions are approximate values, and they will differ in the site-specific projects. As can be seen, the uncertainty of the solar resource is the key element of energy simulation.

Table 2.13: Reference configuration - photovoltaic power plant with fixed-mounted PV modules

Feature	Description
Nominal capacity	Configuration represents a typical PV power plant of 1 MWp or higher. All calculations are scaled to 1 kWp, so that they can be easily multiplied for any installed capacity.
Modules	Crystalline silicon modules with positive power tolerance. Nominal Operating Cell Temperature (NOCT) 46°C and temperature coefficient of the Pmax -0.438 %/K
Inverters	Central inverter with declared datasheet efficiency (Euro efficiency) 97.5%
Mounting of PV modules	Fixed mounting structures facing North with optimum tilt (the range from 13° to 23°). Relative row spacing 2.5 (ratio of absolute spacing and table width)
Transformer	Medium voltage power transformer

Table 2.14: Yearly energy losses and related uncertainty in PV power simulation

	Simulation step	Losses	Uncertainty	Notes
		[%]	[± %]	
1	Global Tilted Irradiation (model estimate with terrain shading)	N/A	**5.0**	Annual Global Irradiation falling on the surface of PV modules
2	Module surface angular reflectivity (numerical model)	-2.4 to -3.0	1.0	Slightly polluted surface is assumed in the calculation of the module surface reflectivity
	Conversion in modules relative to STC (numerical model)	-9.2 to -13.5	3.5	Depends on the temperature and irradiance. NOCT of 46°C is considered
3	Polluted surface of modules (empirical estimate)	-4.0	1.5	Losses due to dirt, dust, soiling, and bird droppings
	Power tolerance (value from the data sheet)	0.0	0.0	Value given in the module technical data sheet (modules with positive power tolerance)
	Module inter-row shading (model estimate)	-0.1 to -0.5	0.5	Partial shading of strings by modules from adjacent rows
	Mismatch between modules (empirical estimate)	-0.5	0.5	Well-sorted modules and lower mismatch are considered.
	DC cable losses (empirical estimate)	-2.0	1.5	This value can be calculated from the electrical design
4	Conversion in the inverter (value from the technical data sheet)	-2.5	0.5	Given by the Euro efficiency of the inverter, which is considered at 97.5%
	AC cable losses (empirical estimate)	-0.5	0.5	Standard AC connection is assumed
	Transformer losses (empirical estimate)	-1.0	0.5	Standard transformer is assumed
5	Availability	0.0	1.5	100% technical availability is considered; the uncertainty considered here assumes a well-integrated system; the real value strongly depends on the efficiency of PV integration into the existing grid.
	Range of cumulative losses and indicative uncertainty	-20.4 to -24.9	6.8	These values are indicative and do not consider the project specific features and performance degradation of a PV system over its lifetime

Map 3.16 shows theoretical potential power production of a PV system installed with a typical technology configuration for open space PV power plants. The technical parameters are described in Table 2.13.

In this study, the reference configuration for the PV potential calculation is a PV system with crystalline-silicon (c-Si) modules mounted in a fixed position on a table facing North and inclined at an angle close to optimum, i.e. at the angle at which the yearly sum of global tilted irradiation received by PV modules is maximized (a range between 13° and 23° depending on latitude and geographical features). The fixed-mounting of PV modules is very common and provides a robust solution with minimal maintenance effort. Geographic differences in potential PV production are shown for six selected sites (Chapter 3.6).

The results presented in Chapter 3.6 do not consider the performance degradation of PV modules due to aging; they also lack the required level of detail. Thus, these results cannot be used for financial assumptions of any specific project. Detailed assessment of energy yield for a specific power plant is within the scope of a site-specific bankable expert study.

2.4 Outline of solar concentrating technologies

Concentrating technologies can only utilize DNI (as diffuse irradiance cannot be concentrated). Instant (short-term) variability of DNI is very high and this is especially relevant for Concentrating PV (CPV) systems. On the contrary, solar thermal power plants, often denoted as Concentrating Solar Power (CSP) technology, have several methods to control short term, as well as daily, variability. This is given by the inertia of the whole system (solar field, heat transfer and storage), which can additionally be supported by storage or fossil fuels.

DNI solar resource availability in Zambia does not give prospects for installation of solar concentrating technologies. This chapter presents only overview information.

2.4.1 Concentrating Solar Power (CSP)

A distinctive characteristic of Concentrated Solar Power technology (CSP) is that, when deployed with thermal energy storage, it can produce electricity on demand, providing a dispatchable source of renewable energy. Therefore, it can provide electricity whenever needed to meet demand, performing like a traditional base-load power plant. There are several groups of solar thermal power plants:

- **Parabolic troughs**: solar fields using trough systems capture solar energy using large mirrors that track the sun's movement throughout the day. The curved shape reflects most of that heat onto a receiver pipe that is filled with a heat transfer fluid. The thermal energy from the heated fluid generates steam, which in turn generates electricity in a conventional steam turbine. Heated fluid in the trough systems can also provide heat to thermal storage systems, which can be used to generate electricity at times when the sun is not shining;
- **Power towers**: they use flat mirrors (heliostats) to reflect sunlight onto a solar receiver at the top of a central tower. Water is pumped up the tower to the receiver, where concentrated thermal energy heats it up. The hot steam then powers a conventional steam turbine. Some power towers use molten salt in place of water and steam. That hot molten salt can be used immediately to generate steam and electricity, or it can be stored and used at a later time.
- **Fresnel reflectors**: they are made of many thin, flat mirror strips to concentrate sunlight onto tubes through which working fluid is pumped. The rest of the energy cycle works similarly as in the above-mentioned systems.

- **Stirling dish**: consists of a stand-alone parabolic reflector that concentrates light onto a receiver positioned at the reflector's focal point. The reflector tracks the Sun along two axes. The working fluid in the receiver is heated and then used by a Stirling engine to generate power.

One of the advantages of technology is thermal storage, often in the form of molten salt. CSP can also be integrated with fossil-based generation sources in a hybrid configuration.

2.4.2 Concentrating photovoltaics (CPV)

A different conversion method of DNI into electricity is Concentrated Photovoltaic (CPV). This technology is based on the use of lenses or curved mirrors to concentrate sunlight onto a small area of high-efficiency PV cells. High concentration CPV requires very precise solar trackers. The advantage of CPV over flat plate PV is a potential for cost reduction due to the smaller area of photovoltaic material required. The necessity of sun tracking partially balances out the smaller price of the semiconductor material used. CPV technology also requires more maintenance during the lifetime of the power plant. Power production from CPV may be more sensitive to changing weather conditions. The advantage of CPV over CSP is full scalability, similar to flat plate PV modules.

3 Solar resource and PV potential of Zambia

3.1 Geography

This report analyses solar and meteorological data for Zambia, which determine solar power production and influence its performance efficiency. We also analyse other geographical factors that influence the development and operation of solar power plants.

Zambia is located in southern Africa, approximately between latitudes 8° and 19° South and longitudes 22° and 34° East. We demonstrate the variability of the solar resource and photovoltaic power potential in two forms:

- At the **country level** in the form of maps
- Graphs and tables for **six selected sites** that, to a large extent, represent the variability of the climate and solar power (ESMAP solar meteorological stations).

The position of these sites is summarised in Table 2.1 and Map 2.1. The data in the tables and graphs shown in Chapter 3 relate to these six sites.

Geographic information and maps bring additional value to the solar data. Geographical characteristics of the country from a regional to local scale may represent technical and environmental prerequisites, as well as constraints, for solar energy development.

In this report, we collected the following data that has some relevance to solar energy:

- Map of the administrative division and important cities/towns informs about the country spatial organization and population distribution (Map 3.1)
- Terrain, where elevation and slope inclination may pose physical limitations for solar development (Maps 3.2 and 3.3)
- Rainfall (precipitation) has impact on efficiency (performance ratio) and operation (modules cleaning effect) of the PV installations (Map 3.4)
- Land cover defines primary areas used for human economic activities and settlements and possible land availability for solar PV installations (Map 3.5)
- Transport network (roads and railways), defining accessibility of sites for location of PV power plants (Map 3.6)
- Population density is a good indicator of electricity consumption (Map 3.7).

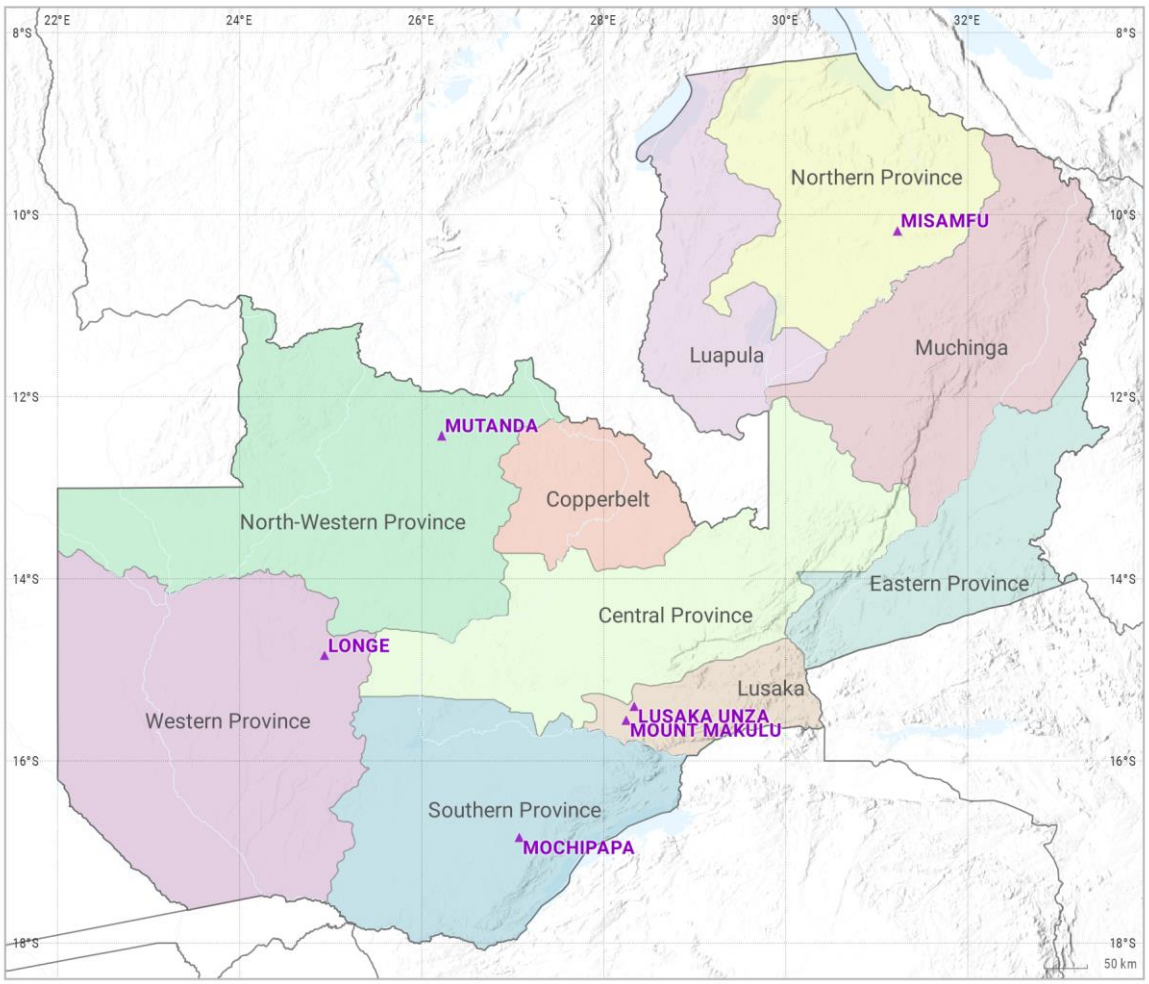

Map 3.1: Administrative division, towns and cities in Zambia.
Source: Administrative boundaries by Cartography Unit, GSDPM (World Bank Group), GeoNames, adapted by Solargis
For reference, position of six solar meteo sites is shown.

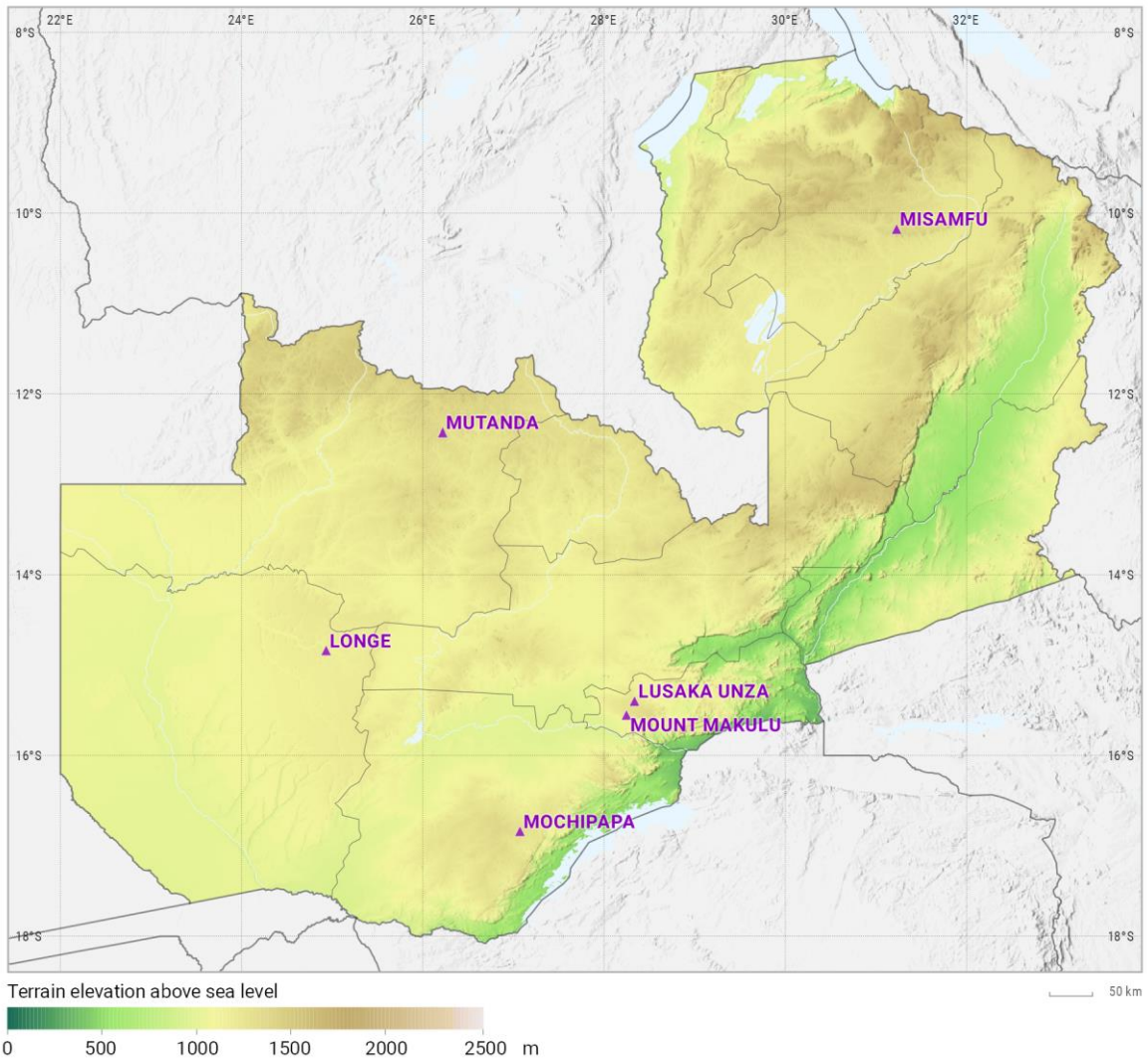

Map 3.2: Terrain elevation above sea level.
Source: SRTM v4.1.
For reference, position of six solar meteo sites is shown.

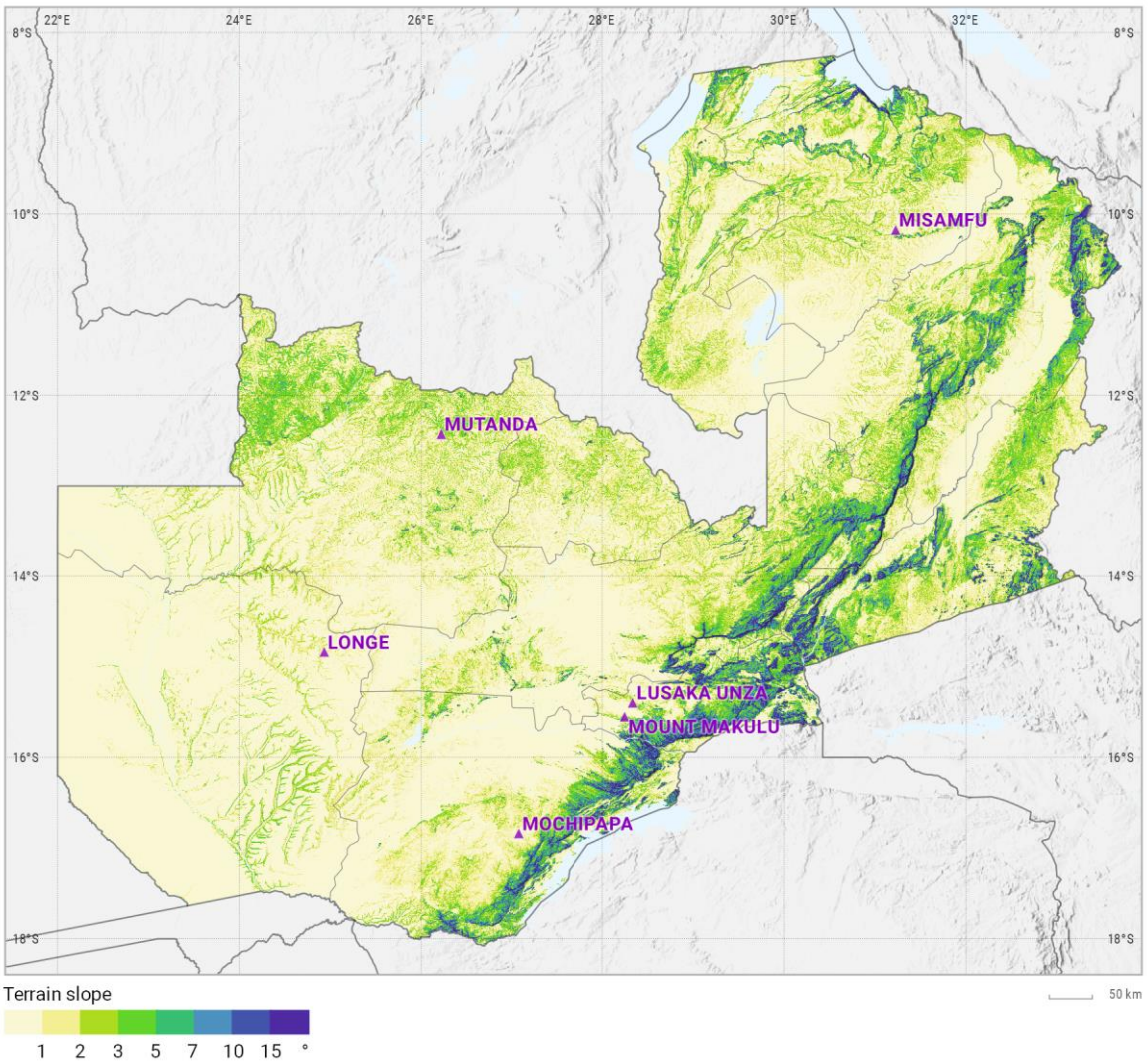

Map 3.3: Terrain slope.
Based on: SRTM v4.1 data, calculated by Solargis.
For reference, position of six solar meteo sites is shown.

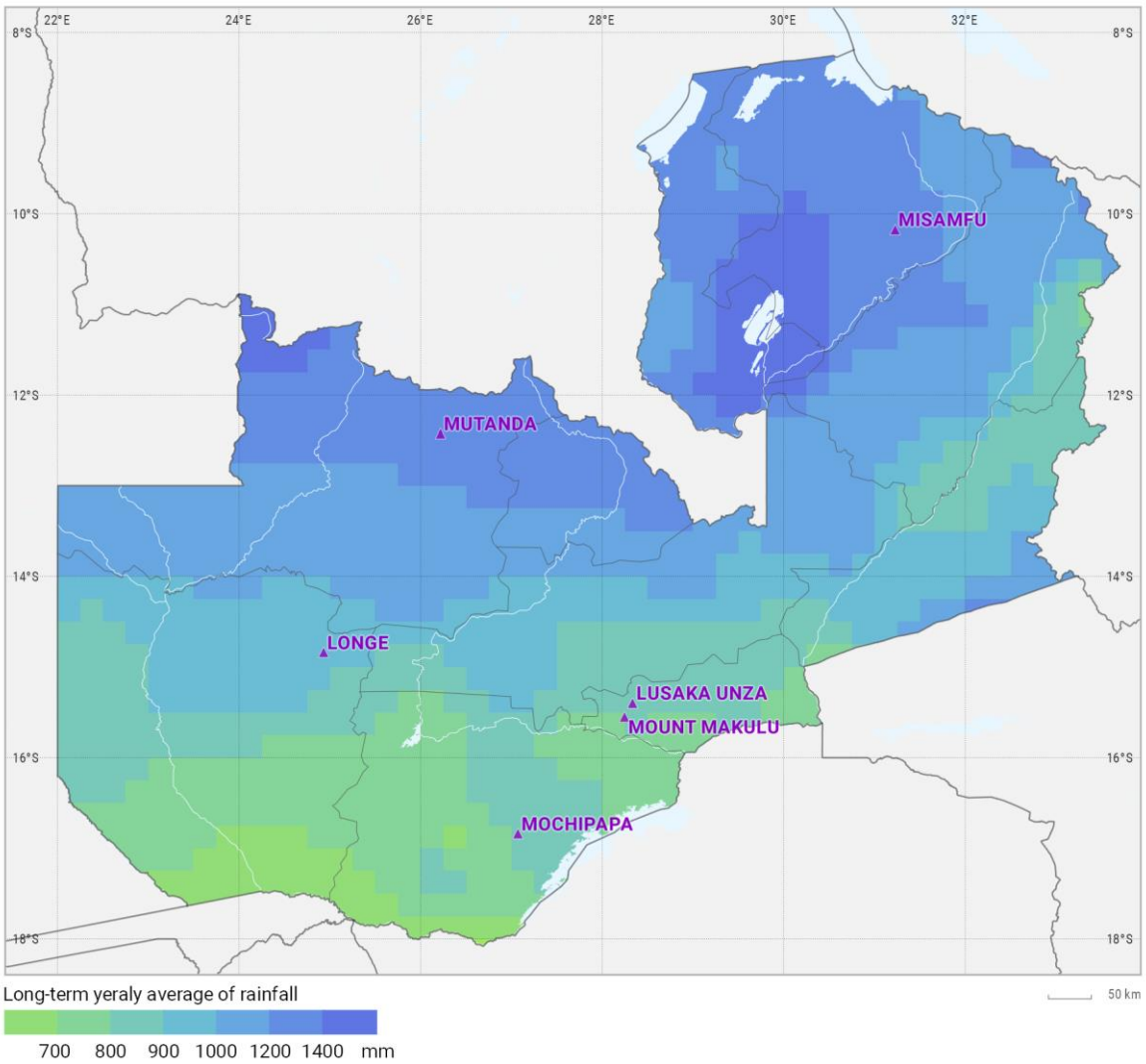

Map 3.4: Long-term yearly average of rainfall (sum of precipitation).
Source: Global Precipitation Climatology Centre (DWD)
For reference, position of six solar meteo sites is shown.

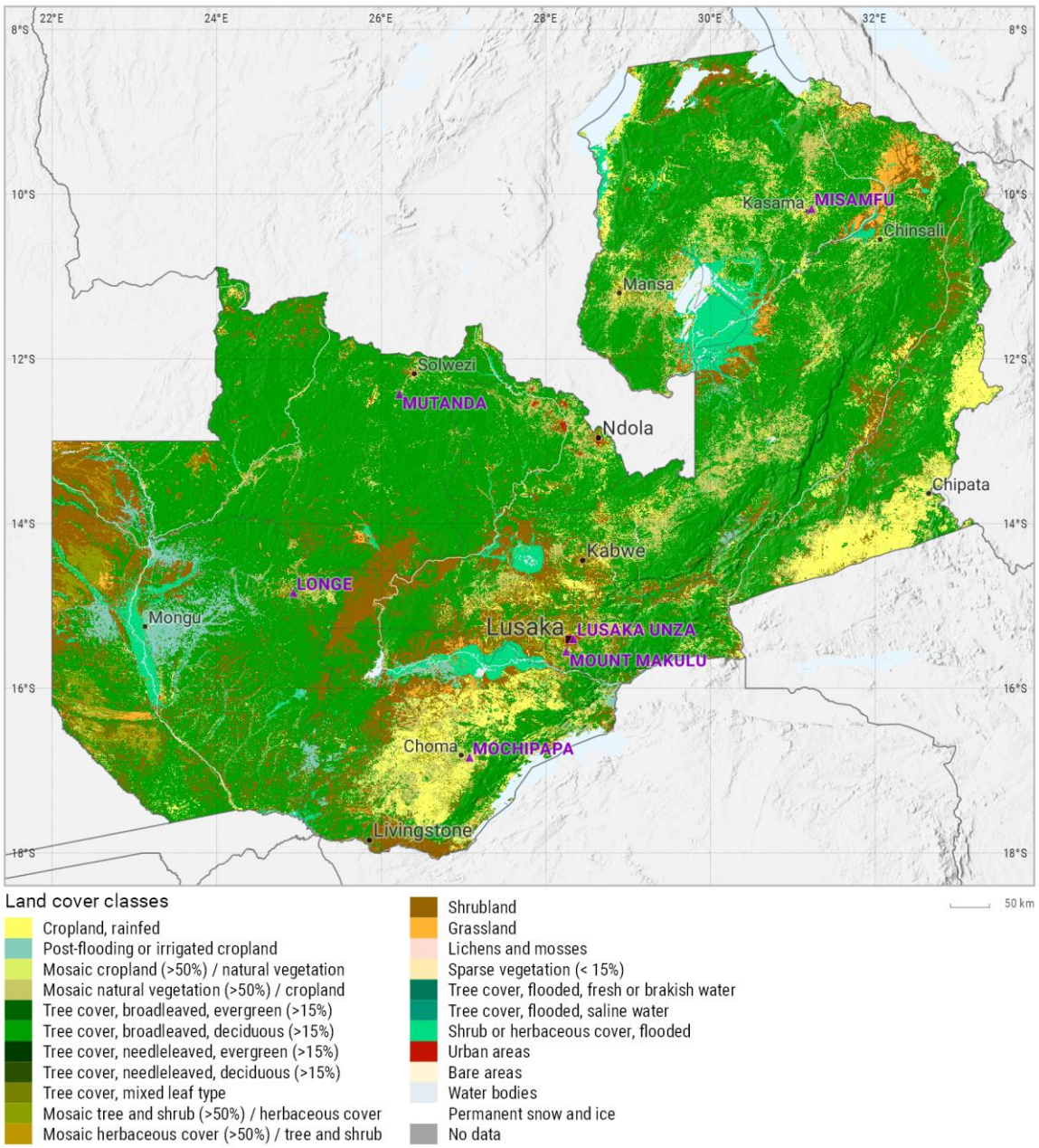

Map 3.5: Land cover.
Source: ESA Climate Change Initiative - Land Cover led by UCLouvain (2017)
For reference, position of six solar meteo sites is shown.

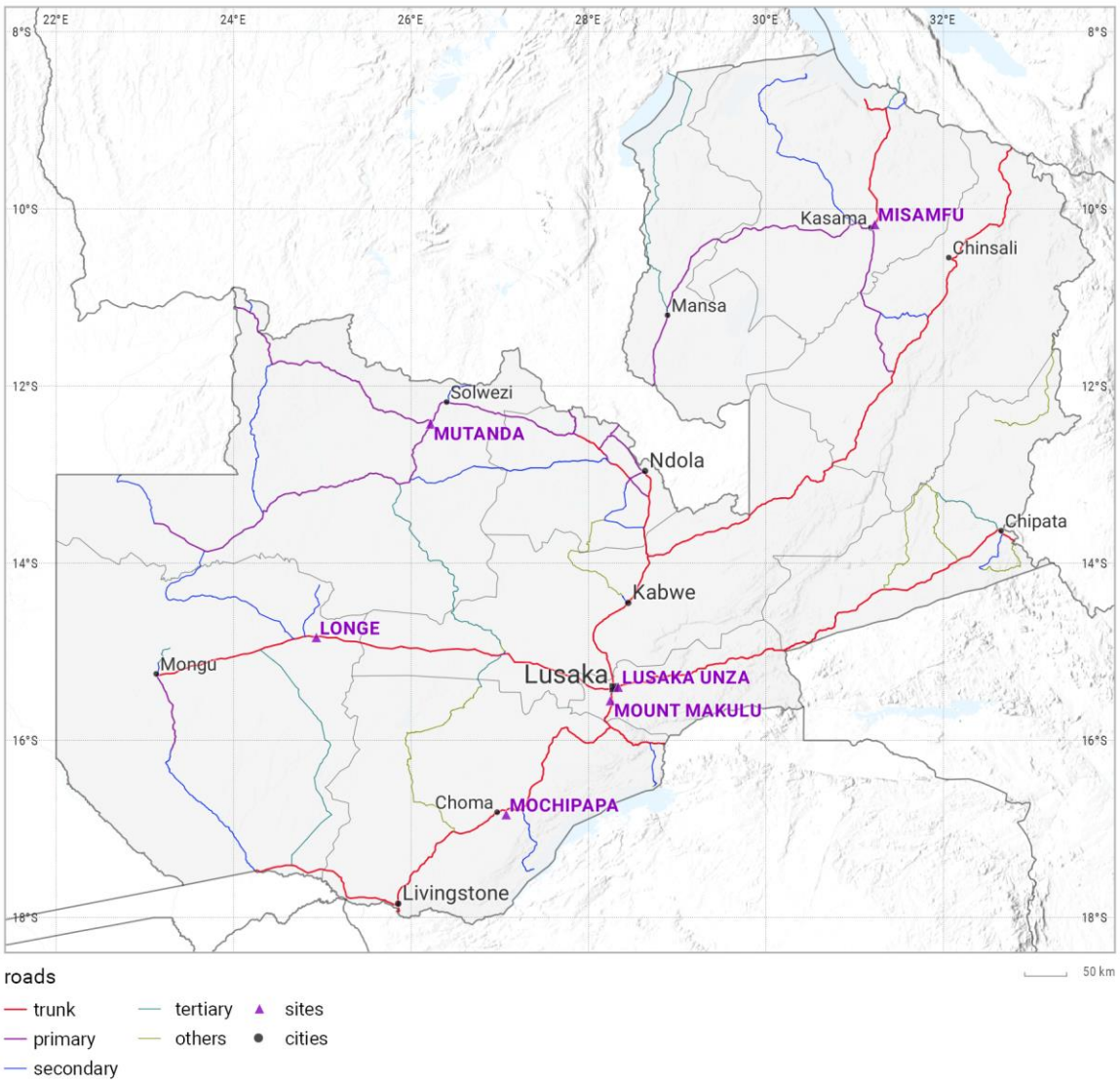

Map 3.6: Transport corridors.
Source: OpenStreetMap.org contributors.
For reference, position of six solar meteo sites is shown.

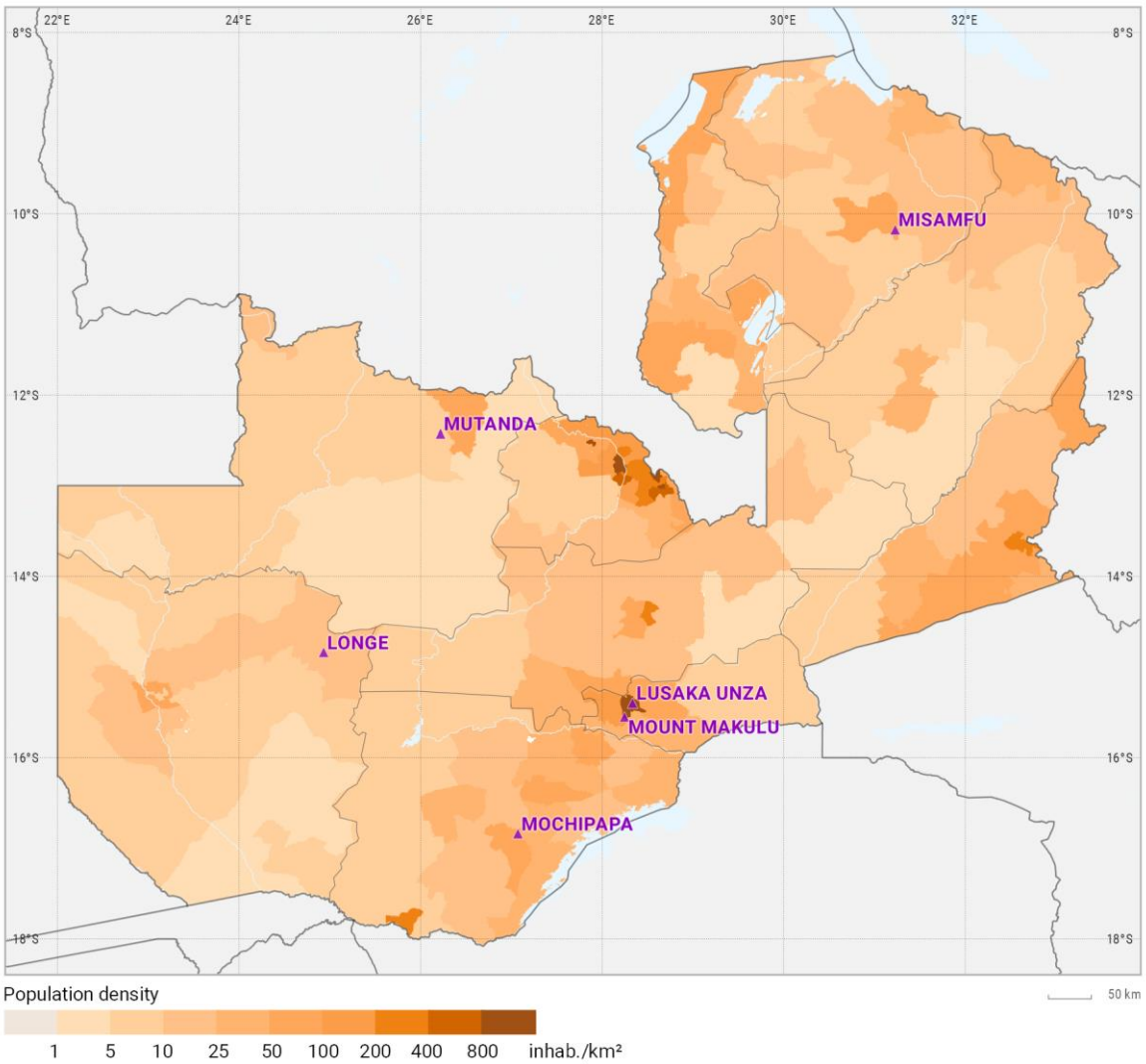

Map 3.7: Population density.
Source: Gridded Population of the World (GPW v4).
For reference, position of six solar meteo sites is shown.

From the geographical viewpoint, Zambia is a diverse country, with Lake Tanganyika, and Great Rift Valley in the North and Northeast to central high plateau and lowlands to the South, all having specific geographical conditions.

The map of the land cover shows the most appropriate conditions for human activities, including settlements and economic activities (industry, agriculture) that require substantial amount of electrical power. These developed regions are mainly on the southern plateaus and lowlands and valleys to the East, with industry (eg. mining in the North). Smaller settlements are dispersed thought Zambia.

More complex orographic conditions (terrain) are generally less populated and are typically unsuitable for large-scale solar energy development; however, they are suitable for smaller, off-grid or hybrid installations.

Urbanisation centres together with mining region in the North constitute the main energy demand centres. At present (statistics update Nov 2018), about 67% of urban inhabitants in Zambia are connected to electricity grid (in rural areas it is only 4%) [39].

3.2 Air temperature

Air temperature determines the operating environment and performance efficiency of the solar power systems. Air temperature is used as one of the inputs in the energy simulation models. In this report, the yearly and monthly average maps are shown. Map 3.8 and Map 3.9 show the yearly and monthly averages.The long-term averages of air temperature are derived from the MERRA-2 and CFSv2 models (see Chapter 2.2) by Solargis post-processing.

In the case of PV power plants, higher air temperature reduces the power conversion efficiency of the PV modules, as well as on other components (inverters, transformers, etc.).

Monthly averages of daily values show the seasonal variation of air temperature at six selected sites in Zambia (Figure 3.1). See Chapter 2.2 discussing the uncertainty of the air temperature model estimates.

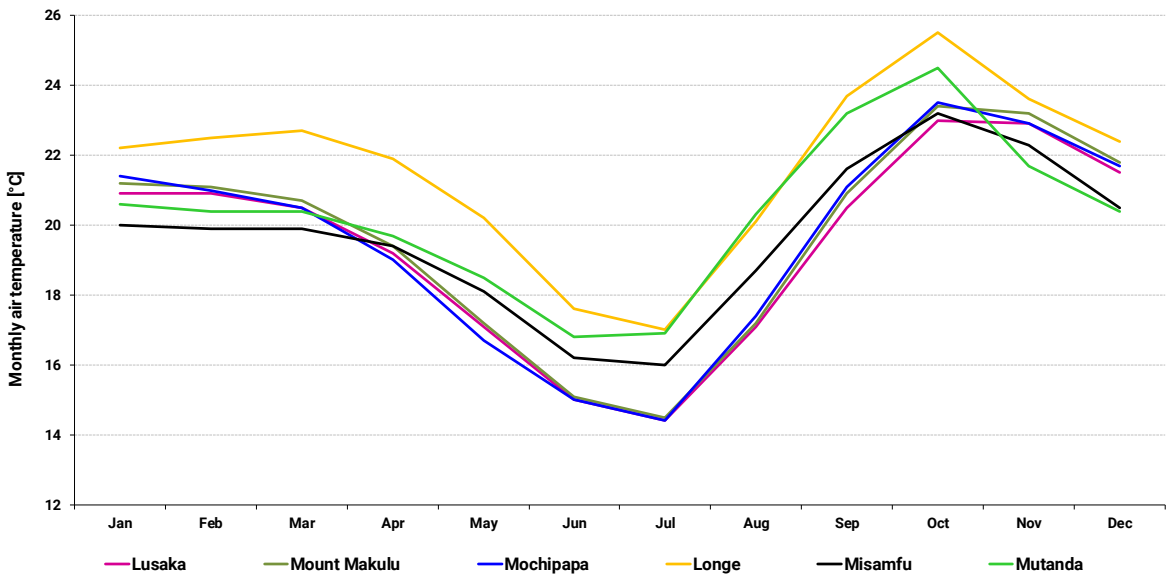

Figure 3.1: Monthly averages of air-temperature at 2 m for selected sites.

Table 3.1: Monthly averages of air-temperature at 2 m at 6 sites

Month	Temperature [°C]					
	Lusaka	Mount Makulu	Mochipapa	Longe	Misamfu	Mutanda
January	**20.9**	**21.2**	**21.4**	**22.2**	**20.0**	**20.6**
February	**20.9**	**21.1**	**21.0**	**22.5**	**19.9**	**20.4**
March	**20.5**	**20.7**	**20.5**	**22.7**	**19.9**	**20.4**
April	**19.2**	**19.4**	**19.0**	**21.9**	**19.4**	**19.7**
May	**17.1**	**17.2**	**16.7**	**20.2**	**18.1**	**18.5**
June	**15.0**	**15.1**	**15.0**	**17.6**	**16.2**	**16.8**
July	**14.4**	**14.5**	**14.4**	**17.0**	**16.0**	**16.9**
August	**17.1**	**17.2**	**17.4**	**20.1**	**18.7**	**20.3**
September	**20.5**	**20.9**	**21.1**	**23.7**	**21.6**	**23.2**
October	**23.0**	**23.4**	**23.5**	**25.5**	**23.2**	**24.5**
November	**22.9**	**23.2**	**22.9**	**23.6**	**22.3**	**21.7**
December	**21.5**	**21.8**	**21.7**	**22.4**	**20.5**	**20.4**
YEAR	**20.2**	**20.5**	**20.4**	**22.5**	**20.5**	**21.1**

Table 3.1 shows monthly characteristics of air temperature at six selected sites; they represent statistics calculated over a 24-hour diurnal cycle.

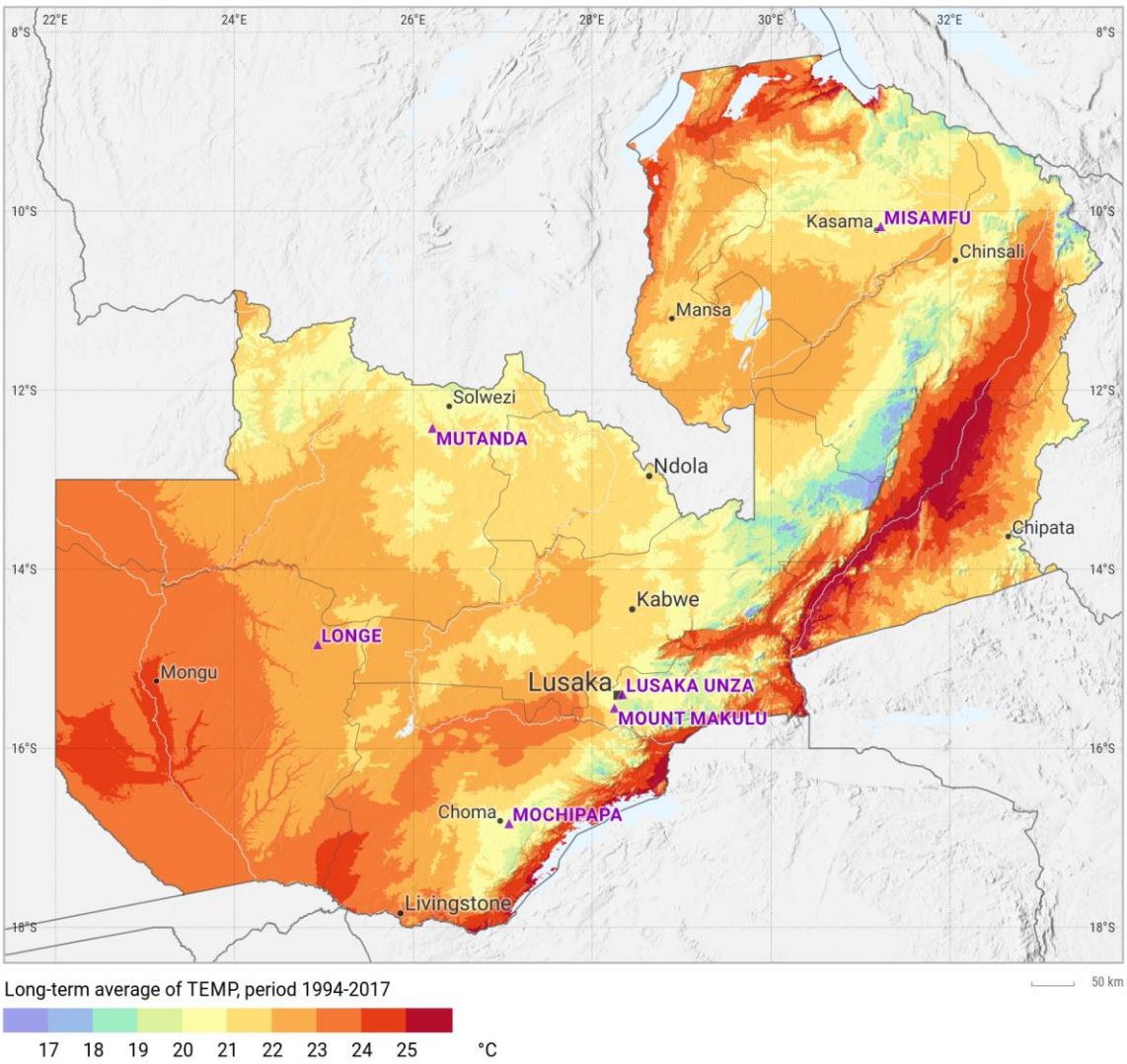

Map 3.8: Long-term yearly average of air temperature at 2 metres, period 1994-2017.
Source: Models CFSv2, MERRA-2, post-processed by Solargis

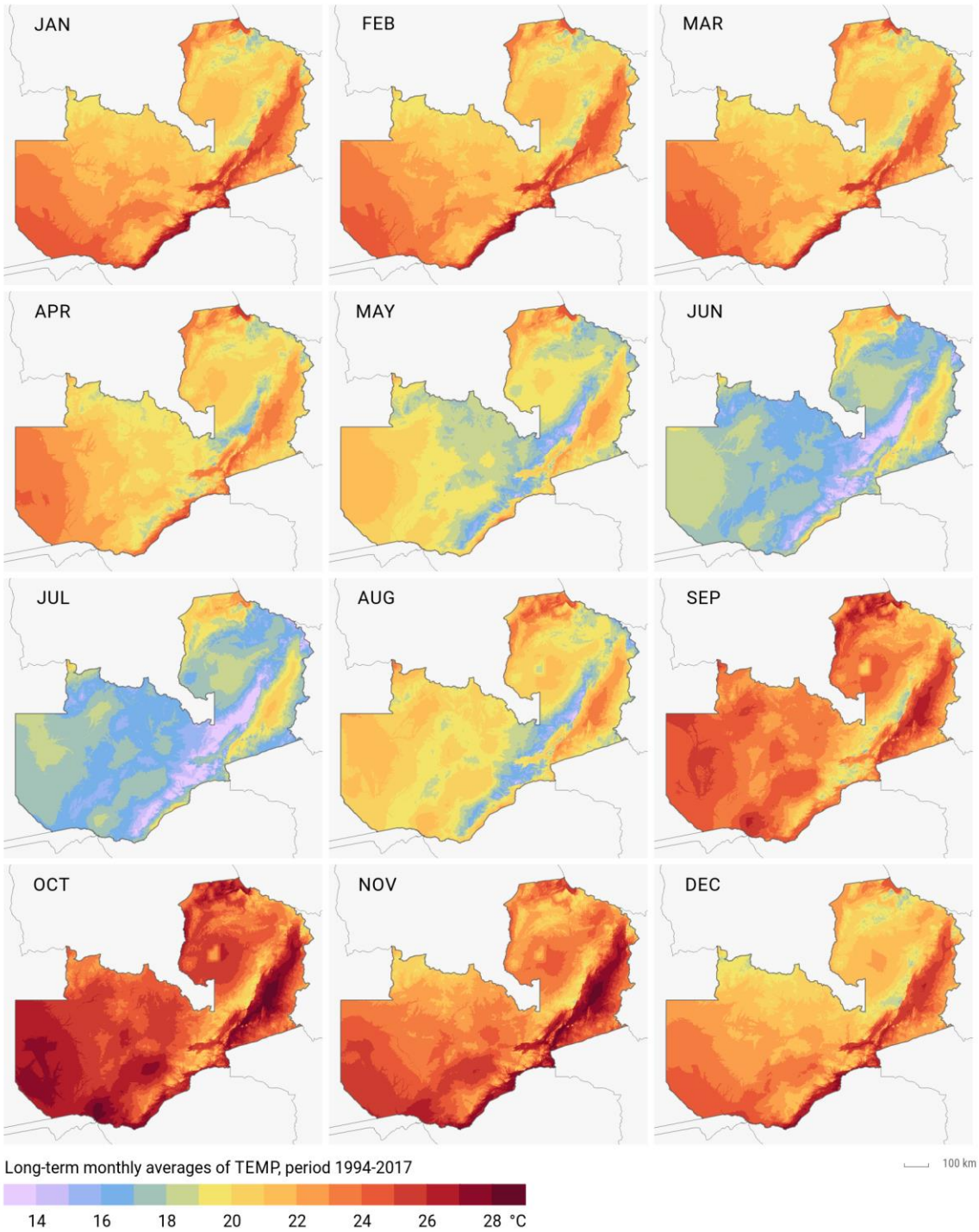

Map 3.9: Long-term monthly average of air temperature at 2 metres, period 1994-2017.
Source: Models CFSv2, MERRA-2, post-processed by Solargis

3.3 Global Horizontal Irradiation

Global Horizontal Irradiation (GHI) is used as a reference value for comparing geographical conditions related to PV electricity systems, as it eliminates possible variations influenced by the choice of components and the PV system design.

Table 3.2 shows long-term average of daily totals of Global Horizontal Irradiation (GHI) for a period 1994 to 2017 for six selected sites.

Figure 3.2 compares daily values of GHI at selected sites. When comparing GHI for these sites, they demonstrate a very similar pattern. The weather with highest GHI values is observed in September and October.

Highest variability of GHI between sites is observed in June and July. Generally annual variability between the sites is small (1.5%), which is determined by similar geographical characteristics. Figure 3.2 indicates that all sites will experience similar PV power performance.

Table 3.2: Daily averages of Global Horizontal Irradiation at 6 sites

Month	Global Horizontal Irradiation [kWh/m^2]						Variability between sites [%]
	Lusaka	Mount Makulu	Mochipapa	Longe	Misamfu	Mutanda	
January	**5.16**	**5.15**	**5.28**	**5.32**	**4.84**	**4.87**	**4.0**
February	**5.18**	**5.13**	**5.37**	**5.45**	**4.99**	**4.89**	**4.2**
March	**5.22**	**5.16**	**5.30**	**5.44**	**5.16**	**5.18**	**2.1**
April	**5.24**	**5.24**	**5.32**	**5.77**	**5.20**	**5.47**	**4.1**
May	**5.11**	**5.08**	**5.08**	**5.48**	**5.37**	**5.49**	**3.8**
June	**4.71**	**4.69**	**4.71**	**5.13**	**5.42**	**5.34**	**6.8**
July	**4.90**	**4.88**	**4.93**	**5.33**	**5.56**	**5.45**	**5.9**
August	**5.71**	**5.69**	**5.81**	**5.98**	**6.08**	**5.90**	**2.6**
September	**6.47**	**6.42**	**6.54**	**6.46**	**6.43**	**6.23**	**1.6**
October	**6.66**	**6.52**	**6.68**	**6.44**	**6.32**	**6.11**	**3.4**
November	**6.05**	**5.86**	**5.86**	**5.77**	**5.84**	**5.41**	**3.7**
December	**5.45**	**5.35**	**5.46**	**5.41**	**5.27**	**5.08**	**2.7**
YEAR	**5.49**	**5.43**	**5.53**	**5.67**	**5.54**	**5.45**	**1.5**

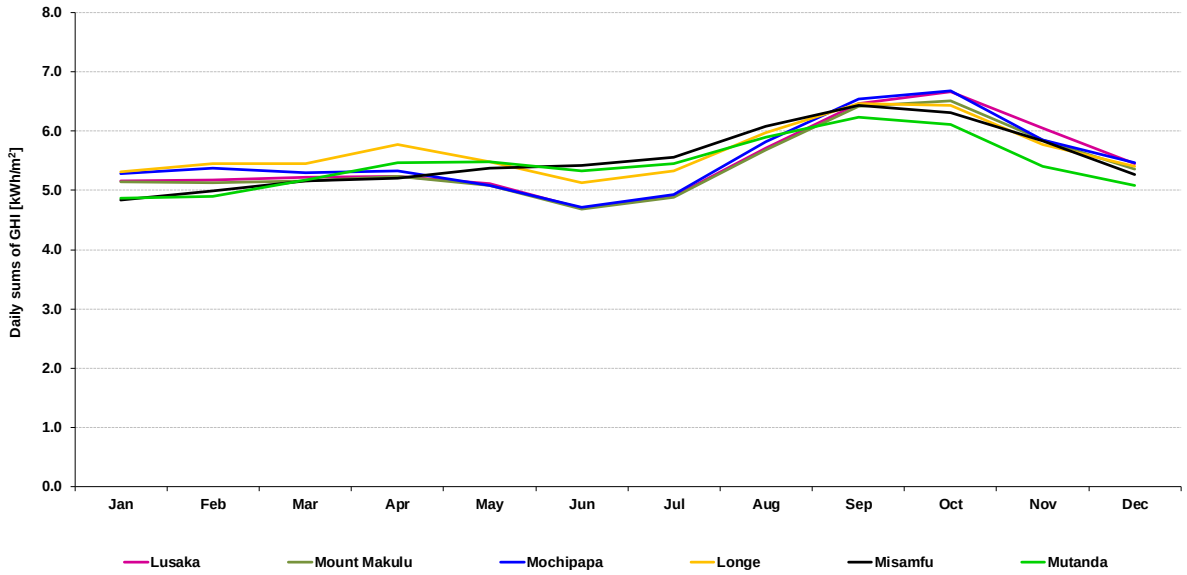

Figure 3.2: Long-term monthly averages of Global Horizontal Irradiation.

Weather changes in cycles and has also stochastic nature. Therefore, annual solar radiation in each year can deviate from the long-term average in the range of few percent. The estimation of the interannual variability shows the magnitude of this change.

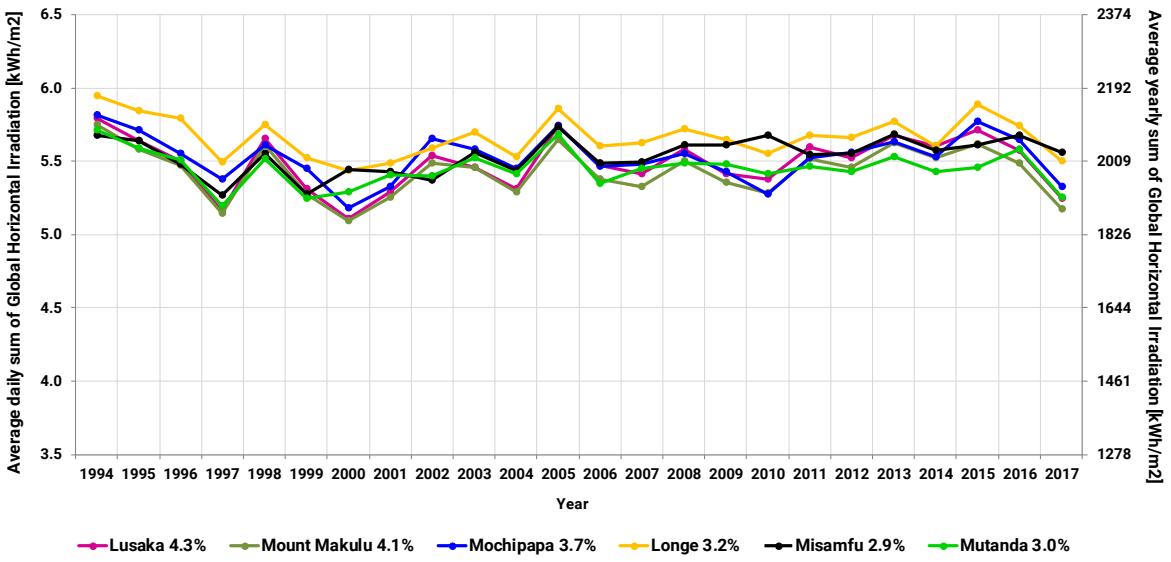

Figure 3.3: Interannual variability of Global Horizontal Irradiation for selected sites.

The interannual variability of GHI for the representative sites is calculated from the unbiased standard deviation of GHI over 24 years taking into consideration the long-term, normal distribution of the annual sums. All sites show similar patterns of GHI changes over the recorded period (Figure 3.3). More stable GHI (the lowest interannual

variability) is observed at Misamfu and Mutanda sites. Highest variability of all sites is observed at Lusaka site (standard deviation of 4.3%).

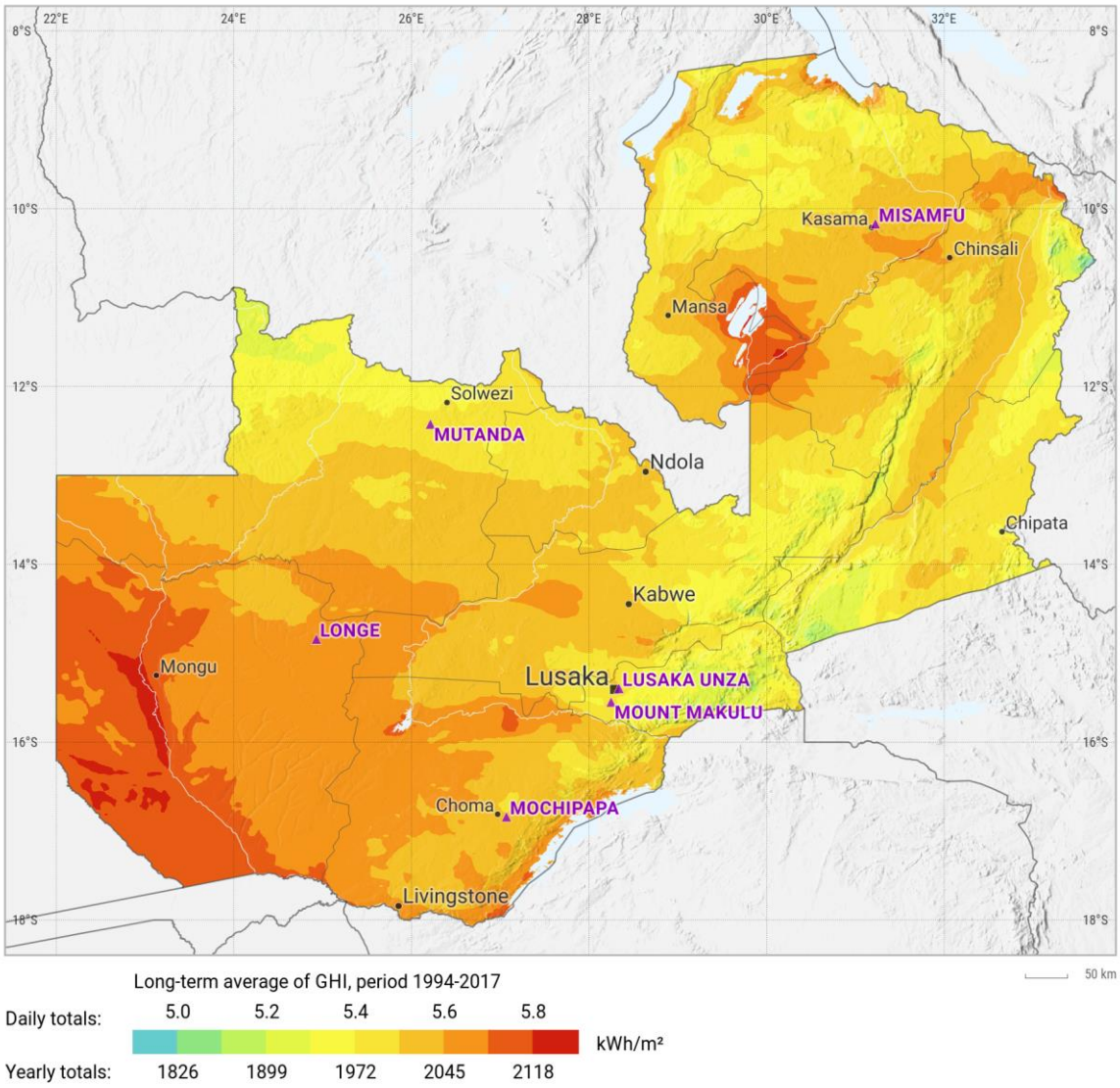

Map 3.10: Global Horizontal Irradiation – long-term average of daily and yearly totals.
Source: Solargis

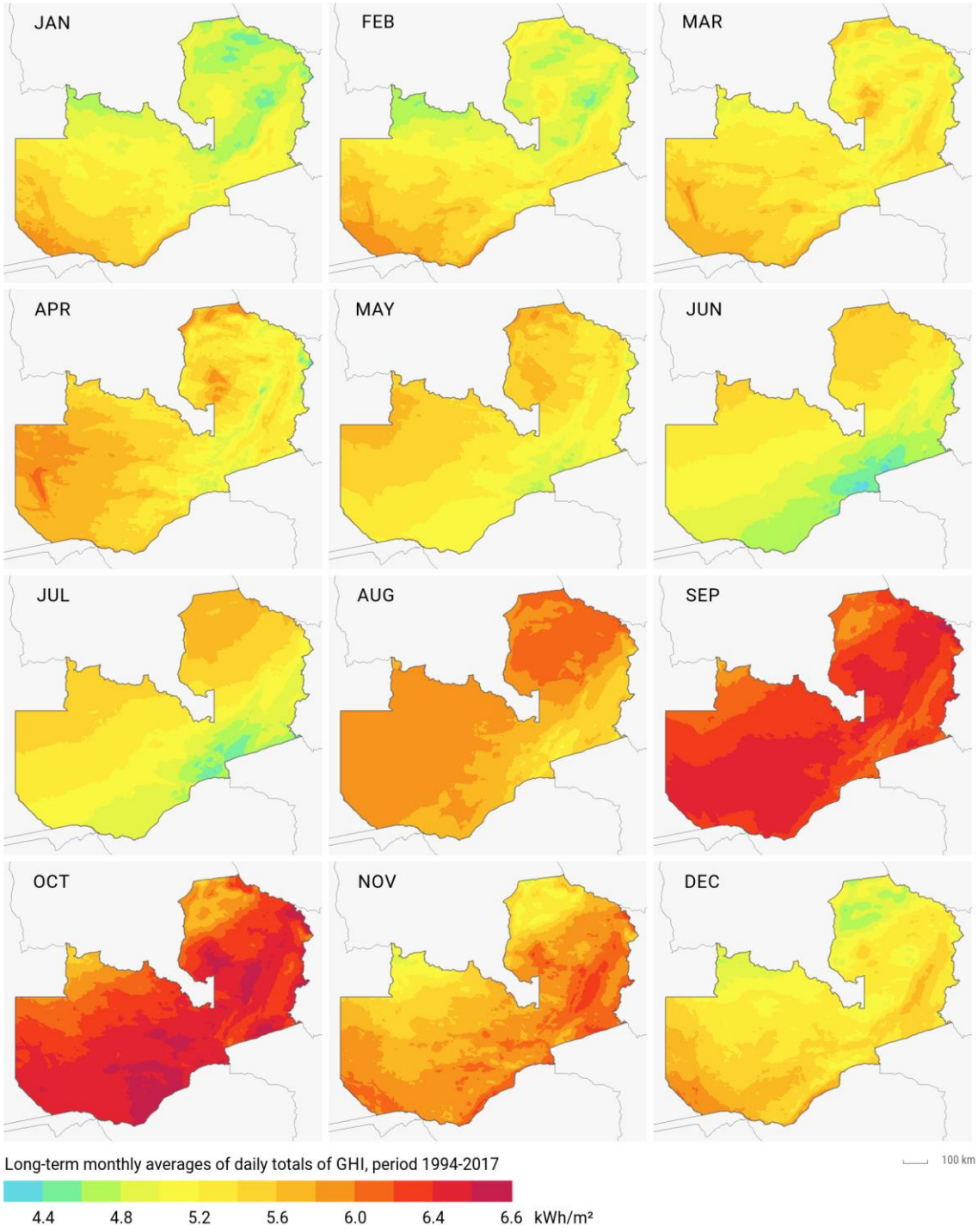

Map 3.11: Global Horizontal Irradiation – long-term monthly average of daily totals.
Source: Solargis

The highest GHI is identified in the South-western part of the Zambia, where average daily totals reach 5.6 kWh/m^2 (yearly sum about 2045 kWh/m^2) or more (Map 3.10). The season of highest irradiation with daily totals up to 6.6 kWh/km^2 lasts two months (from September to October, Map 3.11). The lowest documented GHI values are in January and February for sites Misamfu and Mutanda, while other sites show lowest GHI values in June and July.

Map 3.12 shows the ratio of diffuse to global horizontal irradiation. This ratio is important for the performance of PV systems and may have impact during the consideration process of PV modules technology. A higher ratio of diffuse to global horizontal irradiation (DIF/GHI) indicates less stable weather, higher occurrence of clouds, higher atmospheric pollution or water vapour. In general, higher values occurs along the eastern and northern borders of the country (up to 44%). In the South-west of the country the values fall to 28%.

Lower DIF/GHI values are identified from May to August, highest being in December, January and February. This indicates that the potential for concentrated solar technologies (CSP, CPV) in Zambia is lower due to high DIF/GHI ration and seasonality of solar radiation.

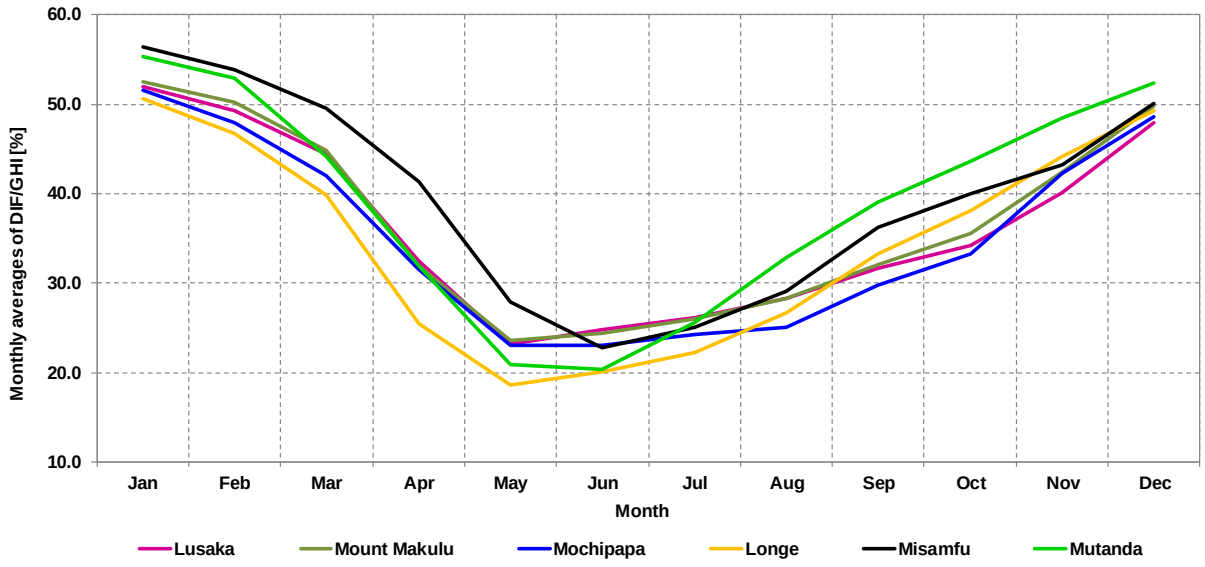

Figure 3.4: Monthly averages of DIF/GHI.

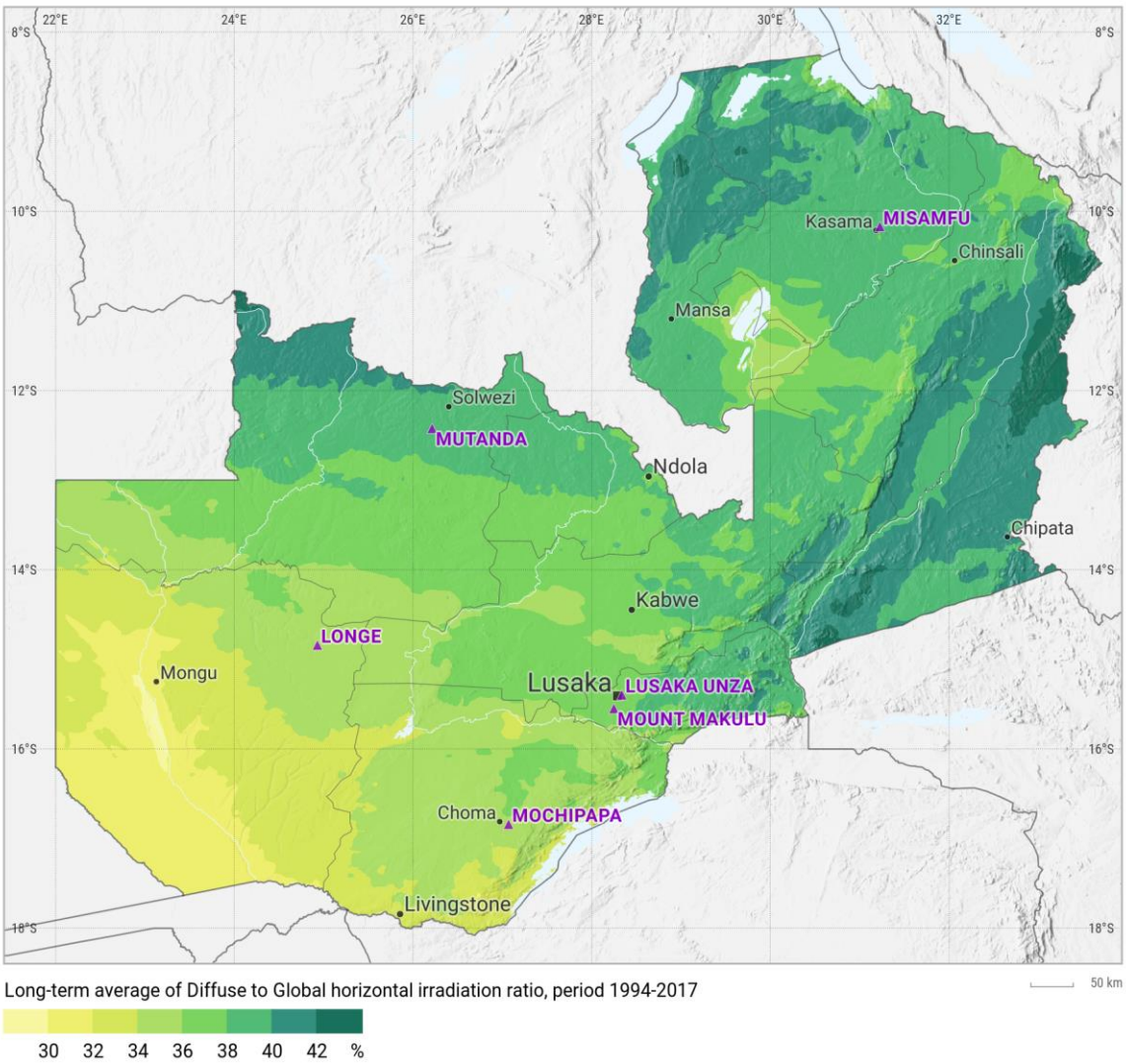

Map 3.12: Long-term average for ratio of diffuse and global irradiation (DIF/GHI).
Source: Solargis

3.4 Direct Normal Irradiation

Direct Normal Irradiation (DNI) is important solar resource parameters needed for the computation of Global Tilted Irradiation (GTI) (Chapter 3.5).

Table 3.3 and Figure 3.5 show long-term average daily totals of DNI for the six selected sites, during the period from 1994 to 2017. The highest DNI is reached in Longe, and the lowest in Misamfu.

Table 3.3: Daily averages of Direct Normal Irradiation at six sites

Month	Direct Normal Irradiation [kWh/m^2]						Variability between sites [%]
	Lusaka	Mount Makulu	Mochipapa	Longe	Misamfu	Mutanda	
January	3.18	3.18	3.36	3.39	2.60	2.74	10.7
February	3.42	3.35	3.71	3.75	2.85	2.88	11.8
March	3.98	3.99	4.29	4.47	3.37	3.82	9.6
April	5.38	5.46	5.66	6.48	4.40	5.51	12.1
May	6.49	6.49	6.67	7.37	6.06	6.94	6.7
June	6.20	6.23	6.49	7.08	6.81	7.10	6.1
July	6.12	6.16	6.50	6.94	6.56	6.52	4.7
August	6.26	6.26	6.84	6.67	6.23	5.77	5.9
September	6.09	6.00	6.42	5.86	5.42	4.99	8.8
October	5.79	5.56	5.97	5.19	4.85	4.40	11.3
November	4.75	4.45	4.48	4.16	4.33	3.53	9.7
December	3.69	3.52	3.71	3.53	3.40	3.07	6.7
YEAR	5.12	5.06	5.35	5.41	4.75	4.78	5.5

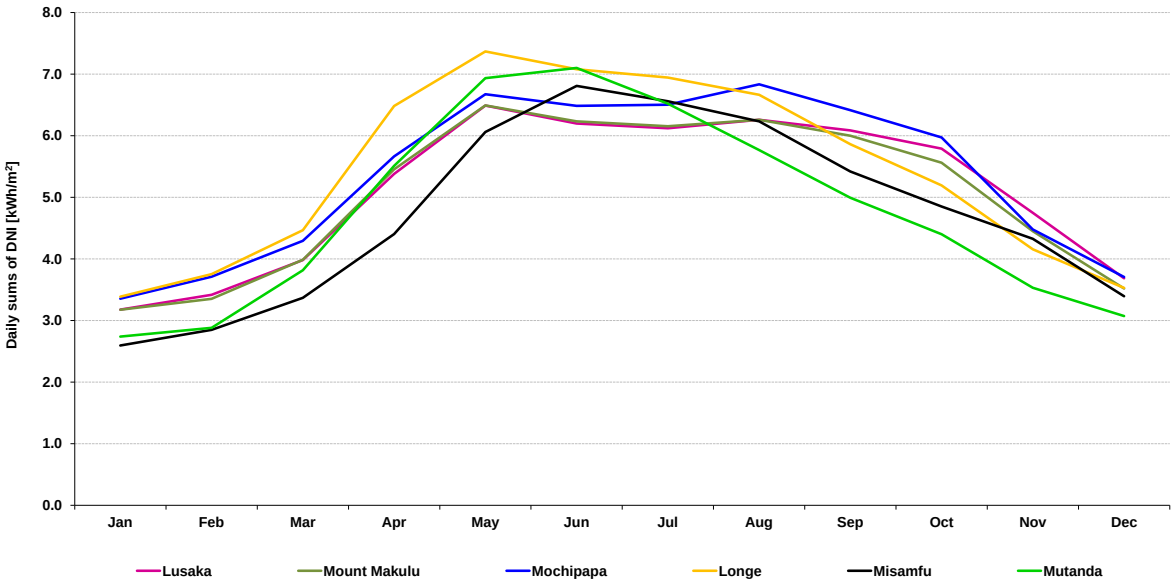

Figure 3.5: Daily averages of Direct Normal Irradiation at selected sites.

Interannual variability of DNI for selected sites (Figure 3.6) is calculated from the unbiased standard deviation of yearly DNI over 24 years and it is based on a simplified assumption of normal distribution of the yearly sums. Six sites show similar patterns of DNI variability over recorded period. The most stable DNI (the lowest interannual variability) is observed in Misamfu.

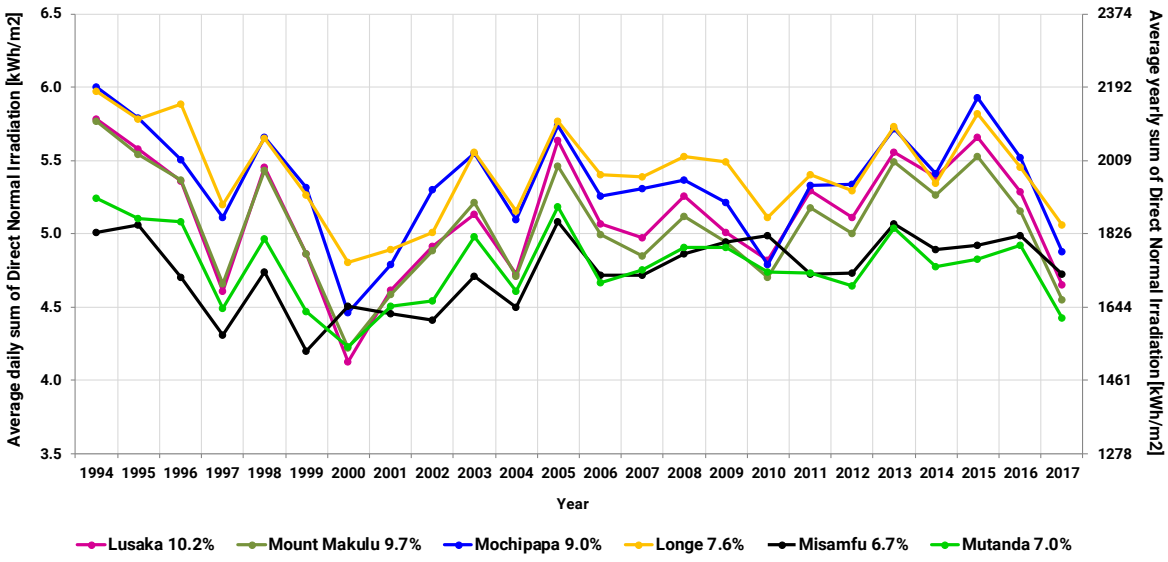

Figure 3.6: Interannual variability of Direct Normal Irradiation at representative sites

The highest DNI observed in the South-west part of Zambia, represents average daily totals over 5.8 kWh/m^2 (equal to yearly sum of about 2118 kWh/m^2, Map 3.13). High DNI occurs during the months from May to August, often exceeding the daily totals of 6.0 kWh/m^2 (Map 3.14). However, in December to February DNI daily totals drop significantly.

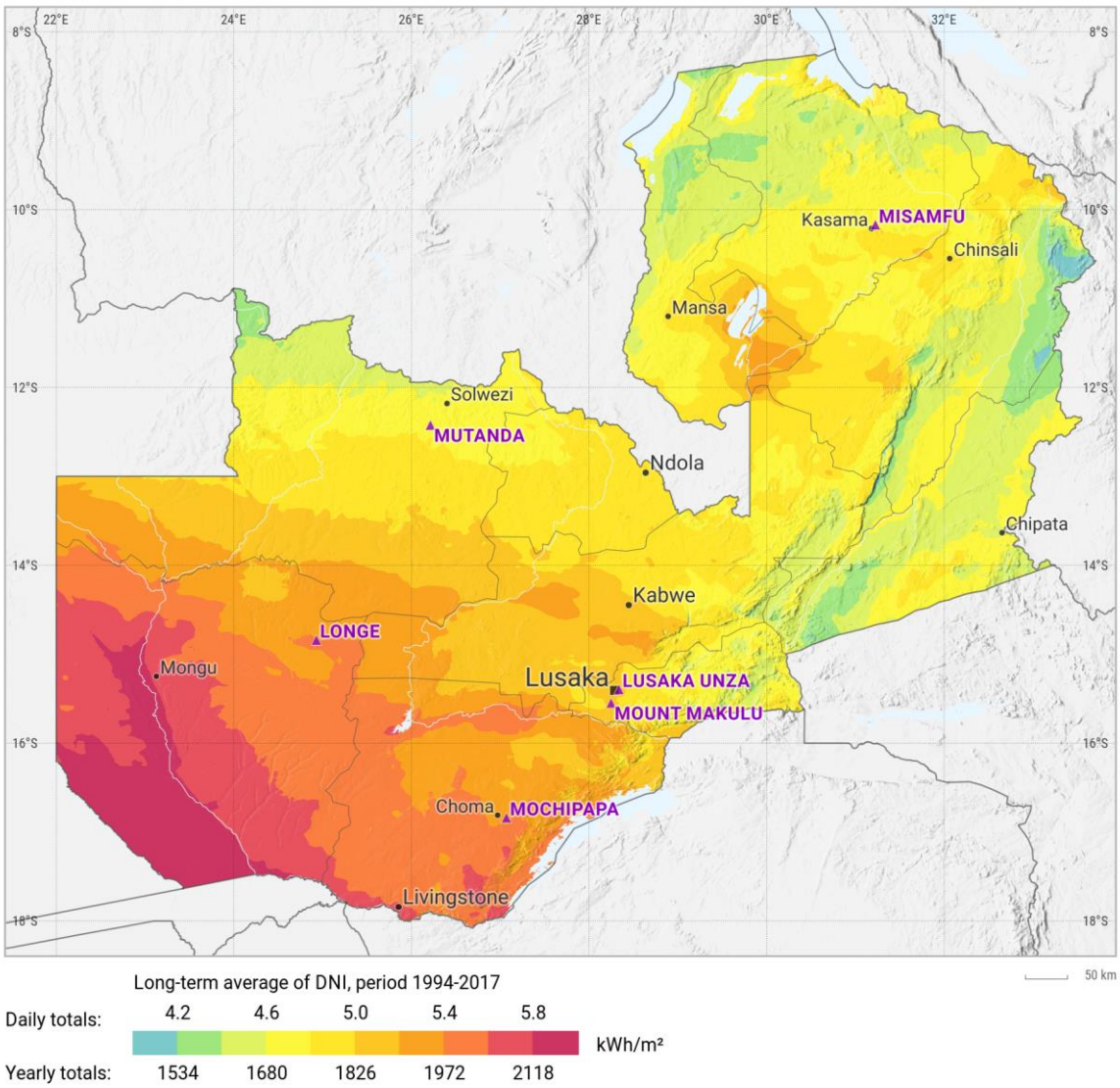

Map 3.13: Direct Normal Irradiation – long-term average of daily and yearly totals.
Source: Solargis

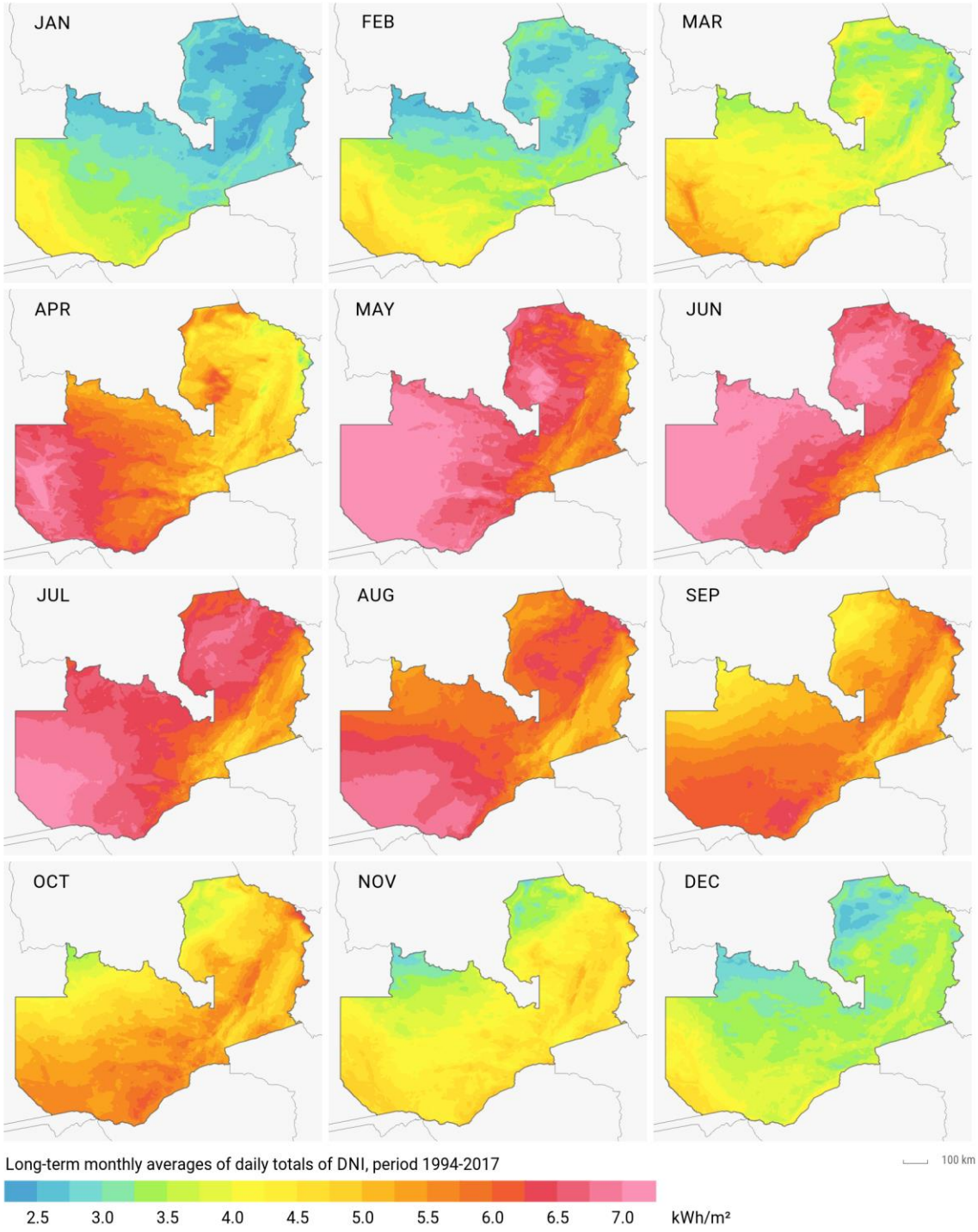

Map 3.14: Direct Normal Irradiation – long-term monthly average of daily totals.
Source: Solargis

3.5 Global Tilted Irradiation

Global Tilted Irradiation (GTI) is the key source of energy for flat-plate photovoltaic (PV) technologies (Chapter 3.6). Optimally tilted PV module produces more energy output annually compared to non-tilted module. The magnitude of the tilt also determines the ability of self-cleaning effect of the modules during the rainfall events (by washing dust and dirt).

Table 3.4 shows the long-term averages of average daily total Global Tilted Irradiation (GTI) for selected sites. It is assumed that solar radiation is received by PV modules with surface at optimum tilt.

Table 3.4: Daily averages of Global Tilted Irradiation at 6 sites

Month	Global Tilted Irradiation [kWh/m^2]						Variability between sites [%]
	Lusaka	Mount Makulu	Mochipapa	Longe	Misamfu	Mutanda	
January	4.72	4.72	4.78	4.82	4.49	4.45	3.3
February	4.95	4.91	5.11	5.17	4.78	4.65	4.0
March	5.33	5.28	5.44	5.55	5.19	5.23	2.6
April	5.82	5.82	6.00	6.46	5.55	5.97	5.1
May	6.17	6.14	6.29	6.68	6.11	6.48	3.6
June	5.88	5.87	6.06	6.47	6.38	6.52	4.8
July	6.00	5.99	6.20	6.59	6.43	6.51	4.1
August	6.58	6.56	6.84	6.90	6.70	6.61	2.1
September	6.86	6.80	6.99	6.82	6.64	6.48	2.6
October	6.53	6.39	6.54	6.27	6.15	5.94	3.7
November	5.57	5.40	5.35	5.28	5.42	4.98	3.7
December	4.91	4.83	4.87	4.83	4.81	4.58	2.4
YEAR	5.78	5.73	5.88	5.99	5.72	5.70	1.9

In Zambia, the optimum tilt of PV modules (for maximized yearly production) is between 13° and 23° (decreasing towards the Equator) with North orientation (Map 3.15).

Figure 3.7 compares long-term daily averages at selected sites. Stable weather with high GTI values is seen from August to November. Variability of GTI in all selected sites is relatively small. Lower daily averages in period from December to March are very similar for all sites, which are related to the rainy season.

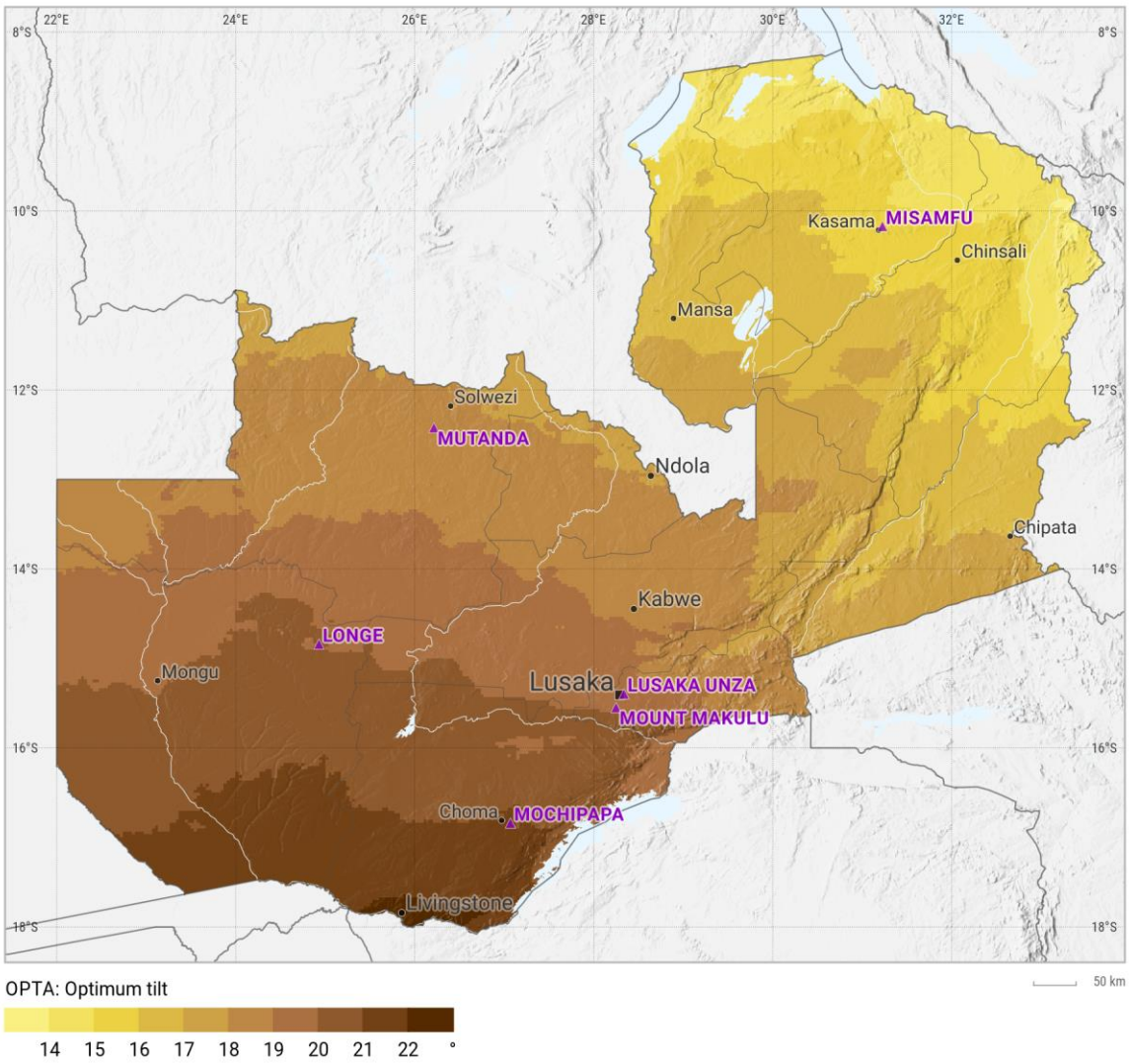

Map 3.15: Optimum tilt of PV modules to maximize yearly PV power production.
Source: Solargis

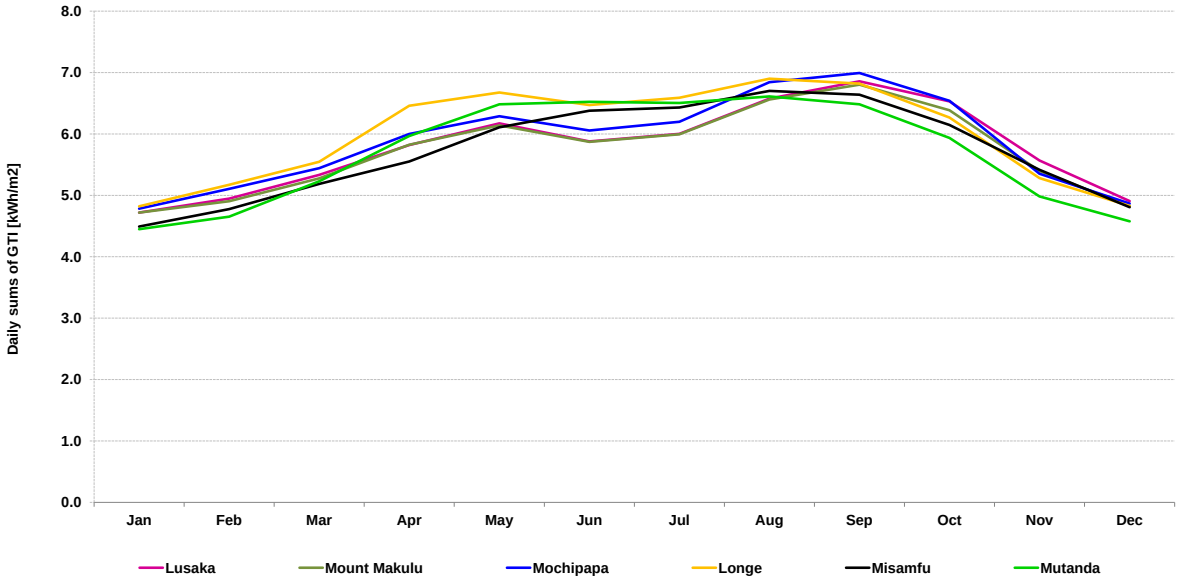

Figure 3.7: Global Tilted Irradiation – long-term daily averages.

A surface inclined at an optimum angle (tilt) gains more yearly irradiation than a horizontal surface (depending on the latitude of a site). In Zambia optimum tilt ranges between 13° and 23°. While seasonal gains of GTI in comparison to GHI are high (between 17% to 28%), the yearly gains of GTI are relatively small. Compared to GHI, GTI gain in the North of the country reaches about 3%, in the South it can be above 6% (Map 3.16 and 3.17). This is documented in Figure 3.8, where a positive gain of GTI is about 3.3% (Misamfu) to 6.3% (Mochipapa).

Despite relatively small yearly gain of GTI compared to GHI, the installation of modules in inclined position has additional positive effect of natural cleaning of the modules by rain.

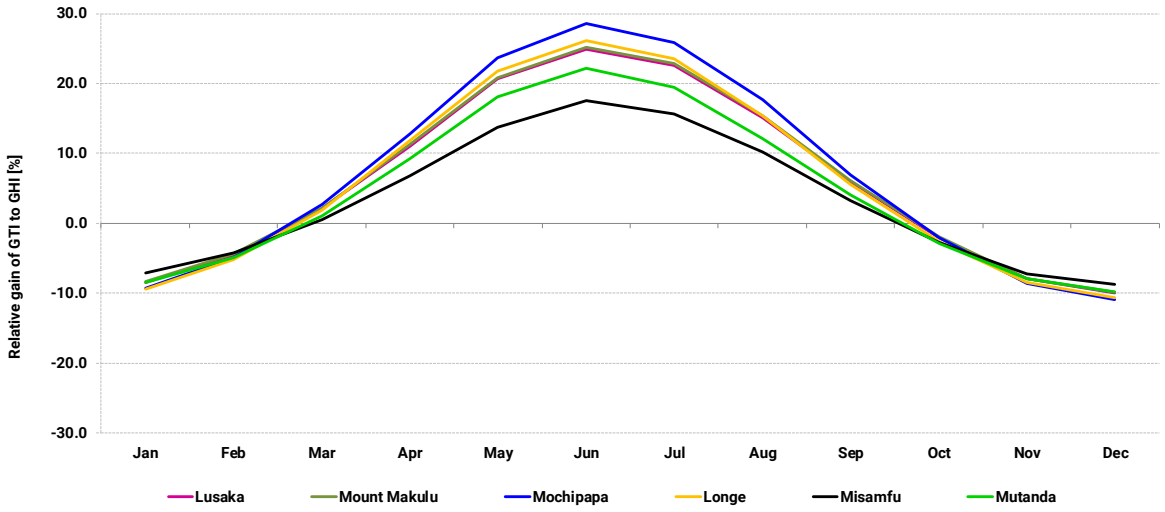

Figure 3.8: Monthly relative gain of GTI relative to GHI at selected sites.

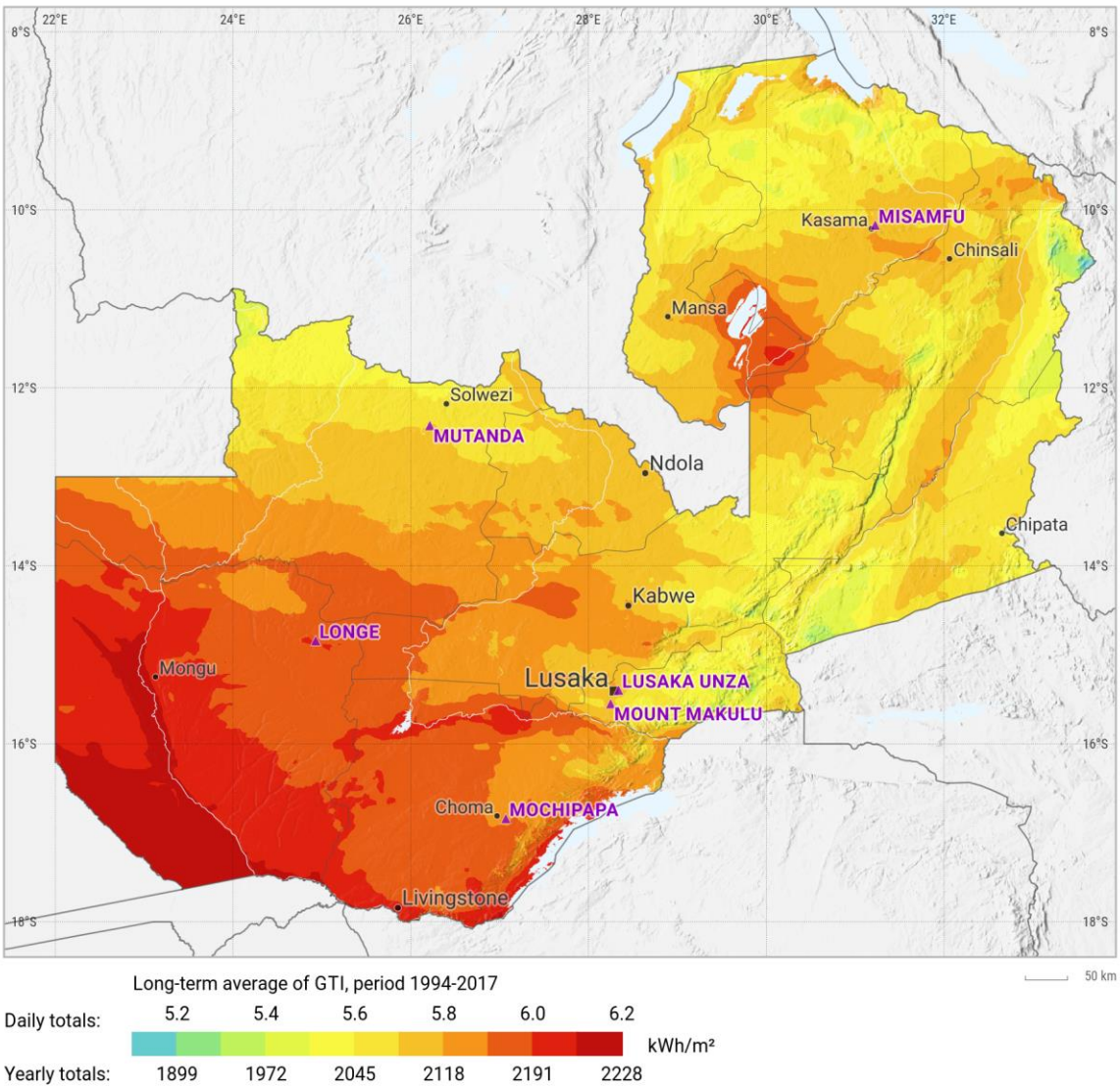

Map 3.16: Global Tilted Irradiation at optimum tilt – long-term average of daily and yearly totals.
Source: Solargis

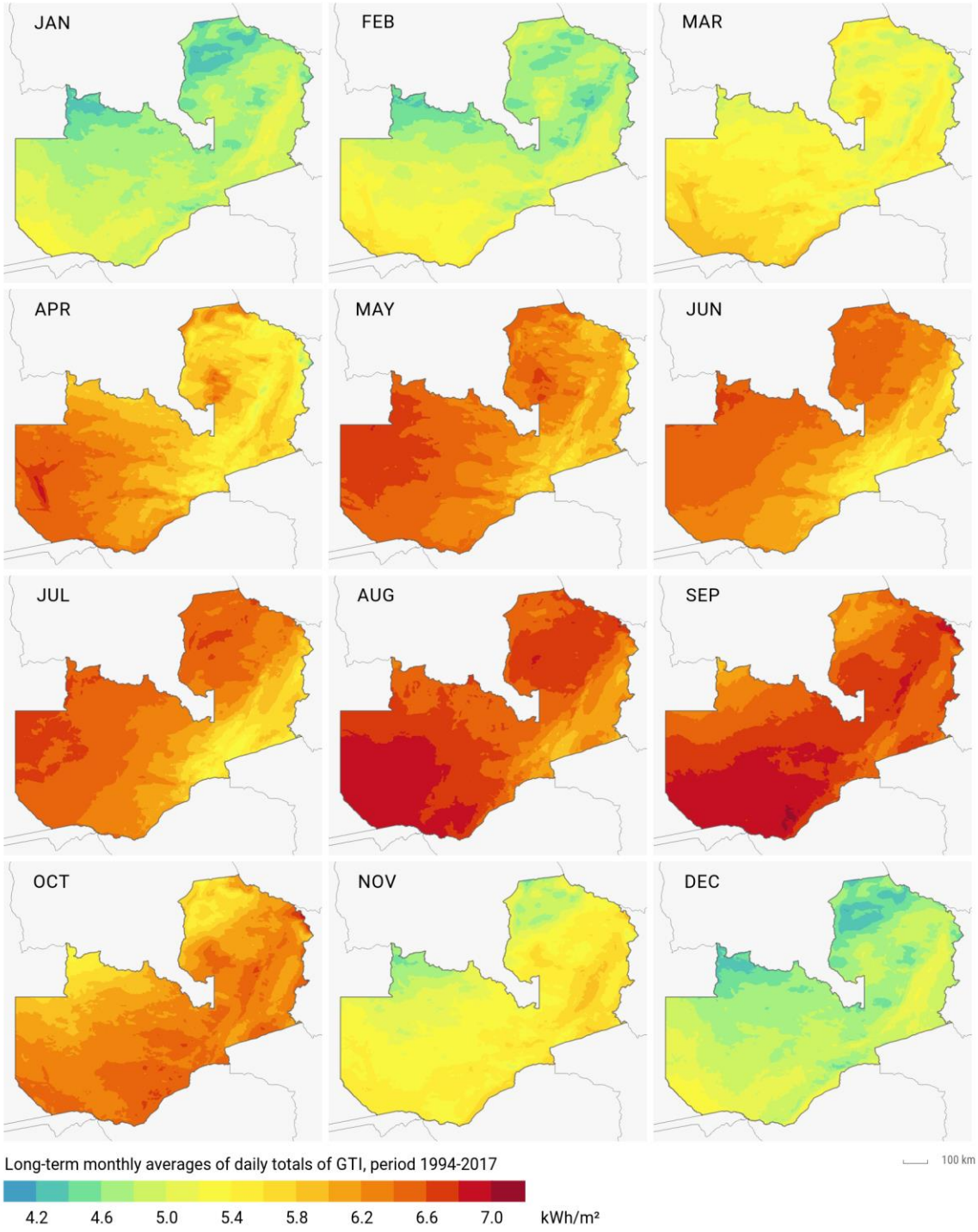

Map 3.17: Global Tilted Irradiation at optimum tilt – long-term monthly average of daily totals.
Source: Solargis

3.6 Photovoltaic power potential

The PV potential from a reference system for six representative sites is shown in Table 3.5. Despite the geographic distribution of selected sites, electricity production from a PV power system is similar for all sites and follows a combined pattern of global solar irradiation and air temperature. Considering six selected sites, the difference between PV production from the "best" site (Longe, 4.66 kWh/kWp) and "the least productive" site (Mutanda, 4.48 kWh/kWp) is very low, only about 4%. Also, monthly power production profiles are very similar for all sites. The highest seasonal production occurs in August and September (Table 3.6).

Table 3.5: Annual performance parameters of a PV system with modules fixed at the optimum angle

	Lusaka	Mount Makulu	Mochipapa	Longe	Misamfu	Mutanda
PVOUT Average daily total [kWh/kWp]	4.56	4.51	4.62	4.66	4.52	4.48
PVOUT Yearly total [kWh/kWp]	1665	1649	1689	1702	1651	1638
Annual ratio of DIF/GHI	36.2%	36.8%	35.2%	34.5%	39.1%	38.6%
System PR	78.9%	78.8%	78.7%	77.8%	79.0%	78.6%

PVOUT - PV electricity yield for fixed-mounted modules at optimum angle; DIF/GHI – Ratio of Diffuse/Global horizontal irradiation;
PR - Performance ratio for fixed-mounted PV

Table 3.6: Average daily sums of PV electricity output from an open-space fixed PV system with a nominal peak power of 1 kW [kWh/kWp]

Site	Average daily sum of electricity production [kWh/kWp]												Year
	Jan	Feb	Mar	Apr	May	Jun	Jul	Aug	Sep	Oct	Nov	Dec	
Lusaka	3.72	3.90	4.22	4.63	4.94	4.75	4.85	5.20	5.30	5.01	4.30	3.85	4.56
Mount Makulu	3.72	3.87	4.18	4.63	4.91	4.74	4.84	5.18	5.25	4.89	4.16	3.78	4.51
Mochipapa	3.75	4.02	4.29	4.76	5.03	4.90	5.01	5.39	5.39	4.98	4.13	3.81	4.62
Longe	3.77	4.04	4.33	5.03	5.23	5.15	5.24	5.35	5.17	4.74	4.08	3.77	4.66
Misamfu	3.57	3.79	4.12	4.43	4.89	5.13	5.15	5.26	5.13	4.73	4.21	3.80	4.52
Mutanda	3.52	3.68	4.14	4.74	5.14	5.20	5.18	5.15	4.96	4.54	3.89	3.62	4.48

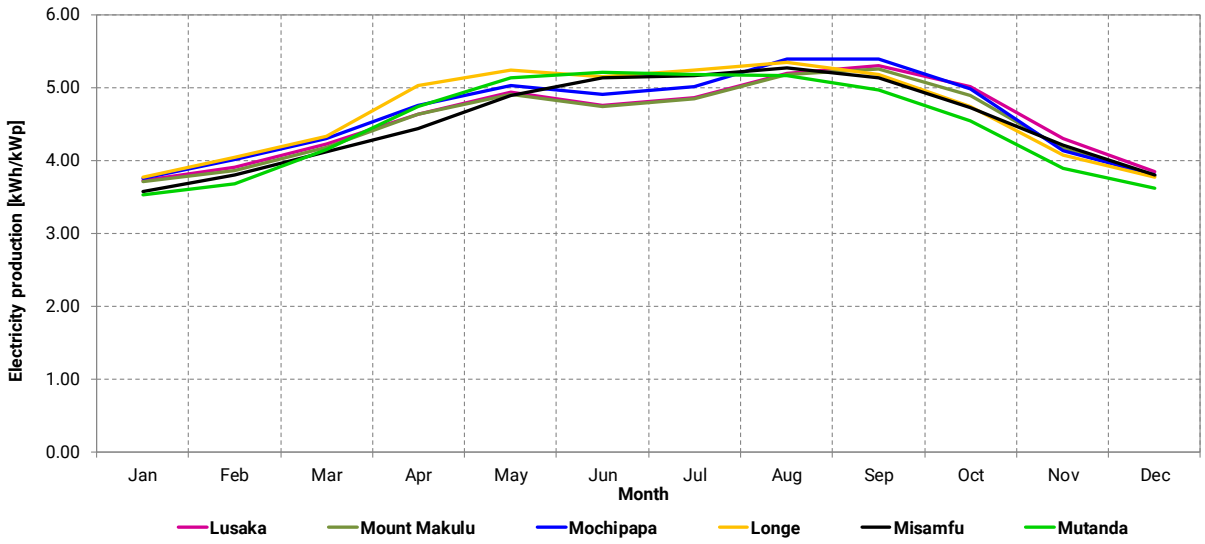

Figure 3.9: Monthly averages of daily totals of power production from the fixed tilted PV systems with a nominal peak power of 1 kW at six sites [kWh/kWp]

Maps 3.18 and 3.19 show yearly and monthly production from a PV power system, and Figure 3.9 breaks down the values for the six sites. The season of relatively high PV yield is long enough for the effective operation of a PV system. As shown in Chapter 3.5, in case of fixed mounted systems it is recommended to install modules inclined, with angle close to the optimum tilt towards equator rather than on a horizontal surface. Besides higher yield, a benefit of tilted modules is improved self-cleaning of the surface pollution by rain.

The monthly and yearly performance ratios (PR) of a reference installation for the selected sites are shown in Table 3.7 and Figure 3.10. The range of yearly PR for the selected sites is between 77.8% and 79.0%, with Misamfu being the site with the highest PR (Chapter 2.3).

Table 3.7: Monthly and annual Performance Ratio of a free-standing PV system with fixed modules

Site	Monthly Performance Ratio [%]												Year
	Jan	Feb	Mar	Apr	May	Jun	Jul	Aug	Sep	Oct	Nov	Dec	
Lusaka	78.9	79.0	79.1	79.6	80.0	80.8	80.9	79.0	77.3	76.7	77.3	78.5	78.9
Mount Makulu	78.7	78.8	79.2	79.5	80.0	80.8	80.7	78.9	77.1	76.5	77.1	78.3	78.8
Mochipapa	78.5	78.7	78.9	79.3	80.0	80.8	80.8	78.8	77.0	76.2	77.1	78.2	78.7
Longe	78.2	78.2	78.0	77.9	78.4	79.6	79.5	77.5	75.9	75.6	77.2	78.2	77.8
Misamfu	79.5	79.4	79.5	79.9	80.1	80.4	80.2	78.5	77.2	76.9	77.7	79.0	79.0
Mutanda	79.1	79.1	79.2	79.4	79.2	79.8	79.6	78.0	76.6	76.4	78.1	79.1	78.6

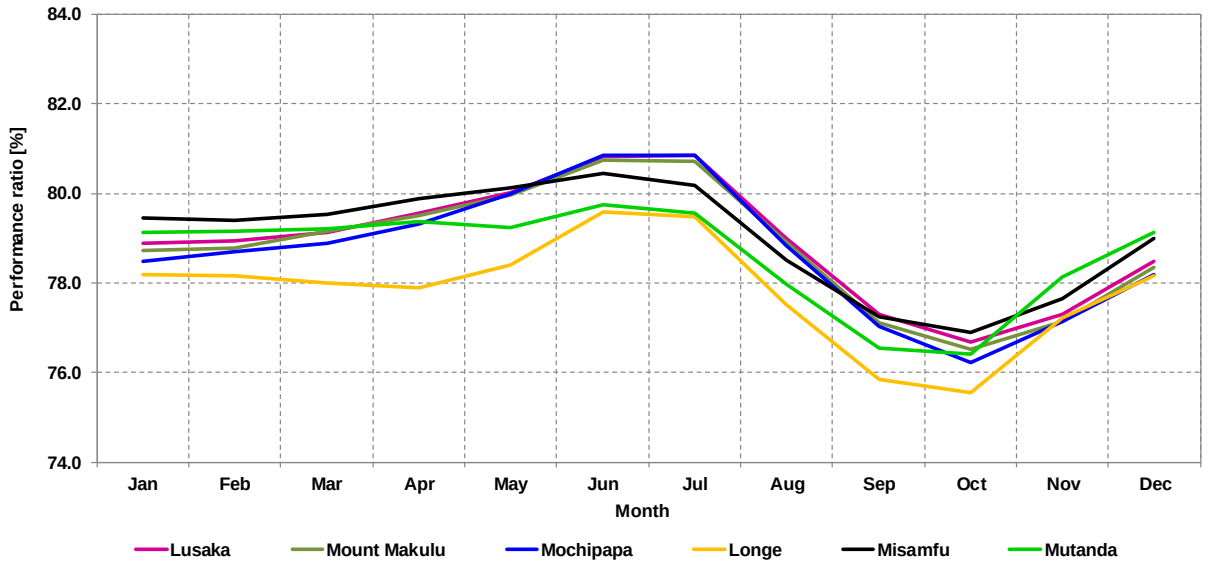

Figure 3.10: Monthly performance ratio of a PV system at selected sites.
Fixed mounted modules at optimum tilt towards equator are considered

Map 3.18 shows the average daily total of specific PV electricity output from a typical open-space PV system with optimally tilted c-Si modules and a nominal peak power of 1 kW (thus the values are in kWh/kWp). Calculating PV output for 1 kWp of installed power makes it simple to scale the PV power production relative to the size of a power plant. Besides the technology choice, the electricity production depends on the geographical position of the power plant.

In most regions of Zambia, the average daily sums of the specific PV power production from a reference system vary between 4.2 kWh/kWp (equals to yearly sum of about 1534 kWh/kWp) and 4.8 kWh/kWp (about 1716 kWh/kWp per year). The best season for PV power production is from May to September, with highest values in August, when they can exceed locally 5.6 kWh/kWp.

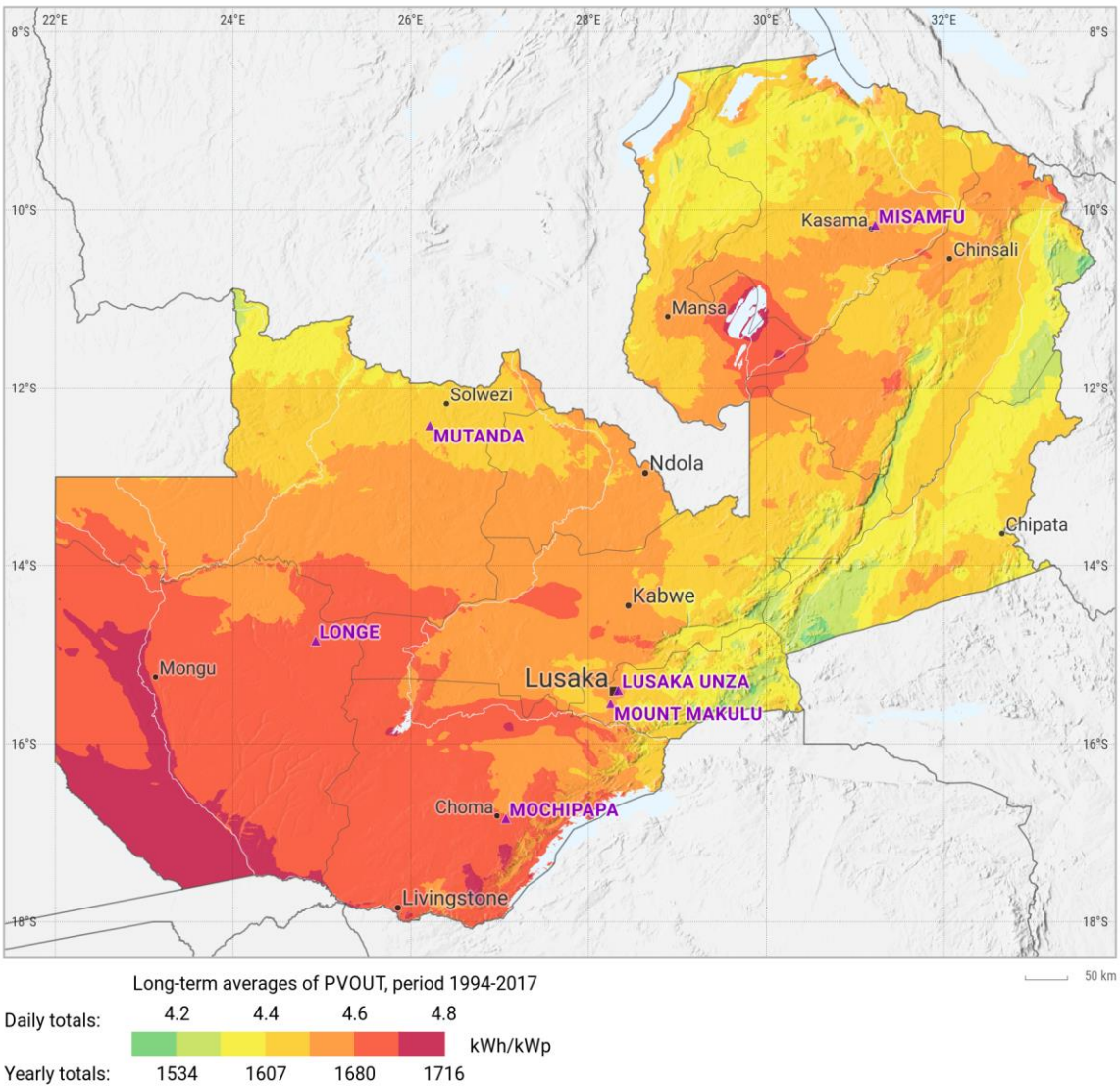

Map 3.18: PV electricity output from an open space fixed-mounted PV system with PV modules mounted at optimum tilt towards equator and a nominal peak power of 1 kWp. Long-term averages of daily and yearly totals.

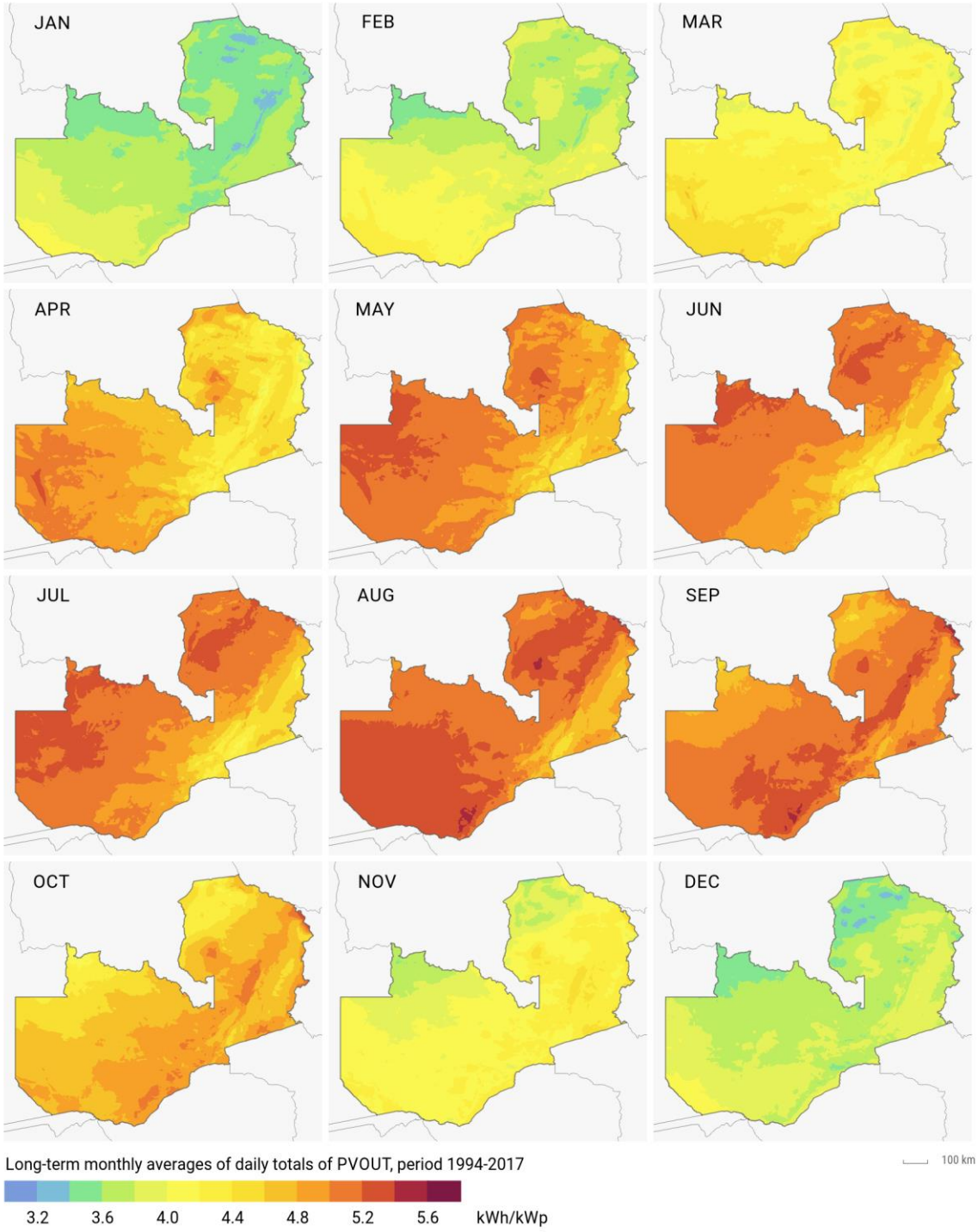

Map 3.19: PV power generation potential for an open-space fixed-mounted PV system.
Long-term monthly averages of daily totals.
Source: Solargis

3.7 Evaluation

The chapters above describe various aspects of PV power generation potential in Zambia, and its relevance for the development and operation of photovoltaic systems. A large extent of the country has an average PV electricity daily output within the range from 4.3 to 4.6 kWh/kWp (equals to average yearly totals between 1550 and 1680 kWh/kWp). **This fact positions Zambia into the category of countries with high potential for PV power generation.**

Additionally, the seasonal variability in the country is low, when compared to regions further away from the equator. The ratio between months with maximum and minimum GHI is about 1.42 in Lusaka, which is better than the ratio for e.g. Upington in South Africa (2.29) or Sevilla in Spain (3.54) (Figure 3.11).

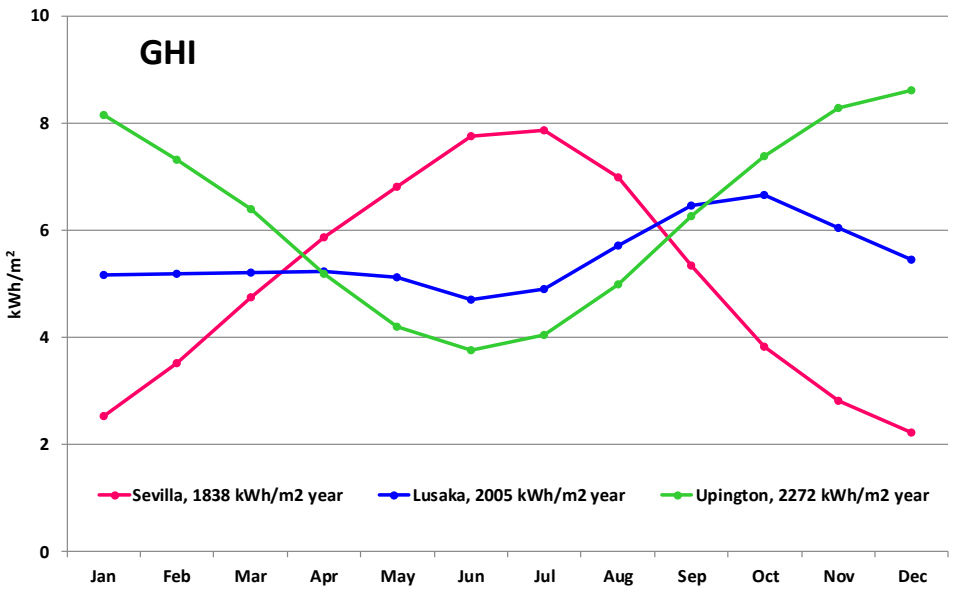

Figure 3.11: Comparing seasonal variability in three locations for GHI

4 Data delivered for Zambia

The following data and maps are delivered for Zambia:

1. Site-specific time series and TMY data

The data for six sites, corresponding to the locations of solar meteorological stations, can be accessed through the web site https://energydata.info/:

- High accuracy **1-minute measurements** (time series) acquired over a period of 24 months (2015-2017)
- High accuracy site-adapted **15-minute historical time series and hourly Typical Meteorological Year** (TMY) data generated by the Solargis model. The data represent history of years 1994 to 2017

2. Country-wide spatial data (GIS files) and maps

These outputs can be accessed as downloadable GIS files and maps through the map-based web application https://globalsolaratlas.info/:

- Harmonized solar and meteorological **GIS-based data**. Regionally adapted solar resource and temperature data for Zambia. The long-term averages represent history of years 1994 to 2017 at 9 arcsec (nominally 250 m) grid resolution.
- High resolution poster **maps** and medium size maps

More information about site specific data products is available in [29]. The information about spatial data products is available in chapters below.

The delivered data and maps offer a good basis for knowledge-based decision making and project development. Solargis database is updated in real time and this data can be further used in solar monitoring, performance assessment and forecasting.

4.1 Spatial data products

High-resolution Solargis data have been delivered in the format suitable for common GIS software. The *Primary data* represent solar radiation, meteorological data and PV power potential. The *Supporting data* include various vector data, such as administrative borders, cities, etc. Tables 4.1 and 4.2 show information about the data layers and the technical specification is summarized in Tables 4.3 and 4.4. File name convention, used for the individual data sets, is described in Table 4.5.

Metadata is delivered with the data files in two formats, according to ISO 19115:2003/19139 standards:

- PDF - human readable
- XML - for machine-to-machine communication

The snapshots of most of the data can be viewed on the maps in Chapter 3.

Table 4.1: General information about GIS data layers

Geographical extent	Republic of Zambia, including approx. 10 km buffer zone along the country border between 19°S and 8°S, 22°E and 34°E
Map projection	Geographic (Latitude/Longitude), datum WGS84 (also known as GCS_WGS84; EPSG: 4326)
Data formats	ESRI ASCII raster data format (asc) GeoTIFF raster data format (tif)

Notes:

- Data layers of both formats (asc and tif) contain the same information; the operator is free to choose the preferential data format. Data layers can be also converted to other standard raster formats.
- More information about ESRI ASCII grid format can be found at http://help.arcgis.com/en/arcgisdesktop/10.0/help/index.html#/ESRI_ASCII_raster_format/009t0000000z000000/
- More information about GeoTIFF format can be found at https://trac.osgeo.org/geotiff/

Table 4.2: Description of primary GIS data layers

Acronym	Full name	Unit	Type of use	Type of data layers
GHI	Global Horizontal Irradiation	kWh/m^2	Reference information for the assessment of flat-plate PV (photovoltaic) and solar heating technologies (e.g. hot water)	Long-term yearly and monthly average of daily totals
DNI	Direct Normal Irradiation	kWh/m^2	Assessment of Concentrated PV (CPV) and Concentrated Solar Power (CSP) technologies, but also calculation of GTI for fixed mounting and sun-tracking flat plate PV	Long-term yearly and monthly average of daily totals
DIF	Diffuse Horizontal Irradiation	kWh/m^2	Complementary parameter to GHI and DNI	Long-term yearly and monthly average of daily totals
GTI	Global Irradiation at optimum tilt towards equator	kWh/m^2	Assessment of solar resource for PV technologies	Long-term yearly and monthly average of daily totals
OPTA	Optimum tilt	°	Optimum tilt of PV modules to maximise the yearly yield	Long-term average
PVOUT	Photovoltaic power potential	kWh/kWp	Assessment of power production potential for a PV power plant with free-standing fixed-mounted c-Si modules, optimally tilted towards equator to maximize yearly PV production	Long-term yearly and monthly average of daily totals
TEMP	Air Temperature at 2 m above ground level	°C	Defines operating environment of solar power plants	Long-term (diurnal) annual and monthly averages

Table 4.3: Characteristics of the raster output data files

Characteristics	Range of values
West – East	21:00:00E – 34:00:00E
North – South	7:00:00S – 19:00:00S
Resolution GHI, DNI, GTI, DIF, PVOUT	00:00:09 (5200 columns x 4800 rows)
Resolution TEMP	00:00:30 (1560 columns x 1440 rows)
Resolution OPTA	00:02:00 (390 columns x 360 rows)
Data type	Float
No data value	-9999, NaN

Table 4.4: Technical specification of primary GIS data layers

Acronym	Full name	Data format	Spatial resolution (pixel size)	Time representation	No. of data layers
GHI	Global Horizontal Irradiation	Raster	9 arc-sec. (approx. 275 x 275 m)	1994 – 2017	12+1
DNI	Direct Normal Irradiation	Raster	9 arc-sec. (approx. 275 x 275 m)	1994 – 2017	12+1
DIF	Diffuse Horizontal Irradiation	Raster	9 arc-sec. (approx. 275 x 275 m)	1994 – 2017	12+1
GTI	Global Irradiation at optimum tilt towards equator	Raster	9 arc-sec. (approx. 275 x 275 m)	1994 – 2017	12+1
OPTA	Optimum tilt	Raster	2 arcmin (approx. 3700 x 3700 m)	-	1
PVOUT	Photovoltaic power potential	Raster	9 arc-sec. (approx. 275 x 275 m)	1994 – 2017	12+1
TEMP	Air Temperature at 2 m above ground level	Raster	30 arc-sec. (approx. 930x930 m)	1994 – 2017	12+1

Explanation:

- MM: month of data – from 01 to 12
- ext: file extension (***asc*** or ***tif***)

Data layers are provided as separate files in a tree structure, organized according to

- File format (ASCII or GEOTIF)
- Time summarization (*yearly* and *monthly*)
- Complementary files: Project files (*.prj) and ESRI ASCII grid files (*.asc)

The support GIS data are provided in a vector format (ESRI shapefile, Table 4.6).

Table 4.5: File name convention for GIS data

Acronym	Full name	Filename pattern	Number of files
GHI	Global Horizontal Irradiation, long-term yearly average of daily totals	GHI.*ext*	1+1
GHI	Global Horizontal Irradiation, long-term monthly averages of daily totals	GHI_*MM.ext*	12+12
DNI	Direct Normal Irradiation, long-term yearly average of daily totals	DNI.*ext*	1+1
DNI	Direct Normal Irradiation, long-term monthly averages of daily totals	DNI_*MM.ext*	12+12
DIF	Diffuse Horizontal Irradiation, long-term yearly average of daily totals	DIF.*ext*	1+1
DIF	Diffuse Horizontal Irradiation, long-term monthly averages of daily totals	DIF_*MM.ext*	12+12
GTI	Global Irradiation at optimum tilt towards equator, long-term yearly average of daily totals	GTI.*ext*	1+1
GTI	Global Irradiation at optimum tilt towards equator, long-term monthly averages of daily totals	GTI_*MM.ext*	12+12
PVOUT	Photovoltaic power potential, long-term yearly average of daily totals	PVOUT.*ext*	1+1
PVOUT	Photovoltaic power potential, long-term monthly averages of daily totals	PVOUT_MM.*ext*	12+12
TEMP	Air Temperature at 2 m above ground, long-term yearly average	TEMP.*ext*	1+1
TEMP	Air Temperature at 2 m above ground, long-term monthly averages	TEMP_*MM.ext*	12+12

Total size of unpacked data layers is 13.6 GB, packed (with ZIP compression) 1.7 GB respectively.

Table 4.6: Support GIS data

Data type	Source	Data format
City location	OpenStreetMap.org contributors, GeoNames.org, adapted by Solargis	Point shapefile
Administrative borders	Cartography Unit, GSDPM, World Bank Group	Polyline shapefile
Road network	OpenStreetMap.org contributors, adapted by Solargis	Polyline shapefile
Large water bodies	SWBD, USGS	Polygon shapefile
Solar meteorological stations	Solargis	Point shapefile

4.2 Project in QGIS format

For easy manipulation with GIS data files, selected vector and raster data files are integrated into ready-to-open QGIS project file with colour styles and annotations (see Figure 4.1). QGIS is state-of-art open-source GIS software allowing visualization, query and analysis on the provided data. QGIS includes a rich toolbox to manipulate data. More information about the software and download packages can be found at http://qgis.org.

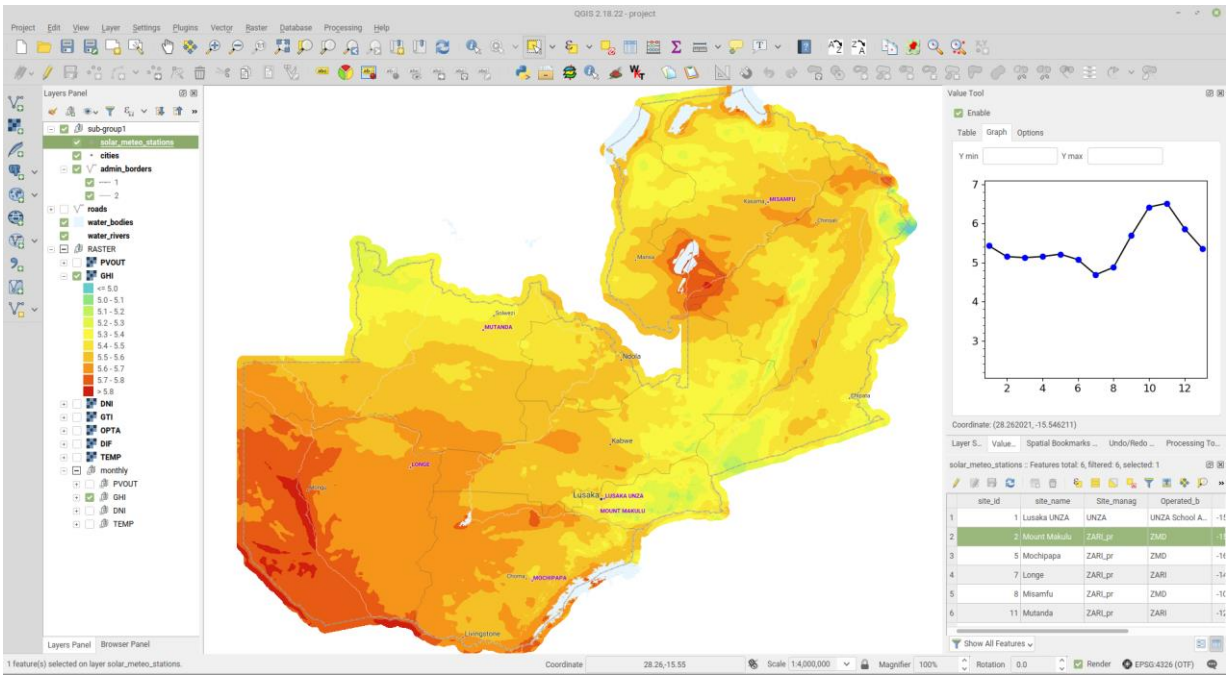

Figure 4.1: Screenshot of the map and data in the QGIS v2.18 environment

4.3 Map images

Besides GIS data layers, digital maps are also delivered for selected data layers for presentation purposes. Digital images (maps) are prepared in two types; each suitable for different purpose:

- High-resolution **poster maps**, printing size 120 x 80 cm, prepared as the colour-coded maps in a TIFF format at 300 dpi density and lossless compression
- **Mid-size maps** suitable for A4 printing or on-screen presentation, prepared in PNG format at 300 dpi density and lossless compression

The following three parameters are processed in the form of maps:

- Global Horizontal Irradiation – Yearly average of the daily totals
- Direct Normal Irradiation – Yearly average of the daily totals
- Photovoltaic electricity production from a free-standing power plant with optimally tilted c-Si modules – Yearly average of the daily totals

The maps will be released to be downloadable from the Download section of Global Solar Atlas (see Figure 4.2):
http://globalsolaratlas.info/downloads/Zambia

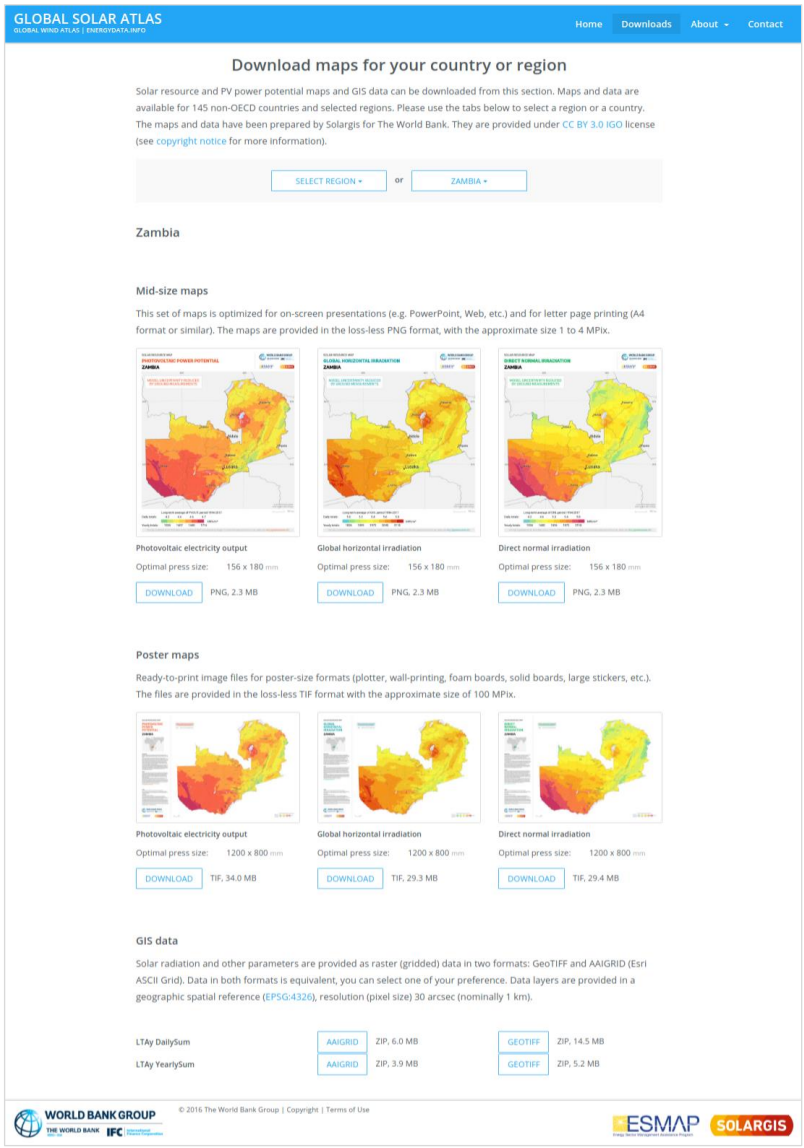

Figure 4.2: Screenshot of the Download section at Global Solar Atlas (Mar 2019) (https://globalsolaratlas.info/downloads/zambia)

5 List of maps

6 List of figures

7 List of tables

8 References

[1] Paul W. Stackhouse, Jr., Zhang T., Westberg D., Barnett A.J., Bristow T., Macpherson B., Hoell J. M., 2018. POWER Release 8 (with GIS Applications) Methodology (Data Parameters, Sources, & Validation), Data Version 8.0.1. https://power.larc.nasa.gov/documents/POWER_Data_v8_methodology.pdf. Web visited on 3 Oct 2018

[2] Šúri M., Wald L., Huld T., Dunlop E., Albuisson M, 2005. Integration of HelioClim-1 database into PVGIS to estimate solar electricity potential in Africa. In: Palz W., Ossenbrink H., Helm P., (eds.) 20th European Photovoltaic Solar Energy Conference, Barcelona, Spain, 6-10 June 2005, Barcelona, pp. 2989-2992" https://www.researchgate.net/publication/43406677

[3] Huld T., Müller R.W., Gambardella A., 2012. A new solar radiation database for estimating PV performance in Europe and Africa. Solar Energy 86 (6), 1803–1815. DOI: 10.1016/j.solener.2012.03.006

[4] Lefèvre M., Wald L., Diabaté L., 2007. "Using reduced data sets ISCCP-B2 from the Meteosat satellites to assess surface solar irradiance". Solar Energy, 81, 240-253. doi:10.1016/j.solener.2006.03.008

[5] ARMINES/MINES ParisTech/TRANSVALOR/ ECMWF – COPERNICUS Atmosphere Monitoring Service. Monthly and yearly average Global Horizontal Irradiation maps from CAMS Radiation Service over Africa. "JADE" volume, April 2018

[6] Meteonorm handbook, Version 7.3, Part II: Theory. Meteotest, 2018

[7] Global Solar Atlas, 2016. The World Bank Group. https://globalsolaratlas.info.

[8] Marcel Suri, Tomas Cebecauer, Branislav Schnierer, Artur Skoczek, Daniel Chrkavy, Nada Suriova, Juraj Betak, 2018. Annual Solar Resource Report for solar meteorological stations after completion of 24 months of measurements. Republic of Zambia, Ref. Nr. 128-07/2018, https://www.esmap.org/node/55906.

[9] Perez R., Cebecauer T., Suri M., 2014. Semi-Empirical Satellite Models. In Kleissl J. (ed.) Solar Energy Forecasting and Resource Assessment. Academic press.

[10] Cebecauer T., Šúri M., Perez R., High performance MSG satellite model for operational solar energy applications. ASES National Solar Conference, Phoenix, USA, 2010.

[11] Šúri M., Cebecauer T., Perez P., Quality procedures of SolarGIS for provision site-specific solar resource information. Conference SolarPACES 2010, September 2010, Perpignan, France.

[12] Šúri M., Cebecauer T., 2014. Satellite-based solar resource data: Model validation statistics versus user's uncertainty. ASES SOLAR 2014 Conference, San Francisco, 7-9 July 2014.

[13] Cebecauer T., Suri M., Gueymard C., Uncertainty sources in satellite-derived Direct Normal Irradiance: How can prediction accuracy be improved globally? Proceedings of the SolarPACES Conference, Granada, Spain, 20-23 Sept 2011.

[14] Šúri M., Cebecauer T., Requirements and standards for bankable DNI data products in CSP projects, Proceedings of the SolarPACES 2011 Conference, September 2011, Granada, Spain.

[15] Ineichen P., A broadband simplified version of the Solis clear sky model, 2008. Solar Energy, 82, 8, 758-762.

[16] Morcrette J., Boucher O., Jones L., Salmond D., Bechtold P., Beljaars A., Benedetti A., Bonet A., Kaiser J.W., Razinger M., Schulz M., Serrar S., Simmons A.J., Sofiev M., Suttie M., Tompkins A., Uncht A., GEMS-AER team, 2009. Aerosol analysis and forecast in the ECMWF Integrated Forecast System. Part I: Forward modelling. Journal of Geophysical Research, 114.

[17] Benedictow A. et al. 2012. Validation report of the MACC reanalysis of global atmospheric composition: Period 2003-2010, MACC-II Deliverable D_83.1.

[18] Cebecauer T., Perez R., Suri M., Comparing performance of SolarGIS and SUNY satellite models using monthly and daily aerosol data. Proceedings of the ISES Solar World Congress 2011, 28 August – 2 September 2011, Kassel, Germany.

[19] Cebecauer T., Šúri M., Accuracy improvements of satellite-derived solar resource based on GEMS re-analysis aerosols. Conference SolarPACES 2010, September 2010, Perpignan, France.

[20] Molod, A., Takacs, L., Suarez, M., and Bacmeister, J., 2015: Development of the GEOS-5 atmospheric general circulation model: evolution from MERRA to MERRA2, Geosci. Model Dev., 8, 1339-1356, doi:10.5194/gmd-8-1339-2015

[21] GFS model. http://www.nco.ncep.noaa.gov/pmb/products/gfs/

[22] MERRA-2 Overview: The Modern-Era Retrospective Analysis for Research and Applications, Version 2 (MERRA-2), Ronald Gelaro, et al., 2017, J. Clim., doi: 10.1175/JCLI-D-16-0758.1

[23] CFSR model. https://climatedataguide.ucar.edu/climate-data/climate-forecast-system-reanalysis-cfsr/

[24] CFSv2 model http://www.cpc.ncep.noaa.gov/products/CFSv2/CFSv2seasonal.shtml

[25] Cano D., Monget J.M., Albuisson M., Guillard H., Regas N., Wald L., 1986. A method for the determination of the global solar radiation from meteorological satellite data. Solar Energy, 37, 1, 31–39.

[26] Perez R., Ineichen P., Maxwell E., Seals R. and Zelenka A., 1992. Dynamic global-to-direct irradiance conversion models. ASHRAE Transactions-Research Series, pp. 354-369.

[27] Perez, R., Seals R., Ineichen P., Stewart R., Menicucci D., 1987. A new simplified version of the Perez diffuse irradiance model for tilted surfaces. Solar Energy, 39, 221-232.

[28] Ruiz-Arias J. A., Cebecauer T., Tovar-Pescador J., Šúri M., Spatial disaggregation of satellite-derived irradiance using a high-resolution digital elevation model. Solar Energy, 84, 1644-1657, 2010.

[29] Marcel Suri, Tomas Cebecauer, Marcel Suri, Branislav Schnierer, Nada Suriova, Juraj Betak, Daniel Chrkavy, Artur Skoczek, 2019. Solar Model Validation Report; Regional adaptation of Solargis model based on data acquired in 24-months solar measurement campaign; Republic of Zambia, Ref. Nr. 128-08/2019. https://www.esmap.org/node/55906.

[30] Ineichen P. Long term satellite hourly, daily and monthly global, beam and diffuse irradiance validation. Interannual variability analysis. University of Geneva/IEA SHC Task 46, 2013. http://www.unige.ch/energie/forel/energie/equipe/ineichen/annexes-iae.html

[31] Cebecauer T., Suri M., 2015. Site-adaptation of satellite-based DNI and GHI time series: overview and Solargis approach. SolarPACES conference, September 2015, Cape Town, North Africa.

[32] King D.L., Boyson W.E. and Kratochvil J.A., Photovoltaic array performance model, SAND2004-3535, Sandia National Laboratories, 2004.

[33] Huld T., Šúri M., Dunlop E.D., Geographical variation of the conversion efficiency of crystalline silicon photovoltaic modules in Europe. Progress in Photovoltaics: Research and Applications, 16, 595-607, 2008.

[34] Huld T., Gottschalg R., Beyer H. G., Topic M., Mapping the performance of PV modules, effects of module type and data averaging, Solar Energy, 84, 2, 324-338, 2010.

[35] Huld T., Friesen G., Skoczek A., Kenny R.P., Sample T., Field M., Dunlop E.D., 2011. A power-rating model for crystalline silicon PV modules. Solar Energy Materials and Solar Cells, 95, 12, 3359-3369.

[36] Skoczek A., Sample T., Dunlop E. D., The results of performance measurements of field-aged crystalline silicon photovoltaic modules, Progress in Photovoltaics: Research and Applications, 17, 227-240, 2009.

[37] Martin N., Ruiz J.M. Calculation of the PV modules angular losses under field conditions by means of an analytical model. Solar Energy Material and Solar Cells, 70, 25–38, 2001.

[38] The German Energy Society, 2008: Planning and Installing Photovoltaic Systems. A guide for installers, architects and engineers. Second edition. Earthscan, London, Sterling VA.

[39] Zambia, Power Africa fact sheet, USAID, https://www.usaid.gov/powerafrica/Zambia

Support information

Background on Solargis

Solargis is a technology company offering energy-related meteorological data, software and consultancy services to solar energy. We support industry in the site qualification, planning, financing and operation of solar energy systems for more than 19 years. We develop and operate the high-resolution global database and applications integrated within Solargis® information system. Accurate, standardised and validated data help to reduce the weather-related risks and costs in system planning, performance assessment, forecasting and management of distributed solar power.

Solargis is ISO 9001:2015 certified company for quality management.

This report has been prepared by Nada Suriova, Branislav Schnierer, Daniel Chrkavy, Juraj Betak, Artur Skoczek, Tomas Cebecauer, Marcel Suri and Veronika Madlenakova from Solargis

All maps in this report are prepared by Solargis

Solargis s.r.o., Mytna 48, 811 07 Bratislava, Slovakia

Reference No. (Solargis): 128-09/2019

http://solargis.com


SOLARGIS